MyD88 mutations in B cell tumors: constitutive signaling by TIR domain oligomerization

Dissertation

der Mathematisch-Naturwissenschaftlichen Fakultät

der Eberhard Karls Universität Tübingen

zur Erlangung des Grades eines

Doktors der Naturwissenschaften

(Dr. rer. nat.)

vorgelegt von

Dipl. Biol. Olaf-Oliver Wolz

aus Großsanktnikolaus/Rumänien

Tübingen

2015

Gedruckt mit Genehmigung der Mathematisch-Naturwissenschaftlichen Fakultät der Eberhard Karls Universität Tübingen.

Tag der mündlichen Qualifikation:	08. März 2016
Dekan:	Prof. Dr. Wolfgang Rosenstiel
1. Berichterstatter:	Jun.-Prof. PhD Alexander N.R. Weber
2. Berichterstatter:	Prof. Dr. Hans-Georg Rammensee

Acknowledgement

First I would like to thank my supervisor Alexander N.R. Weber for giving me the opportunity to perform the experimental work of my doctoral thesis in his laboratory. His confidence in me, the never-ending personal support and the valuable scientific advices contributed to the accomplishment of this work. The time spent in his research group with many inspiring discussions has been a precious experience.

I would also like to thank Prof. Dr. Hans-Georg Rammensee from the University of Tübingen. He allowed me to carry out the project at the department of Immunology in an excellent scientific working environment through the financial support by the SFB685. I am grateful to get known to other areas of research and for cooperation with colleagues by taking part in the Integrated Research Training Group (IRTG) “Immunotherapy".

I am very thankful for the help gained from all former and actual members of the Weber laboratory who greatly assisted me with experiments and good advises and who accounted to the success of the project.

In the end I am especially pleased for the constant patience and understanding obtained from my parents and Leonie. I am deeply grateful for their encouragement and I highly appreciate their support.

Abstract

Myeloid differentiation primary response 88 (MyD88) is the key adaptor protein that mediates signals upon activation of Toll-like receptors (TLR) and the IL-1 receptor (IL-1R). MyD88 consists of a Toll/IL-1R (TIR) domain that interacts with TIR domains of receptors or other adaptor proteins, whereas the death domain (DD) recruits downstream IL-1R-associated kinases (IRAKs) to form the so-called Myddosome signaling complex. A leucine to proline substitution of the amino acid residue 265 (L265P) within the TIR domain of MyD88 has recently been described as a very frequent somatic mutation in several types of B cell non-Hodgkin lymphomas, all of which are associated with considerable mortality; i.e. diffuse large B cell lymphoma (DLBCL), Waldenström's macroglobulinemia (WM), mucosa-associated lymphoid tissue lymphoma (MALT) and chronic lymphocytic leukemia (CLL). Recent reports revealed MyD88 L265P strongly increases binding and activation of IRAK1 as well as Bruton's tyrosine kinase (BTK), thus these interactions are suggested to sustain cancer cell survival by constitutive activation of the transcription factor NF-κB (nuclear factor kappa-light-chain-enhancer of activated B cells). However, the precise molecular events leading to NF-κB hyperactivation and whether other B cell-intrinsic pathways are affected still remains unknown. In an effort to address these questions we found that the hyperactive phenotype of MyD88 L265P is caused by increased oligomerization propensity of the mutated TIR domain. L265P TIR domains in contrast to WT TIRs were alone able to trigger cell activation by strongly interacting with and therefore utilizing WT MyD88, possibly explaining why heterozygous mutation could be sufficient to trigger tumorigenesis. Confocal microscopy revealed cytosolic aggregation of TIR-mutants. MyD88 L265P colocalized with IRAKs indicating that L265P mutant assembly of oligomeric Myddosome post-receptor complexes leads to cell activation. Furthermore, cell lysates of L265P-mutated lymphoma cell lines contained complexes of high molecular weight including MyD88 and IRAK1, indicative for Myddosomes and confirming the aggregation phenotype of the mutant. Consequently blocking MyD88 oligomerization induced death of L265P-mutated but not WT DLBCL cells. Preliminary data indicate that L265P alters binding of MyD88 to several proteins which are important for regulatory circuits in B cell carcinogenesis. We plan to corroborate these findings in primary tumor cells and in vitro murine models, and propose to evaluate and utilize novel insights of how L265P may modulate tumor cell persistence by using small molecule inhibitors targeting the newly discovered interaction partners.

Zusammenfassung

MyD88 (myeloid differentiation primary response 88) ist ein wichtiges Adapter-Protein das Signale von aktivierten Toll-like Rezeptoren (TLRs) und dem Interleukin-1-Rezeptor (IL-1R) weiterleitet. MyD88 besteht aus einer Toll/IL-1R-Proteindomäne (TIR) welche mit TIR-Domänen von Rezeptoren oder weiteren Adapter-Proteinen interagiert. Über die sog. DD-Proteindomäne (death domain) von MyD88 werden IL-1R-assoziierte Kinasen (IRAKs) rekrutiert wobei alle Proteine zusammen sog. Myddosomen bilden, aktivierte Signalkomplexe von hohem Molekulargewicht. In Studien wurde gezeigt, dass die MyD88 TIR-Domäne häufig in diversen B-Zell Non-Hodgkin-Lymphomen mutiert ist. Dazu gehören Neoplasien mit hoher Todesfolge wie z.B. das diffuse großzellige B-Zell-Lymphom (DLBCL), Waldenströms Makroglobulinämie (WM) oder die Chronische lymphatische Leukämie (CLL). Meistens entsteht durch Punktmutation im *MYD88*-Gen ein Austausch der 265. Aminosäure von Leucin zu Prolin (L265P). Studien konnten belegen, dass die L265P-Mutation eine starke Bindung von MyD88 mit IRAK- und BTK (Bruton-Tyrosinkinase) verursacht. Beide Kinasen waren dabei phosphoryliert und somit aktiv, was eine konstitutive Aktivierung des Transkriptionsfaktors NF-κB (nuclear factor kappa-light-chain-enhancer of activated B cells) auslöste. Es ist davon auszugehen, dass letztendlich die erhöhte Expression anti-apoptotischer Gene durch hyperaktives NF-κB zur Persistenz von malignen Tumorzellen führt. Jedoch sind die genauen Vorgänge die zu dieser Hyperaktivierung führen nicht im Detail verstanden. Die vorliegende Arbeit beschreibt einen bisher unbekannten Mechanismus der Krebsentstehung: Expression von L265P-mutierten TIR-Domänen waren im Vergleich zu WT TIRs alleine ausreichend um NF-κB zu aktivieren. Die Mutante offenbarte dabei eine starke Bindungsaffinität zu sowohl mutierten, als auch WT TIR-Domänen, was eine wirksame Oligomerisierung von MyD88 Molekülen zur Folge hatte. Dieser Umstand wäre auch eine Erklärung dafür, dass eine heterozygot vorliegende MyD88-Mutation, wie es in den allermeisten Fällen von Lymphomen der Fall ist, ausreichend für die Krebsentstehung wäre. Fluoreszenzmikroskopische Untersuchungen zeigten Protein-Aggregation von L265P-mutierten TIR-Domänen im Zytoplasma. Weiterhin konnten wir Co-Lokalisation von MyD88 L265P mit verschiedenen IRAK Kinasen nachweisen, was vermuten lässt dass es sich bei beschriebenen Aggregaten um Myddosomen handelt, welche letztendlich zur Aktivierung von Signalwegen führen. Nach Zentrifugation von DLBCL Zelllysaten konnten wir mutiertes MyD88 in Komplexen mit hohem Molekulargewicht nachweisen. Diese Komplexe in L265P-mutierten Zellen enthielten auch mehr IRAK1 im Vergleich zu den MyD88 WT Zellen. Das weist darauf hin, dass eine

L265P-bedingte Bildung von aktiven Myddosom-Aggregaten auch in DLBCL stattfindet. Folgerichtig konnten wir durch Blockieren der TIR-Oligomerisierung ein gezieltes Abtöten von MyD88 L265P-mutierten DLBCL Zelllinien erreichen. Weiterhin deuten vorläufige Daten an, dass die MyD88 L265P-Mutation auch die Affinität zu weiteren Proteinen verändert, welche eine wichtige Funktion in der B-Zell Onkogenese einnehmen. Diese Erkenntnisse sollen sowohl in primären Tumorzellen als auch in einem in vitro Mausmodell bestätigt werden. Wir hoffen, dass sich unsere Neuentdeckungen als nützlich erweisen und planen deshalb zur Evaluierung, konstitutiv-aktivierte Signalwege in MyD88-mutierten Lymphomen pharmakologisch zu inhibieren.

Content

Figures

Tables

Abbreviations

ABC-DLBCL	Activated B cell type of DLBCL
ADCC	Antibody-dependent cell-mediated cytotoxicity
ALR	AIM2-like receptor
APC	Antigen presenting cells
BCR	B cell receptor
BMDM	Bone marrow-derived macrophages
BSA	Bovine serum albumin
BTK	Bruton’s tyrosine kinase
CARD11	Caspase recruitment domain 11
CCD	Charge-coupled device
CD	Cluster of differentiation
CLL	Chronic lymphocytic leukemia
CLR	C-type lectin receptor
COPII	Coat protein complex II
CSR	Class-switch recombination
CTL	Cytotoxic T cell
DAMP	Danger-associated molecular pattern
DC	Dendritic cell
DD	Death domain
DLBCL	Diffuse large B cell lymphoma
DLR	Dual-Luciferase Reporter Assay
dsDNA	Double-stranded DNA
dsRNA	Double-stranded RNA
DTT	Dithiothreitol
DUSP4	Dual-specificity phosphatase 4
ER	Endoplasmatic reticulum
ERK	Extracellular signal-regulated kinase

EV	Empty vector
FCS	Fetal calf serum
FRET	Fluorescence resonance energy transfer
GOI	Gene of interest
HA	Hemagglutinin
HEK	Human embryonic kidney
HLA	Human leukocyte antigen
HRP	Horseradish peroxidase
IB	Immunoblot
IFN	Interferon
Ig	Immunoglobulin
IL	Interleukin
IL-1R	Interleukin-1 receptor
IP	Immunoprecipitation
IRAK	IL-1R-associated kinase
IRF	Interferon regulatory factor
JNK	C-Jun N-terminal kinase
LPL	Lymphoplasmacytic Lymphoma
LPS	Lipopolysaccharide
Mal	MyD88 adaptor-like protein
MALT1	Mucosa associated lymphoid tissue lymphoma translocation gene 1
MAPK	Mitogen-activated protein kinases
MGUS	Monoclonal gammopathy of undetermined significance
MHC	Major histocompatibility complex
MyD88	Myeloid differentiation primary response protein 88
NF-κB	nuclear factor kappa-light-chain-enhancer of activated B cells
NLR	NOD-like receptor
NTD	N-terminal domain
OS	Overall survival
PAGE	Polyacrylamide gel electrophoresis

PAMP	Pathogen-associated molecular pattern
PCR	Polymerase chain reaction
pDC	Plasmacytoid dendritic cell
PFS	Progression free survival
PI3K	Phosphatidylinositol 3-kinase
PKC	Protein kinase C
PRR	Pattern recognition receptor
RLR	RIG-1-like receptor
RLU	Relative light units
RNAi	RNA interference
SARM	Sterile alpha and TIR motif containing protein
SD	Standard deviation
SDS	Sodium dodecyl sulfate
SEM	Standard error of the mean
SH2	Src-homology 2
SNP	Single nucleotide polymorphism
SOCS1	Suppressor of cytokine signaling 1
Strep	Streptavidin
ssRNA	Single-stranded RNA
Syk	Spleen tyrosine kinase
TCR	T cell receptor
Th	T helper cell
TIR	Toll/interleukin-1 receptor (TIR) homology domain
TLR	Toll-like receptor
TRAF6	Tumor necrosis factor receptor-associated factor 6
TRIF	TIR-domain-containing adapter-inducing interferon-β
UPD	Uniparental disomy
WM	Waldenström’s macroglobulinemia

1 Introduction

1.1 The Immune System

The immune system is an interactive network of lymphoid organs, cells, humoral factors and cytokines to protect the host from microbes, toxic and allergic substances that threaten normal homeostasis. It is central to the host for mobilizing defense to distinguish between non-self and self. For this purpose two systems have developed which differ by the speed and specificity of defense reactions. They are known as the innate and adaptive immune system. Although they are defined as two different systems their function is not strictly separated since there is considerable cross-talk and cooperation for a fully integrated and efficient immune response.

One should not exclude that in addition to the function of the immune system, barriers play a crucial role in preventing the bulk of infectious agents from entering the host organism. Those barriers could be physical surfaces like skin and mucosa, chemical such as acidic pH in the stomach lumen or even microbiological as in the gut where the symbiotic microbiome creates a protective environment[1].

1.1.1 Innate immune responses

The innate immune system comprises defense mechanism such as cytokine secretion, the complement system and acute phase protein, challenges which are typically fulfilled by cell types such as macrophages, dendritic cells (DCs), neutrophils and monocytes. The innate immune system represents the first line of defense against invading microbial pathogens and is conserved among vertebrates and some components like receptors are also found in plants.

Innate immune responses were first assumed to operate in a more rude non-specific sense but Janeway hypothesized in 1989[2] that “nonclonal recognition of nonself patterns plays a major role in immune system function and in host defense. The receptors mediating such recognitive events were the original, nonclonal triggers for immune effector mechanisms.” Furthermore he postulated that “primitive effector cells bear receptors that allow recognition of certain pathogen-associated molecular patterns that are not found in the host.” And he named these receptors as ‘pattern recognition receptors’.

The first proof of a germline encoded receptor that recognizes highly conserved microbial structures and thus initiates the immune reaction came with the discov-

ery of the *Drosophila melanogaster* protein Toll. Originally Toll was detected to play a role in the dorso-ventral development of the embryo but later in the adult fly it was found out that it was critical for resistance to the fungus *Aspergillus fumigatus*[3]. Soon after this discovery a human paralogue of the *Drosophila* Toll was found (later declared to be Toll-like receptor 4)[4] which responded to bacterial lipopolysaccharide (LPS)[5]. Today we know a variety of so-called Pattern recognition receptors (PRRs) which recognize specific pathogen-associated molecular patterns (PAMPs) and danger-associated molecular patterns (DAMPs). The term PAMP has been controversially discussed because most microbes, as i.e. commensal *Escherichia coli* in the gut and not solely pathogens express molecules such as LPS being detected by PRRs. Therefore the term microbe-associated molecular patterns (or MAMPs) has been proposed[6,7]. PRRs can be subdivided into five different families: Toll like receptors (TLRs), NOD-like receptors (NLRs), RIG-1-like receptors (RLRs), AIM2-like receptors (ALRs) and C-type lectin receptors (CLRs)[8]. In case of the best characterized PRRs, the TLRs, up to date 13 were identified in mammalian cells, with 10 different in humans[9]. All specifically recognize MAMPs which are unique to microbes and not found in the host. Following recognition of MAMPs by PRRs multiple inflammatory cytokines are secreted in order to initiate an immune response. These networks of signaling are mandatory for the regulation of inflammation, antiviral defense, the control of inflammatory or autoimmune diseases and the consequent activation of the adaptive immune system[10].

1.1.2 The adaptive immune system

In contrast to the innate immune system which is seen even in simple organisms like insects, the adaptive immune system is a hallmark of higher organisms like mammals. Whereas innate immune responses are much faster, they lack a certain kind of specificity. Therefore the adaptive immunity has evolved, a precise but delayed response that could take days to weeks and includes memory, and which consists of antigen-specific reactions through B and T lymphocytes. In B and T cells recognition specificity is encoded by multiple gene elements that rearrange somatically to generate a highly diverse repertoire of antigen-binding B and T cell receptors (BCRs, TCRs) with outstanding specificity for foreign structures. The adaptive response is of long duration and has a memory function so that recapitulated exposure to invaders has a more rapid and vital response to attenuate the damage. Long-lived B and T memory cells persist in a dormant state but rapidly after another encounter with their specific antigen they re-express their effector functions.

The characteristic of the adaptive immune system is the use of antigen-specific receptors on B and T lymphocytes that mediate effector responses in two stages. At first, the antigen is presented and recognized by T cells, which leads to their cell priming, activation and differentiation. Secondly, effector responses are triggered which cause that activated effector CD8 T cells leave the lymphoid organs and home to the site of the infection, or that activated plasma B cells, helped by CD4 T cells, secrete antigen-specific antibodies.

Dendritic cells or macrophages i.e. are so-called antigen-presenting cells (APCs). In addition to MAMP/DAMP-mediated defense, these cells ingest and process antigens which they present on the cell surface on the major histocompatibility complexes MHC class I or II. The TCR recognizes MHC-antigen-complexes together with the co-receptors CD8 (for MHC class I) or CD4 (for MHC class II, respectively) which leads to T cell priming, activation and differentiation. CD8 and CD4 T lymphocytes have distinct functions which are determined by the MHC class they recognize. It is seen as a general rule that endogenous antigens derived i.e. from viruses or intracellular pathogens are complexed with MHC class I on infected cells which activates CD8 cytotoxic T cells (CTL). Activated CTLs induce apoptosis of infected cells by releasing cytotoxins, perforin and granzymes or via cell surface interactions between the so-called death receptors, whereby Fas ligand (FasL) on CTLs binds to Fas on infected target cells. On the other hand CD4 T cells are seen to recognize antigens derived from extracellular pathogens which are presented on MHC class II. Activation of CD4 T cells leads to an extensive production of cytokines which in turn activate a wide range of surrounding effector cells like B lymphocytes and CTLs. CD4 T cells could be further subdivided, depending on the cytokines they secrete, in the two main groups of T helper cells Th1 or Th2. Th1 cells are known to produce e.g. interleukin 2 (IL-2) which stimulates CTL cytotoxicity and induces T cell proliferation of CD4 T cell in an autocrine loop. Cells of this type also produce interferon γ (IFN- γ) which is an important activator of macrophages and inducer of MHC class II molecule expression. On the contrary, Th2 cells produce cytokines as interleukin 4, 5, 6 and 10 that are important for B cell maturation and the antibody response. For example, IL-4 triggers class switch recombination (CSR) of B cell, a process were the constant region of the immunoglobulin heavy chain is changed to modulate the interaction of an antibody with different effector molecules.

The main purpose of B cells is to generate antibodies (immunoglobulins, Ig) which function i.e. to sensitize infected or tumor cells for antibody-dependent cellular cytotoxicity (ADCC) which is mediated by CTLs and Natural killer (NK) cells, to opsonize microorganisms for phagocytosis, activate the complement system or neutralize toxins. The BCR is a membrane bound form of an immunoglobulin which is

crucial in the whole procedure of B cell maturation. BCRs recognize antigens, and mediate the internalization and presentation on antigen-fragments on the MHC class II complex. Therefore B cells also act as antigen-presenting cells for T cells. In turn when primed CD4 T cell recognize antigen-bound MHC class II with their specific TCRs they can mediate a Th2 response what triggers B cells to divide, mature and secrete different classes of Ig. There are also further crucial interactions between T and B cells known, in particular direct binding of CD40 ligand (CD40L or also known as CD154) on T to CD40 on B cells which for example induces antibody isotype switching[11]. Furthermore, B cells can respond to several antigens in a T cell-independent fashion by stimulation of TLRs expressed in B cells, i.e. TLR4 activation by bacterial LPS[12].

1.2 Toll-like Receptor pathways of the innate immune system are central for host defense

Toll-like receptor signaling is central in host immune defense against a bulk of pathogenic microorganisms. TLR-pathway malfunctioning contributes to many human diseases (see 1.4). Therefore it is of great interest to understand the regulation and underlying mechanisms of TLR signal transduction.

1.2.1 Signaling pathways of TLRs

TLRs are evolutionary conserved transmembrane receptors consisting of an extracellular ligand-recognition domain, a membrane-bridging section and a TIR (abbreviation for Toll/Interleukin-1 receptor) domain protruding into the cytosol (reviewed in [13-18]).

After binding of activating ligands to the TLR's ectodomain, TIR dimerization is induced which in turn forms a platform for downstream signal transduction. Cytosolic adaptor proteins such as MyD88 and Mal also contain TIR domains and interact with activated receptors by TIR-TIR interplay. In turn adaptor proteins recruit and activate the IL-1 receptor associated kinases (IRAK) 1, IRAK2 and IRAK4 by death domain (DD) interactions[10]. MyD88 has a fundamental role in initiating the hierarchical assembly of this high molecular weight signaling complex, which finally mediates the activation of nuclear factor-κB (NF-κB). Therefore, these complexes are referred to as 'Myddosomes'. Activation of IRAKs involves both auto- and reciprocal phosphorylation leading to oligomerization and activation of the E3 ubiquitin ligase TRAF6 (tumor necrosis factor receptor (TNFR)-associated factor 6)[19] and the kinase TAK1[20]. Ubiquitination of TRAF6 and TAB2 recruits both TAB1 and TAB2 leading to activation of the kinase TAK1. TAK1 activates the IKK complex which consists of the two catalytic subunits IKKα and IKKβ and the regulatory

subunit IKKγ (also known as NEMO). The transcription factor NF-κB resides inactive in the cytosol where it is bound to its repressor IκBα. Phosphorylation of IκBα by the activated IKK complex leads to the ubiquitination and proteasome-mediated degradation of IκBα which allows NF-κB to translocate into the nucleus to initiate gene transcription. TLR pathways do not exclusively lead to activation of NF-κB but also include several other transcription factors described in the following.

1.2.1.1 Stimulation of TLRs activates NF-κB transcription factors

Nuclear factor kappa-light-chain-enhancer of activated B cells (NF-κB) is one of the most studied transcription factors because of its important role in regulating gene expression during inflammation and immune response. The family of NF-κB transcription factors comprises five members that form homo- or heterodimers in various combinations: p65 (or RelA), RelB, c-Rel, p105 (or NF-κB1) and p100 (or NF-κB2)[21]. Thereby p105 and p100 are expressed as large precursors and are subsequently proteolytically processed by the proteasome to the mature subunits p50 and p52, respectively. In TLR signaling the heterodimer composed of p65/p50 is the most common activated form and named as canonical NF-κB pathway.

1.2.1.2 Stimulation of TLRs activates AP-1 transcription factors

During TLR-signaling, mitogen-activated protein kinases (abbreviated as MAPK) are activated by complex phosphorylation cascades. It has been suggested that TAK1 is the kinase which connects NF-κB and MAPK signaling. TAK1 activates MAPKs such as MKK3, MKK4 and MEK1/2 which further triggers downstream MAPKs like p38, JNK (C-Jun N-terminal kinase) and ERK (extracellular signal-regulated kinase)[9]. This in turn consequently leads to the activation of transcription factors of the AP-1 family controlling the expression of several cytokine genes[21].

1.2.1.3 Stimulation of TLRs activates IRF transcription factors

Whereas NF-κB and MAPK-pathways are activated by several inflammatory stimuli, interferon regulatory factors (IRFs) are manly activated in response to viral infections. They initiate the expression of type I interferons. For example, TLR3 is stimulated by viral double-stranded RNA (dsRNA) which leads to a TRIF (explained under 1.3.2.3) adaptor-dependent activation of IRF3 and consequent secretion of IFN-β[21].

1.2.2 Distinct TLR receptors modulate signaling

So far ten different TLRs are described (compare to Table 1.1) for humans that recognize ubiquitous conserved motifs on microbes and pathogens, the MAMPs. Due to the relatively small number of TLRs each individual receptor recognizes

and responds to a large number of microorganisms ranging from viruses, bacteria, fungi and protozoa since they all have conserved structures not present in humans.

For human TLRs it is known (see Table 1.1) that TLR2 forms heterodimers together with TLR1 and TLR6. While the TLR1/TLR2 heterodimer recognizes triacylated lipopeptides, the TLR2/TLR6 dimer senses diacylated lipopeptides. Heterodimerization of TLRs 1, 2, and 6 has the useful effect to increase the repertoire of ligands to be detected. Thus, independently of TLR1 or TLR6, the TLR2 homodimer can also recognize lipoteichonic acid (LTA) or mycobacterial cell wall components. Against viral infections TLR3 is crucial because it senses double-stranded RNA (dsRNA). TLR4 is associated with a co-receptor named MD-2 which together sense LPS found in the outer membrane of Gram-negative bacteria. Bacterial flagella are huge filaments composed of many subunits of the protein flagellin, which was shown to be the ligand for TLR5. Both TLR7 and 8 can associate with single-stranded RNA (ssRNA) from viruses and bacteria. TLR9 recognizes bacterial and viral unmethylated CpG-rich DNA, motifs where a cytosine nucleotide occurs next to a guanine nucleotide in the linear DNA sequence. CpG motif sites are very frequent in the bacterial and viral genome. In vertebrates they are found rarely where they are often methylated at so-called CpG islands due to gene-regulatory functions. TLR10 is expressed in humans but not in mice, but its biological function, ligands and mode of signaling still remains unclear[22].

1.2.3 TLRs signal from different cellular compartments

TLRs could be subdivided by their cellular localization (compare to Table 1.1). Broadly speaking, TLRs 1, 2, 4, 5 and 6 are mainly located at the cell surface and bind protein and lipid ligands. On the other hand TLRs 3, 7, 8 and 9 reside in the endosomal compartment and are activated by foreign nucleic acids. Restriction to the endosomal compartment prevents TLRs from engaging hosts' self-derived nuclear acids. TLRs lack specificity compared to BCR and TCR immune receptors and in that way self-derived nucleic acids are prevented from entering the endosome whereas foreign material including nucleic acids is endocytosed and processed at this locus. Interestingly while TLRs expressed on the surface mainly detect bacterial components, TLRs located in endosomal membranes rather sense viral products. TLR4 was shown to signal in response to LPS from two locations[23]. When expressed at the plasma membrane TLR4 recruits the bridging adaptor Mal which than recruits MyD88, leading to NF-κB activation. When TLR4 is endocytosed and activated it recruits the two other TIR-domain adaptors TRAM and TRIF (compare to sections 1.3.2.3 and 1.3.2.4). This leads to the activation of the kinase

TBK1 which shifts the signal transduction towards induction of transcription factor IRF3 required for interferon expression/secretion.

TLRs are differentially expressed in a wide range of different cell types and tissues. Most hematopoetic innate cell types stemming from the myeloid linage such as macrophages or dendritic cells express almost the full repertoire of TLRs[24]. On the other hand for lymphoid-derived B cells it is known, that primarily TLR9 is important for their function[12,25]. But TLRs are also abundant and play a crucial role in non-hematopoetic cells, i.e. on the basolateral surface of epithelial cells of the small intestine[26].

Table 1.1: Toll like receptors expressed in humans and exemplary activating ligands.
Summarized information from reviews[9,13-18,22]. dsDNA: double stranded DNA; LPS: lipopolysaccharide; ssRNA: single stranded RNA; CpG DNA: regions of DNA where a cytosine nucleotide occurs next to a guanine nucleotide in the linear sequence; IRF: Interferon regulatory factor

TLR	Dimer-formation with TLR	Activating ligands	Cellular localization	TIR-containing adaptor	Comments
1	2	lipopeptides	surface	MyD88	
2	1, 6	lipopeptides	surface	MyD88/Mal	
3		dsRNA	endosome	TRIF	activates IRFs
4	2	LPS	surface or endosome	MyD88/Mal, TRAM/TRIF	co-receptor MD2 bound to LPS is the ligand
5		flagellin	surface	MyD88	
6	2, 1	lipopeptides	surface	MyD88/Mal	
7		ssRNA	endosome	MyD88, Mal	
8		ssRNA	endosome	MyD88, Mal	
9		CpG DNA	surface or endosome	MyD88, Mal	highly expressed in B cells
10		unknown	surface		present only in humans; role unclear

1.2.4 Various domains of TLRs mediate signal transduction over membranes

Ligands are recognized by the extracellular/endosomal ectodomains of TLRs. Such ectodomains comprise of N-terminal leucine-rich repeats (LRRs), protein motifs which form into a horseshoe-like structure with free N termini and juxtamembrane C-termini which pass over into a transmembrane sequences. These flexible LRR structures provide several binding interfaces for TLR ligands of characteristic sizes and chemical properties such as proteins, lipids and nucleic acids. Generally TLR-induction brings the juxtamembrane C-termini of the ectodomains into close proximity, independently form the type of receptor dimerization. The juxtamembrane C-termini (and therefore linked transmembrane sequences and cytosolic TIR domains) seem to have a natural propensity to form dimers and some TLRs are expressed as pre-formed dimers prior to ligand binding (see below). Expression of truncated TLR endodomains (lacking LRRs) is accompanied by constitutive signaling proposing an inhibitory role of LRR ectodomains which is abrogated by ligand binding[27]. In the following there are two known mechanisms described for TLR activation in humans.

1.2.4.1 TLR activation by dimerization

TLRs 1, -2, -4, -5, -6 reside monomeric in the cell membrane but when exposed to their proper ligands they can form homo- or heterodimers. For example, it was shown that bacterial flagellin prompts TLR5 homodimerization[28] and that lipoproteins or -peptides induce the formation of TLR2 heterodimers together with TLR1 or TLR6[29,30], whereby the TLR1-TLR2 heterodimer ligated with tri-acylated lipopetide was crystalized. TLR3 signals from the endosomal compartment, but in exception for TLRs7-9 which also reside in endosomes, it remains monomeric when inactive. TLR3-crosslinking with double-stranded RNA leads to clustering and activation of the receptors[31].

1.2.4.2 Activation of preformed TLR-dimers by conformational changing

TLRs sensing nucleic acids (TLR7, -8, -9), in contrast to TLR3 and their cell membrane counterparts, are integrated into endosomal membranes as preformed homodimers as it was shown by fluorescence resonance energy transfer (FRET) techniques. In the case of TLR9, dimer conformations were also investigated by circular dichroism spectroscopy[32]. CpG-motif rich DNA stimulates TLR9 whereas DNA lacking CpG could also associate with TLR9 and even inhibit its activation. Steady state (unliganded) TLR9 was homodimerized, but formed in an inactive conformation. After binding of CpG-DNA TLR9 underwent allosteric conformational changes in the cytoplasmic TIR domain, which is required for the recruitment of

adaptor proteins like MyD88. Another study solved the structures of the single-stranded RNA-sensing TLR8 homodimer both in an unliganded and ligand-induced activated state[33]. Remarkably in both reports TLR ligand binding induced structural reorganization of the dimer, which enables downstream signaling processes.

1.2.5 TLR trafficking and arrangement in lipid rafts sensitize signal strength

TLR pathways underlie a complex regulation that is not only restricted to signal transduction but also includes TLR synthesis and trafficking to their locus of action (cell surface or endosomal compartment) or their recycling by endocytosis.

1.2.5.1 TLR-trafficking determines localization to cellular compartments

After protein translation TLR-folding happens in the membrane of the endoplasmic reticulum (ER) with the help of diverse chaperones. For example in case of the endosomal TLRs 3, -7, -8 and -9, the membrane intrinsic chaperone UNC93B accomplishes this function. Patients with deficiencies in UNC93B were described to suffer under severe herpes simplex encephalitis to the same extent like patients with TLR3-mutations[34]. From the ER, folded TLRs are packaged into coat protein complex II (COPII) vesicles which direct the transport to the Golgi-apparatus. From there further protein processing happens such as glycosylation which aids to export the receptors to the plasma membrane or to incorporate them into endosomal membranes. TLR signaling could be also negatively regulated by receptor endocytosis as an example of TLR4 illustrates: LPS-stimulation induces the internalization of receptors which is mediated by clathrin-coated vesicles. After endocytosis protein components are recycled[14].

Furthermore, a recent study suggests that TLR9 could be activated from different subcellular locations and not only from the endosomal compartment. In this case Mal has been proposed to act as a sorting adaptor which directs TLR9 trafficking to either endosomes or the plasma membrane. In both cases Myddosomes were assembled leading to inflammatory cytokine production. The location of TLR9 is determined by the promiscuity of the Mal phosphoinositide-binding domain which targets several lipids found in both endosomal and plasma membrane[35].

1.2.5.2 TLRs cluster in lipid rafts

Lipid rafts, also known as membrane microdomains, are regions of biological membranes with different composition of lipids compared to the surrounding area[36]. Frequently, lipid rafts are defined by a high concentration of cholesterol in the plasma membrane. It was demonstrated that they can modulate strength of TLR-mediated immune responses. In Macrophages for example, TLR4-mediated in-

flammatory signaling was increased after stabilization of lipid rafts with cholera toxin B which cross-links the lipid GM2 ganglioside[37]. The adaptor protein Mal which localizes to rafts by its phosphatidylinositol 4,5-bisphosphate (PIP_2) binding domain, may facilitate the recruitment of TLRs to these membrane areas[38]. Generally it is thought that lipid rafts facilitate the proximity-induced activation and thus the cooperative assembly of oligomeric signaling scaffolds[13].

1.3 Activated TLRs induce the assembly of the Myddosome signaling complex by TIR oligomerization

TLRs (except TLR3) that bind their proper ligands are activated and mediate the hierarchical assembly of downstream protein complexes, named Myddosomes. This is initiated by oligomerization of TIR domains which come together at three different interfaces both in a homotypic and a heterotypic way: the receptor-receptor interface, for example of TLR9 homodimers or TLR2/6 heterodimers; the receptor-adaptor interface i.e. TLR-MyD88 and the adaptor-adaptor interface which could be homotypic (i.e. MyD88-MyD88) or heterotypic (i.e. Mal-MyD88 in case of TLR4 signaling). A scaffold of TIR domains brings death domains (DDs) of MyD88 in close proximity which initiates the cooperative assembly of the Myddosome by further recruitment of DD-containing proteins.

1.3.1 The TIR domain structure and dimerization interface

The cytoplasmic domains of TLRs, the IL-1 receptor (IL-1R) and the carboxy-terminal domains of TLR-adaptor proteins (see 1.3.2) share a high grade of homology and are therefore termed as Toll/IL-1R (TIR) domains. These domains are roughly 200 residues in length. Different TIR domains both from receptors and adaptor proteins have been crystalized and structurally solved[39,40]. In common these domains consist of a core of four to five parallel β-strands (see Figure 1.1, sheets βA - βD) which are surrounded by five α-helices (αA - αD). The alternating α-helices and β-strands along the backbone indicate a common α/β protein fold whereby secondary structures are connected by loops that are very crucial for signaling as stated for the so-called BB loop which is connecting sheet βB with the helix αA[5]. In contrast to DDs, isolated TIR domains do not form stable complexes in vitro due to their only moderate interactions[13,18] and up to date no crystal structure was published from a TIR homo- or heterodimer. This together with very flexible unstructured loops, playing an important role in binding processes, makes it difficult to draw a clear image of TIR-TIR interaction-interfaces. However, structural modeling and mutagenesis studies have revealed some information. In example, work from Bruce Beutler et al. demonstrated that the exchange of a conserved

proline residue in the BB loop of the murine TLR4 TIR abolished responsiveness against LPS. In another study the MyD88 pathway was targeted by BB loop peptidomimetic and eradicated the IL-1β response of the IL-1R[41].

In general, the sequence conservation among TIR domains is only about 20-30% and most of the conserved residues are buried in the core of the protein domain[15]. This may indicate that there are substantial alterations among the structure, especially on the TIR surfaces including loops, which would influence specificity towards binding partners and the signaling process as a whole.

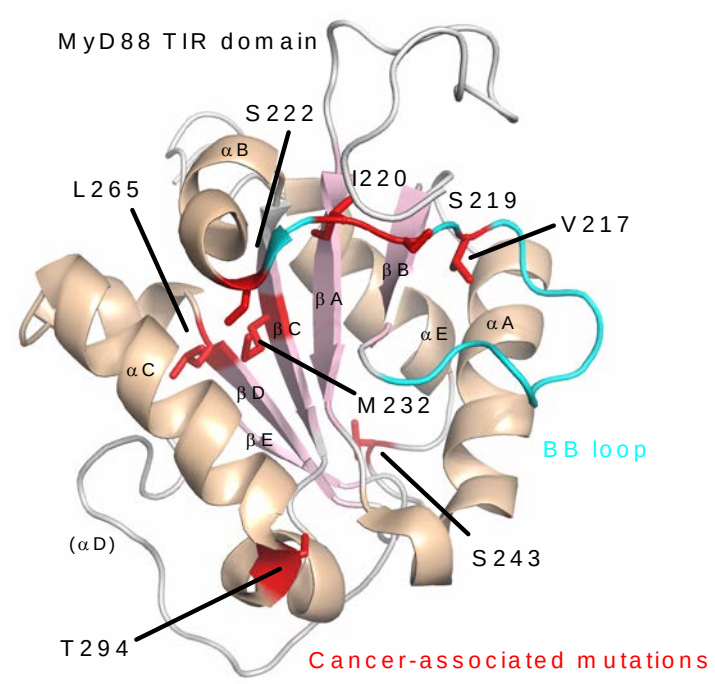

Figure 1.1: Structure of a human MyD88 TIR monomer with lymphoma-associated mutations.
Figure adapted from Avblej, Wolz et al.[42], structure from Protein Data Bank accession number 2JS7. Five α helices (αA - αD) shown in beige are surrounding a core of five β sheets (βA - βD) colored in pink. The BB loop important for TIR dimerization is shown in cyan. For lymphoma-associated mutations highlighted in red please refer to section 1.4.2.

1.3.2 TIR domain-containing TLR adaptor proteins transmit signals

Five different intracellular adaptor proteins for TLRs are described which all have in common a Toll/interleukin-1 receptor (TIR) homology domain[15,18]. Via heterotypic TIR-TIR interactions they are recruited to the cytosolic parts of activated receptors or as bridging adaptors they employ further TIR-domain-containing proteins to form a scaffold to transduce signaling. Often multiple adaptor proteins are used by one TLR-species and they are additionally targeted by a complex regulation process to fine-tune innate immune reactions.

1.3.2.1 MyD88-dependent signaling pathways

MyD88 (abbreviation for myeloid differentiation primary response protein 88) is the key adaptor for TLRs and central in inflammatory responses. The protein consist of 296 amino acid residues with an N-terminal death domain (DD, amino acids 1-110) and a C-terminal TIR domain (residues 155-296), which are connected by an intermediate linker domain (residues 110-155). Except TLR3 which utilizes exclusively TRIF (TIR-domain-containing adapter-inducing interferon-β) all TLRs require MyD88 as an intracellular adapter. In case of TLR4 MyD88 is not directly coupled to activated receptors but it is linked indirectly via the bridging adaptor Mal (MYD88 adaptor-like), which is also termed TIRAP. In resting cells MyD88 is dispersed throughout the cytosol[43]. It has been proposed that without stimulus MyD88 resides in an autoinhibitory conformation by intramolecular interactions between its own TIR and DD. Pathway stimulation would disturb auto-inhibition by assembling MyD88 into the post-receptor complex via its TIR domain[13].

In contrast to the MyD88 DD or TIR domain where a lot of functional studies proofed their importance, little is known about the linker connecting them, the so-called intermediate domain. In vitro studies and structural analysis of Myddosome complexes lack this domain but it was shown to be crucial for signal transduction in vivo. Expression of an alternatively spliced form of MyD88 lacking the intermediate domain (MyD88s for “short” MyD88) shuts down IL-1- and LPS-induced NF-κB activation due to a lost interaction with IRAK4. Consequently, IRAK1 is not activated by phosphorylation proofing MyD88s as a negative regulator of TLR/IL-1R triggered signals[44]. Furthermore a peptide designed from the intermediate domain inhibited TLR4, -5, -2, -9 and IL1R signaling, but not TLR3 which uses the TRIF adapter protein to induce IFN-β. It was surmised that those intermediate domain peptides were targeting IRAK4, confirming that the intermediate domain mediated interaction with IRAKs and therefore contributes to Myddosome formation[45]. Another interesting aspect of the intermediate domain is that it was shown to take part in the binding of the B cell specific transmembrane activator TACI[46]. Most B cells switch their immunoglobulin isotypes in a $CD4^+$ T cell-dependent fashion, whereby CD40L on T cells physically interacts with CD40 receptors on B cells. This leads to differentiation of follicular B cells to immunoglobulin-secreting plasma cells and to memory B cells providing long-term protection. But the T cell-dependent pathway takes 5-7 days, a period which may last too long to efficiently defend fast-replicating pathogens. For extrafollicular B cells a more rapid mechanism is known to overcome these limitations. Therefore, cells of the innate immune system release the factors BAFF and APRIL in response to various MAMP-signals. BAFF and APRIL in turn engage the receptor TACI which triggers class-

switch recombination in a MyD88-dependent way leading to the fast secretion of IgG and IgA immunoglobulins.

It was shown that MyD88 also participates in the activation of several transcription factors of the interferon regulatory factors, like IRF1, IRF5 and IRF7. In case of IRF7 for example, MyD88 acts downstream of TLRs 7-9 in plasmacytoid dendritic cells (pDCs) which leads to the expression of IFNα in response against viral infections. Activated TLRs 7, 8, 9 recruit a complex consisting of MyD88, IRAK1, IRAK4 and TRAF6, whereby IRF7 gets phosphorylated by IRAK1 and activated to initiate transcription[15,21]. Since many of these interactions have been studied in overexpression systems, the composition of these signaling complexes in primary cells remains elusive and the influence of cell type and which TLR is activated have not been studied systematically.

1.3.2.2 Mal-dependent signaling pathways

The bridging adaptor protein Mal (abbreviation for MYD88 adaptor-like protein, also known as TIRAP) is used by TLR4 and to a lesser extent by TLR2 whereby it recruits MyD88 to the post receptor complex[13,47]. Mal is highly regulated which provides an extra control circuit for TLR4 signaling in response to LPS. Regulation mechanisms include phosphorylation by IRAK1 and IRAK4 which leads to Mal ubiquitination and degradation[48]. Furthermore BTK (Bruton's tyrosine kinase) was reported to phosphorylate the Mal TIR domain which in turn leads to recruitment of SOCS1 (suppressor of cytokine signaling 1) by the SH (Src homology) 2 domain and results in Mal polyubiquitination and subsequent degradation[49,50]. It was also shown that Mal is cleaved by caspase-1, the enzyme that processes the precursors of the proinflammatory cytokines IL-1β and IL-18. During this process a fragment of Mal is released which inhibits Mal in its own function[51].

Mal is localized at the cytosolic surface of the cell membrane. At the amino-terminus before the TIR domain there is a basic sequence motif binding to the head group of phosphatidylinositol 4,5-bisphosphate (PtdIns(4,5)P_2, also known simply as PIP_2) a phospholipid manly integrated into the cytosol-facing site of the plasma membrane.

There are two single nucleotide polymorphisms (SNPs) described for the Mal TIR domain which are related to high susceptibility against infectious disease[52,53]. It is believed that the substitutions D96N and S180L interfere with the predicted binding interface of MyD88. Especially residue D96 attracts MyD88 residue R196 electrostatically. Interestingly, homozygous carriers of the MyD88 variant R196C are malfunctioning in MyD88 pathways causing susceptibility to pyogenic infections[54] which proposes an important role of Mal-MyD88 associations. On the other hand D96N mutation does not lead to abrogated MyD88-Mal interactions but fails to in-

duce Myd88 redistribution to the plasma membrane[55], which is supposed to be the main function of Mal in cellular signaling[38].

1.3.2.3 TRIF-dependent signaling pathways

TRIF (TIR-domain-containing adapter-inducing interferon-β) is much bigger with 712 amino acids and more complex in its structure. An important structural determinant of function is the additional amino-terminal domain (TRIF-NTD) composed of α-helices. As a negative regulator TRIF-NTD binds to the TIR domain and prevents the access of downstream effector proteins like TRAF3, TRAF6 and TBK1 in non-stimulated cells[56]. TRIF-NTD is released when TRIF binds to activated TLR3 or TLR4-TRAM complexes via heterotypic TIR interactions. In resting cells TRIF is dispersed throughout the cytosol but stimulation of TLR3 and 4 leads to the assembly of higher-order molecular complexes including downstream effector proteins[43]. Precise stoichiometry and composition remain unclear but according to Myddosomes this TRIF-containing complexes are named ‘Triffosomes’. TRIF is exclusively used by TLR3 for signaling. TLR4 signals through both MyD88 and TRIF but in this process additionally the bridging adapter proteins Mal and TRAM are involved. Contrary to MyD88 and NF-κB activation, TRIF primary induces transcription factors of the IRF-family such as IRF3, which is essential for a potent antiviral defense by expression of i.e. IFN-β. In line with this, children with TRIF-deficiencies suffer under herpes simplex encephalitis, similar as reported for TLR3- and UNC93B-deficiencies, underlying the importance of TRIF-depend production of antiviral IFNs in the central nervous system[57].

1.3.2.4 TRAM-dependent signaling pathways

TRAM (TRIF-related adaptor molecule) is exclusively used by TLR4 and is needed to recruit TRIF. After TLR4 engagement the activated receptor complex is endocytosed which leads to the recruitment of cytosolic TRAM to the endosomal membrane[18]. The acidic pH in the endosomal compartment probably causes structural changes in the TLR4 dimer which would be a possible explanation why TRAM is only recruited to endosomal TLR4 and not to activated receptor residing in the plasma membrane[58]. TRAM is modified by addition of a myristoyl group to an amino-terminal glycine residue during translation, which directs the protein to the plasma membrane[59]. Phosphorylation of serine residues by PKCε (protein kinase C) within a basic motif of TRAM releases the protein from the plasma membrane. Similarly, to the role of Mal as a ‘bridging-adaptor’ for MyD88, TRAM is believed to recruit TRIF to the plasma membrane for efficient TLR4 signaling. This mechanism provides additional control on the pathway and is relevant for a solid TLR4 response by the activation of the TRIF[59,60].

1.3.2.5 SARM-dependent signaling pathways

Sterile alpha and TIR motif containing protein (SARM) is the fifth described TLR adaptor protein. It acts as a negative regulator of TRIF-dependent TLR3 signaling. SARM associated with TRIF and RNA interference-mediated knockdown of SARM enhanced TLR3-/TRIF-dependent cytokine and chemokine production[61].

1.3.3 Death domain assembly completes Myddosome formation

In general, death domain family members play an important role in apoptotic (i.e. FADD, FAS associated death domain) and inflammatory pathways (i.e. IRAKs) by formation of oligomeric molecular scaffolds. By topology, DDs are conserved small globular domains which consist of anti-parallel α-helices. They self-associate by three types of DD-DD binding interfaces in distinct regions of the domain's surface, allowing a variety of different complexes[62].

During TLR and IL-1R signal transduction MyD88 DDs assemble with DDs of IRAK family members into Myddosomes. It is not really clear how this very ordered process of sequential assembly is determined since homotypic interactions (f. e. between MyD88 DDs) are structurally comparable to heterotypic (f. e. between DDs of MyD88 and IRAK4) and DDs concede only minor conformational changes. Two studies revealed that in contrast to TIR domains, isolated DDs can form stable homo- and hetero-oligomers reflecting the backbone of Myddosomes. Plausibly these strong associations would stabilize the more instable TIR-complexes which consist of TLR receptors and adaptors. In the first study isolated DDs from MyD88 and IRAK4 formed into a closed hetero-complex with a variable stoichiometry of 6 to 8 units of MyD88 to 4 molecules of IRAK4 DDs[37]. In a more recent study by Lin et al. the structure of a very ordered ternary complex of DDs which consisted of 6 MyD88 DDs forming a ring of 3 layers, followed by 4 IRAK4 DDs and 4 IRAK2 DDs that are arranged in a left-handed helix with 3.7 subunits per turn[63]. The second study revealed a different stoichiometry in the complex indicating that Myddosome composition might be redundant and may be a target of a complex regulation.

In humans two rare germline variants described located in the MyD88 DD: SNPs S34Y and R98C exhibited reduced homo-oligomerization of MyD88 DD and interaction with IRAK4 which lead to a severely reduced NF-κB induction[64]. This study highlights the importance of DDs in the assembly of the Myddosome post receptor complex.

1.3.4 The Myddosome activates kinases of the IRAK-family

Members of the family of IL-1R-associated kinases (IRAKs) are classified by sharing some structural similarities. Amino-terminally they consist of DDs, followed by a so-called proST domain. In the center there is a conserved kinase domain located, followed by the so-called C-terminal domain, except in case of IRAK4. During active signaling by TLRs or IL-1R, MyD88 assembles with members of the IRAK family by forming a hetero-complex of DDs as a kind of signaling tower. It is assumed that the formation of these Myddosomes brings the IRAK kinase domains into close proximity for mutual self- or cross-phosphorylation and activation[63]. The proST motif is rich in serine, threonine and proline and thought to undergo auto- and hyper-phosphorylation events to fully activate the protein and target it for degradation. After incorporation in Myddosomes and activation, IRAK1 and IRAK4 are consequently degraded by Lys48-linked ubiquitination. Lastly, the C-terminal domain was reported to be important for the recruitment of TRAF6 which is necessary for further signal transduction. Therefore, all IRAKs except IRAK4 were shown to have TRAF6 interaction motifs.

1.3.4.1 IRAK kinases are partially redundant in their functionality

For vertebrates there are four different IRAK homologues described: IRAK1, IRAK2, IRAK3 (alternatively known as IRAKM) and IRAK4 (reviewed in Flannery et al.[10]). IRAK1, IRAK2 and IRAK4 kinase activity is critical for mediating TLR signaling, while IRAK3 was reported to act predominantly as a negative regulator of TLR signaling. It is thought that MyD88 first engages IRAK4[65] which also seems to be the most critical kinase for signal transduction as severe disturbances of TLR-mediated pathways indicate in IRAK4-deficient patients[66,67]. Interaction of MyD88 and IRAK4 further promotes the recruitment of IRAK1 or IRAK2. In juxtaposition IRAK4 phosphorylates IRAK1 or alternatively IRAK2, which in turn become active to transduce the signal. Single mouse knock-outs of IRAK1 or IRAK2 suggest a redundancy between both kinases, since only partial deficiencies in TLR-signaling were observed[68,69]. On the other hand this redundancy is not completely since it was reported that IRAK1 acts more in fast and early induction of NF-κB while IRAK2 seems to be important for later and sustained TLR responses[68,70].

1.3.4.2 IRAKs share a unique kinase domain

Crystal structures of the IRAK4 kinase domain are available and served to model kinase domains of the other family members[71,72]. The structures revealed an exclusive conserved tyrosine gatekeeper residue that controls access to the ATP binding pocket. The gatekeeper makes the IRAK family unique among other ki-

nases and represents an attractive target for the development of small molecule inhibitors[73,74].

1.3.4.3 Regulation of IRAKs as an additional control to shape TLR responses

Composition of IRAKs in the Myddosome complex may differ in different cell types and deliver a further level of regulation of a stimulus and its prospective answer. Or in addition, it might simply depend on the abundancy of components involved. For example, IRAKs are regulated by small non-coding miRNAs (microRNAs) which repress their expression by targeting the 3'-UTR of respective mRNAs. An example is the mir146a miRNA which regulates expression of IRAK1 and IRAK2[75].

1.4 Myddosome pathways in human disease

Intact TLR/IL-1R signaling is crucial for protective immune responses but on the other hand deficient or uncontrolled transductions could potentially cause severe human pathologies and serious diseases. It has become apparent that abnormalities in the former described signaling pathways lead to severe immunodeficiencies or likewise, cause immunopathologies if insufficiently controlled and overactivated. In the following it is discussed how deregulation at the level of the Myddosome post receptor complex contributes to malignancies.

1.4.1 Deficiencies in MyD88 and IRAK4 cause severe pyogenic infections

There are several common polymorphisms in variable genes encoding for TLR-pathway proteins described, which are associated with both infectious and autoimmune disease. In the following two disorders are described which result in a complete deficiency in certain pathways (see review about TLR pathway SNPs and disease associations[76]). First, children with a very rare form of autosomal recessive MyD88 deficiency were described to suffer from life-threatening and recurrent pyogenic bacterial infections such as invasive pneumococcal disease. The clinical status of those patients improved with age indicating that MyD88-dependent host defense against pyogenic bacteria is redundant with the function of the adaptive immune system[54]. Second, a case report of a 14-year old boy with healthy parents underwent a long history of severe infections with pyogenic bacteria together with abrogated MyD88-dependent cytokine responses[77]. Analysis of the *IRAK4* gene revealed compound heterozygosity for two SNPs (different mutations of maternal and paternal allele) with one mutation (R12C) and a loss of function frameshift allele (splice site mutation in intron 7 which leads to skipping of exon 7 in the kinase domain). Despite expression of non-truncated protein there was a functional deficiency of IRAK4 which resulted in a lack of IRAK1 phosphorylation

after stimulation with TLR agonists in a flow cytometry analysis. Another recent report showed that IRAK4 R12C interferes in the heterodimerization of IRAK4 with MyD88 DDs and confirms that the SNP variant fails to assemble Myddosomes and therefore to activate NF-κB[78].

1.4.2 MyD88 is frequently mutated in many B cell cancers

Germline *MYD88* loss-of-function mutations were previously discussed playing a role in infectious disease but on the other hand recently somatic *MYD88* gain-of-function mutations were discovered in B cell cancer entities. In some types of B cell Non-Hodgkin lymphoma, such as diffuse large B cell lymphoma (DLBCL), Waldenström's macroglobulinemia (abbreviated WM, also known as lymphoplasmacytic lymphoma or LPL) and chronic lymphocytic leukemia (CLL), somatic mutations of MyD88 were found[79-81] (see Table 1.2). Most of these somatic MyD88 mutations affected highly conserved residues in the core of the TIR domain, neighboring to the functionally important BB loop, box3 or to the surface of the domain (see Table 1.3 and Figure 1.1). In the majority of the mentioned cancers, a point mutation (c.794T>C) in the *MYD88* gene was found that results in the residue substitution L265P (source catalogue of somatic mutations in cancer, COSMIC). In nearly all cases reported so far the L265P mutation appeared to be heterozygous with one parental WT copy of MyD88 still present. From 382 lymphoma biopsy samples only six were homozygous for the mutation and one ABC-DLBCL derived cell line, OCI-LY3[80]. In a cohort of 67 patients with WM, MyD88 L265P mutation was acquired in 79% of patients and in 2 of them (3%) it appeared to be homozygous for the mutation[82]. Homozygous status could potentially be explained by uniparental disomy (UPD) at the *MYD88* locus of chromosome 3. UPD could happen due malfunctioning mitotic machinery and describes a mechanism when a cell receives two copies of a locus or even whole chromosomes from only one parent and no copies from the other parent. In the previously described case UPD is therefore suggested to be a potentiating mechanism of gene deregulation by duplication of the MyD88 L265P driver mutation.

Table 1.2: Somatic MyD88 mutation frequency in different B cell Non-Hodgkin lymphomas. Table adapted from Avbelj, Wolz et al.[42]. MGUS: monoclonal gammopathy of undetermined significance

B cell malignancy	Frequency of MyD88 mutations	Reference
Diffuse large B cell lymphoma (DLBCL)	6.5-8.2% (29% ABC subtype)	80,83,84
Mucosa-associated lymphoid tissue lymphoma (MALT)	7-9%	80,85
Chronic lymphocytic leukemia (CLL)	2.9-4%	86,87
Waldenström's Macroglobulinemia (WM)	90% (54% MGUS)	88-90
Primary cutaneous large B cell lymphoma (PCLBCL), leg type	61%	91
Primary central nervous B cell lymphoma (PCNBL)	71%	92
Ocular adnexal extranodal marginal zone lymphoma (OAEMZL)	6.7%	93
Splenic marginal zone lymphoma (SMZL)	4-5%	85,94

Table 1.3: Somatic MyD88 mutations, location in the TIR domain and chemical properties. Table adapted from Avbelj, Wolz et al.[42]. Listed are frequent oncogenic mutations discussed in this study. Compare to Figure 1.1 to trace mutations in the globular structure of the MyD88 TIR domain.

Amino acid mutation	Position in secondary structure element	% burial	Expected consequence of amino acid change
M232T	β-sheet	100	nonpolar to polar
L265P	β-sheet	100	nonpolar to nonpolar
V217F	BB loop	95,7	nonpolar to nonpolar
S219C	BB loop	85,5	polar to nonpolar
I220T	BB loop	97,8	nonpolar to polar
S222R	Surface	23,2	polar to charged
S243N	Surface	76,7	polar to polar
T294P	box 3	80	polar to nonpolar

1.4.3 MyD88 L265P mediates hypersignaling by constitutive activation of kinases

Somatic MyD88 L265P, along with other mutations, was firstly discovered in the hematological malignancies DLBCL and CLL. Especially an aggressive subtype of DLBCL called the activated B cell type of DLBCL (ABC-DLBCL) generally relies on constitutive NF-κB activation[95] and interestingly accumulation of MyD88 mutations was much more frequent in this subtype (frequency of MyD88 L265P in total DLBCL ~8% and in ABC-DLBCL 29%, compare to Table 1.2). It was shown that MyD88 L265P strongly associated with IRAK1 in primary CLL cells[81] and that bound IRAK1 was hyperphosphorylated in DLBCL cell lines[80]. Meanwhile during compilation of this thesis, two other kinases TAK1 and BTK were identified to mediate MyD88 L265P hypersignaling. TAK1 is redundant for both NF-κB and MAPK-pathway induction (discussed under 1.2.1 and 1.2.1.2) and was shown to be an essential mediator of MyD88 L265P-driven signaling because it is activated by heightened MyD88/IRAK/TRAF6 oligomerization to Myddosomes[96]. Furthermore, co-IP studies in WM cells identified MyD88 L265P complexed with Bruton's tyrosine kinase (BTK) with preferential binding of MyD88 to phosphorylated BTK[97]. The mutant MyD88-mediated activation of BTK resulted in enhancement of NF-κB activation in an IRAK-independent way. In conclusion, MyD88 L265P interferes in activating critical kinases of TLR (IRAKs, TAK1, BTK) and B cell receptor (BCR, BTK) pathways which are important for B cell proliferation, differentiation and survival[12] and uncover L265P as gain-of-function mutation.

1.4.4 MyD88 L265P mediates malignant cell persistence by hyperactivation of transcription factors interfering in cellular survival

Somatic MyD88 mutants are dominant positive on signaling and cause constitutive activation of the transcription factor NF-κB which was determined by many studies[80,81,95-97]. TLR-mediated NF-κB induction plays an important role in B cell development and differentiation[12]. For example, NF-κB triggers the expression of B lymphocyte-induced maturation protein-1 (Blimp-1), a transcriptional repressor crucial for memory B cell and plasma cell maturation[98] which maintains B cell survival by directly suppressing apoptosis signal-regulating kinase 1 (ASK1)[99]. NF-κB also regulates expression of apoptosis regulator proteins of the BCL-2 family[100]. An example is BCL2A1 which was shown to be upregulated in ABC-DLBCL and therefore mediates resistance to apoptosis[95]. During our investigations Wang et al published that ectopically expressed MyD88 L265P in a mouse B cell setting cooperates with dysregulated BCL2 to sustain cell proliferation. In addition to MyD88 mutations, DLBCL cancers often exhibit translocations of the *BCL-2* gene leading to overexpression of BCL2. Because BCL2 inhibits B cell apoptosis induced by

Bim, Bax and Bak proteins, these translocations sustain malignant B cell survival[101]. Taken together NF-κB hyperactivation in MyD88-mutated lymphomas attenuates apoptosis of cancer cells and transduces pro-survival signals.

The effects of the MyD88 L265P mutation also included elevated signaling of JAK-STAT3 pathways[80,81] and augmented production of many cytokines such as IL-6, IL-10 and IFN-β that are integral to disease pathogenesis by contributing to a favorable microenvironmental niche for tumor cells to survive and proliferate[102].

1.4.5 The Somatic MyD88 L265P mutation is a driver of B cell tumorigenesis

MyD88 mutations are strong drivers of B cell tumorigenesis and malignant cells depend on deregulated pathways initiated by respective mutations to survive. Due to this shRNAs directly targeting *MYD88*, or kinases downstream of MyD88 like *IRAK1* in DLBCL or WM cells, provoked killing of MyD88-mutated cells whereas cells expressing non-mutated MyD88 survived[80,97].

Other studies further highlight the crucial role of MyD88 mutations in hematopoetic B cell tumors and unraveled them as an early event of tumorigenesis. Monoclonal gammopathy of undetermined significance (MGUS) is a symptomless condition where high titers of monoclonal IgM are diagnosed in the blood. MGUS patients are regularly clinically monitored since there is a probability of progression to lymphoproliferative disorders, such as Waldenström's macroglobulinemia, in case malignant plasma cells infiltrate the bone marrow. The frequency of MyD88 L265P mutations is about 54% in MGUS and patients carrying the mutant allele had an increased risk of progression to WM (~90% with L265P incidence[103]) than patients with MyD88 WT. These findings indicate the potency of the L265P mutation as a driver and define MyD88 mutations as an independent predictor of progression of MGUS to WM[88,103,104]. Principally cancer has the ability to evolve and adapt. This leads to the co-existence of manifold, genetically heterogenous subpopulations within a cancer entity. To study intratumoral heterogeneity, whole-exome sequencing and gene copy number analysis of 149 CLL cases was performed and identified *MYD88* mutations (only together with trisomy 12 and del(13q)) as predominantly clonal[87,105]. Although *MYD88*-mutations are not so frequent in CLL (~6% in the appropriate study), clonal outgrowth of MyD88-mutant cells uncovers the L265P mutation as a strong driver which exerts positive effects on selection in a Darwinian fashion. However, effects of MyD88 L265P on the outgrowth are strengthened by accumulation of later appearing, more frequent driver mutations, as i.e. mutations in *SF3B1* and *TP53*. Therefore presence of increasing numbers of subclonal driver mutations is an independent risk factor for rapid disease progression[87].

1.4.6 Activation of endosomal TLRs may trigger Myd88 L265P-mediated effects

It is known that MyD88 mutations constitutively associate with downstream kinases like IRAK1 which consequently leads to pathway activation. We planned to if an external trigger upstream of MyD88 (i.e. by TLRs) is necessary to fully administrate mutational driver forces. By now, a recent study by Wang et al.[101] addressed this question the first time. MyD88 mutants were introduced in murine B cells by retroviral gene transfer and found that the L265P mutation alone was sufficient to drive limited rounds of B cell proliferation both in vitro and in vivo, independently from external mitogen stimuli. However proliferation of transduced cells was dependent on nucleic acid sensing TLRs which signal from the endosomal compartment. Consequently, L265P-transduced mouse cells but deficient for *TLR9* (CpG sensing) or with the *Unc93b1*^{3d} mutation (chaperone for TLR3, 7, 8, 9; mutation leads to incomplete processing of TLRs, see 1.2.5.1) were inhibited in their proliferation.

1.4.6.1 MyD88 L265P influences disease outcome

CLLs with MyD88 L265P are almost all found in the *IGHV*-mutated subgroup[81]. Patients with mutations in the TLR/MyD88 pathway were diagnosed at much younger age (median 43 years, range 38–63, versus median 63 years, range 27–94; $p<0.001$) and had a generally better overall survival (OS) outcome (10-year OS: 100% vs. 62%; $p=0.002$)[81,106]. Remarkably those patients with MyD88 L265P mutation, which was the most frequent mutation in the young subgroup, had a lower expression of CD38 and ZAP-70 which could be a possible explanation for the more favorable outcome: CD38 is important for physical interaction and differentiation of B cells and signals in a ZAP-70-dependent fashion by augmenting BCR pathways. For example, interaction of CD38 with its natural ligand CD31 rescues cells from apoptosis[107].

In case of WM some characteristics differed between patients with MyD88 WT and expressing mutant MyD88 L265P[82]. There was a predominance for the male gender to gather the L265P mutation ($p=0.004$) whereas patients with WT had a higher risk for splenomegaly ($p=0.015$). Nevertheless no difference in terms of survival was observed for the Myd88 mutational status.

MyD88 mutation status and histological expression was retrospectively investigated in a Korean cohort of 124 DLBCL patients[108]. The incidence of MYD88 L265P mutation in Korea was found to be lower than previously reported and mutation status was not associated with changed clinicopathological parameters. But interestingly, high MyD88 expression in the cytosol of DLBCL cells negatively correlated with survival of patients whereupon this was independent if MyD88 was mutat-

ed or not. Another study analyzing clinically relevant impact of *MYD88* mutations in DLBCL is contradictory to the previous report[109]. Off note, patients with L265P mutation had significantly inferior OS and progression free survival (PFS) compared with patients with WT *MYD88* (p=0.001), independently if they were treated with Rituximap and CHOP/CHOP-like regimens. The study also revealed that the L265P mutation is more frequently found in DLBCL in male (p=0.019) as it was reported for WM. In summary, it was shown for the first time that at least in case of DLBCL, MyD88 L265P is an independent prognostic factor which is associated with poor prognosis.

1.5 Aims of this study

MyD88 mutations and especially the L265P mutation were shown to be crucial drivers for frequent B cell malignancies that are associated with considerable mortality and morbidity. A basic understanding of Myddosome processes at the molecular levels is central for the development of new therapies that specifically target malignant innate signaling in human disease. Additionally, since most functional studies have been conducted in mice, many aspects of Myddosome function in human cells remain unclear, precluding a safe and specific exploitation of the MyD88-axis. Therefore this study addresses following tasks:

Therefore it remains to be ascertained how MyD88 mutations influence the structural and molecular properties of the Myddosome underlying hyperactivation of NF-κB in human B cell Non-Hodgkin lymphomas. A very important aim is to target malignant mechanism and validate if this might be an elementary opportunity to develop therapies against lymphomas.

2 Materials and Methods

2.1 Molecular biology methods

2.1.1 Polymerase chain reaction (PCR)

PCR based methods were used for cloning i.e. to generate Gateway®-compatible entry clones (2.1.11). PCR reactions were performed using a standard protocol (Table 2.1) with oligonucleotides purchased from biomers.net GmbH and enzymes and buffers from Thermo Scientific. DNA was amplified in a peqSTAR 2X Gradient Thermocycler supplied by Peqlab (Table 2.2).

Table 2.1: Standard PCR reaction used to generate inserts for Gateway entry clones.
Reactions were pipetted on ice. Oligonucleotides were diluted in sterile DNase free water.

Components	Volume	Final concentration
Sterile DNase free water	64 µl	
5x Phusion HF Buffer	20 µl	1x
10 mM dNTP mixture	2 µl	0.2 mM each
Primer forward/reverse (10 µM)	5 µl each	0.5 µM each
Template plasmids 20 ng/µl	1 µl	20 ng/100 µl
Phusion Hot Start II DNA Polymerase (2 U/µl)	1 µl	2 U
Final volume	100 µl	

Table 2.2: Thermocycler protocol of standard PCR reactions.
Steps 2.-4. were repeated in 35 cycles.

Step	°C	Duration
Heat lid	110	
1. Initial denaturation	98	30 s
2. Denature	98	10 s
3. Anneal	64	30 s
4. Extend	72	30 s
5. Final extension	72	10 min
Hold	4	∞

2.1.2 Plasmid DNA isolation from transformed bacterial cultures

Plasmids were propagated in *Escherichia coli*. Transformed Bacteria were grown in an overnight culture in 2-4 ml (for mini-prep) or in 100-200 ml (for midi-prep) LB media supplied with appropriate antibiotics. Cultures were harvested by centrifugation and plasmid DNA was isolated from bacterial pellets according to the manufacturer's instructions (Promega kits PureYield™ Plasmid Miniprep or Midiprep System). After alkaline lysis of cells[110] DNA binds under high concentrations of salt to a silica gel membrane. After washing with a buffer containing ethanol the plasmid DNA was eluted in 20-50 µl (mini-prep) of or 500-800 µl (midi-prep) sterile water. The obtained isolated plasmid DNA concentration was between 150-1000 ng/µl.

2.1.3 Purification of PCR-amplified DNA

Purified and concentrated DNA from PCR reactions enables a higher efficiency of Gateway BP reaction during cloning (2.1.11). Therefore amplified DNA sourcing from PCR reactions was purified from Enzymes and buffer salts according to instructions of the Qiagen QIAquick Gel Extraction Kit.

2.1.4 Restriction digest of DNA

In order to test cloned plasmids, restriction digest of DNA was done by using reagents supported by Life Technologies according to the manufacturer's instructions. Gateway® constructs in particular were tested by using the *att*-site specific nuclease BsrGI in combination with TANGO buffer. Digested DNA was separated by molecular size and analyzed by agarose gel electrophoresis (section 2.1.5).

2.1.5 Analysis of DNA by agarose gel electrophoresis

DNA fragments were separated by molecular size by running 1% w/v agarose (Roth)/sodium borate buffer[111] gels containing 0.5 µg/ml ethidium bromide or SERVA DNA Stain according to the manufacturer's instructions. DNA samples were diluted with 10x DNA loading dye (NEB). The 2-Log DNA Ladder (NEB) standard was used as a molecular size marker and samples run in sodium borate buffer (for recipe refer to appendix) in horizontal agarose gel chambers supplied by Peqlab at 100 V for 1 h. Separated DNA fragment bands were visualized and recorded by UV light exposure with the Peqlab Fusion SL system and analysis was performed with the system's Fusion software.

2.1.6 Determining DNA concentrations

DNA concentrations were quantified by UV spectroscopy with the NanoDrop 1000 Spectrophotometer by Peqlab Biotechnologie GmbH, Erlangen.

2.1.7 DNA sequencing and computer based analysis

Sequencing reactions of plasmid DNA were done by the service provider GATC Biotech in accordance to the website's protocol using standard primers offered by the company. DNA sequences were analyzed with Geneious software (version 5.56). Gene and protein sequences were retrieved from the NCBI (http://www.ncbi.nlm.nih.gov/gene/) and Ensembl (http://www.ensembl.org/) databases.

2.1.8 Transformation of *Escherichia coli* with Plasmid DNA

Competent *E. coli* DH5α cells were prepared using a standard protocol. In principle, treatment with $CaCl_2$ prepares the bacterial plasma membrane to become permeable to plasmid DNA. Plasmid DNA (50-200 ng) was added to 50 µl of chemical competent DH5α cells and the mixture was incubated on ice for 30 min. After heat shock (42 °C for 45 s) and following incubation on ice for 2-5 min, 200 µl of preheated (42 °C) S.O.C. media (recipe in appendix) was added. Cells were shaken 1 h at 37 °C to recover and express antibiotic resistance before plating on LB agar supplemented with appropriate antibiotics for selection. Culture plates were incubated at 37 °C overnight and colonies were cultured and analyzed the next day.

2.1.9 Culturing of plasmid-transformed bacterial cells

E. coli cultures were grown under standard conditions at 37 °C in LB-media[112] (recipe in appendix). For selection appropriate antibiotics were added (final concentrations: ampicillin 100 µg/ml, kanamycin 50 µg/ml, spectinomycin 100 µg/ml, gentamycin 15 µg/ml)

2.1.10 Cryo-preservation of transformed bacteria cells

Bacterial glycerol stocks were used to culture plasmid transformed strains by circumventing plasmid transformation. Plasmid-transformed *E. coli* were cultivated in LB media supplemented with adequate antibiotics overnight. 500 µl of the bacterial suspension were mixed with 150 µl of 100% sterile glycerol. Afterwards the bacterial glycerol stocks were frozen and stored at -80 °C.

2.1.11 Cloning strategies for plasmid constructs

2.1.11.1 Cloning of different MyD88 expression plasmids

In order to clone different MyD88 expression constructs, sequences were amplified first by PCR (2.1.1) from the template plasmids pEX127 (MyD88 WT) and pHW142 (L265P). The primers were designed the way that PCR-amplified *MYD88* was flanked by *attB* sites, contained a KOZAK consensus sequence to initiate translation (only for N-terminal protein fusion tags), contained the start codon ATG to initiate translation (only open constructs for C-terminal tags), contained a stop codon (only for N-terminal protein fusion tags) or that the stop codon was deleted (only open constructs for C-terminal tags). MyD88 full length (amino acids 13-296) closed constructs (resulting in entry clones pOW011 and pOW012) were amplified with the primer pair AWx275/AWx277 (or AWx340/AWx277 for the desired untagged entry clones pOW035 and pOW036), TIR (amino acids 155-196) closed constructs (resulting in pOW013 and pOW014) with primers AWx276/AWx277, and TIR open constructs (resulting in pOW005 and pOW006) with primers AWx273/AWx274. Detailed information about sequences of primers and description of plasmid constructs is listed in the appendix. *attB*-sites-flanked PCR products were purified (Qiagen Gel Extraction kit, see 2.1.2) and cloned into pEX234 (pDONR207) Gateway entry clone by BP reaction (BP Clonase II Enzyme mix from Life Technologies). Resulting entry clones were analyzed by restriction digest and sequencing (see 2.1.4 and 2.1.7) and afterwards used to generate expression clones with desired fusion tags by LR reaction (description see 2.1.12).

2.1.11.2 Cloning of TLR9 cytoplasmic domain

A plasmid construct encoding for TLR9 (Q9NR96) cytoplasmic domain was ordered from GENEWIZ. Therefore truncated TLR9 (amino acids 840-1032) was synthesized as a closed construct (with stop codon) with flanking *attL* sites and cloned into pUC57 resulting in plasmid pEX467. Afterwards TLR9 expression clone pOW143 for LUMIER protein interaction studies was generated by LR reaction (2.1.12).

2.1.12 Gateway® recombination cloning to generate expression plasmids

The Gateway® recombination cloning technology by Life Technologies enables the systematic shuffling of genes of interest (GOI) between various plasmid vectors by making use of specific *att*-recombination sites. The GOIs were purchased as Gateway-compatible entry clones (alternatively named donor vector) or cloned into an entry clone (in this study pDONR207-derived pEX234 used) where the insert is flanked by *attL* sites. Cloning of gene Gateway expression vectors (alterna-

tively named destination vectors) was performed by using the Gateway LR Clonase II Enzyme mix (Life Technologies) according to the manufacturer's instructions, whereby the GOI inserted in the entry clone (flanked by *attL* sites) is shuttled into a destination vector (containing *attR* sites followed by sequences encoding for desired protein fusion tags). 1-4 µl of the reactions were transformed to DH5α *E. coli* and colonies grown in the presence of selective antibiotics were isolated and further cultured. In order to confirm that GOIs were inserted into proper destination vector and are expressed as correct proteins, plasmids were digested with the *att*-site-specific restriction enzyme BsrGI (Life Technologies, see 2.1.4) and transfected into HEK293-derived cells (2.3.2). Protein lysates were analyzed by immunoblot (see 2.2.2) for expression of the respective proteins. All donor- and destination vectors used during this study are listed in the appendix.

2.1.13 Quantitative real-time PCR

Quantitative PCR was used to asses *MYD88* mRNA expression in different B cell lymphoma cell lines. The mRNA was isolated using the RNeasy Mini Kit (Qiagen) and transcribed into cDNA (High Capacity RNA-to-cDNA Kit from Life Technologies). The relative expression of *MYD88* mRNA was studied using TaqMan Gene Expression Assays (Hs01573837_g1, Life Technologies). Data were normalized to *TBP* housekeeper expression (Hs00427621_m1, Life Technologies). The samples were analyzed on a real time cycler (Applied Biosystems; 7500 fast).

2.2 Biochemical methods

2.2.1 Determination of protein concentration

Protein concentrations of cell lysates were colorimetrical determined according to manufacturer's instructions of the Pierce BCA Protein Assay Kit. Bovine serum albumin (BSA) diluted in concentrations from 0.125 mg/ml to 2 mg/ml served as a standard. 15 µl of protein lysates were mixed with 200 µl of working reagent (solutions A and B from kit mixed in a 50:1 ratio) in 96 well flat bottom microplate format and incubated at 37 °C for 30 min. Protein concentrations were determined in duplicates at a wavelength of 562 nm in a 96 well microplate reader (Fluostar Optima from BMG Labtech).

2.2.2 SDS-PAGE and immunoblot for protein separation and detection

Lysate samples were diluted with Invitrogen's NuPAGE 4x LDS loading dye supplemented with 10x Sample Reducing Agent and boiled for 5 min. Proteins were separated by molecular weight by sodium dodecyl sulfate polyacrylamide gel elec-

trophoresis (SDS-PAGE). According to the expected molecular size of proteins to study polyacrylamide concentrations of the gels ranged from 8% to 12%. Gels incubated in SDS running buffer (see appendix) at 150 V in the Invitrogen Xcell Surelock Mini Cell chamber system for 1.5 h. PageRuler™ Prestained Protein Ladder form Life Technologies was used as molecular size marker.

Thereafter proteins were transferred on nitrocellulose blotting membranes (0.45 µm pore size, GE Healthcare) by either wet blot (transfer at 30 V in Invitrogen Xcell Surelock Mini Cell chamber system for 1.5 h or at 12 V for 13 h) or semi-dry blot (Bio-Rad Trans-Blot® Turbo™ Transfer System, protocol “STANDARD SD”, transfer for 35 min) whereby NuPAGE Transfer Buffer (20x, Life Technologies) was used.

The nitrocellulose membrane with transferred protein was incubated in blocking buffer (TBS, 0.05% Tween® 20, 5% w/v BSA Fraction V from Biomol GmbH) at room temperature for 30 min. Primary as well as secondary antibodies were diluted in blocking buffer at indicated concentrations (see appendix) and membranes incubated at room temperature for 1-2 h. Afterwards membranes were washed (TBS containing 0.05 % Tween® 20) three times for 10 min. Alternatively immunoblots were automatically processed and incubated at 4 °C overnight (BlotCycler™ from Precision Biosystems, with blocking for 1.5 h, primary antibody incubation for 7 h, secondary antibody incubation for 4 h, three washing steps after each antibody incubation with each taking 15 min).

Secondary antibodies (see appendix) were horseradish peroxidase (HRP) conjugated and addition of luminal-based reagent (Pierce™ ECL Western Blotting Substrate from Life Technologies) results in a chemiluminescense signal which was captured on film (Amersham Hyperfilm ECL from GE Healthcare). Alternatively, ECL signal quantification was conducted on the Peqlab Fusion SL charge-coupled device (CCD) system with the AceGlow™ chemiluminescence substrate.

2.2.3 Analysis of MyD88 and IRAK1 aggregation by immunoblot

MyD88 and IRAK1 protein aggregation was analyzed in different B cell lymphoma lines by lysing $3x10^6$ cells (Promega passive lysis buffer supplemented with Roche Protease and Phosphatase inhibitors and Sigma Benzonase Nuclease). Insoluble high molecular weight aggregates were pelleted (16000xg, 4 °C, 10 min), washed with cold PBS and finally dissolved in Invitrogen 4x LDS sample buffer supplemented with 10x Reducing Agent by boiling (99 °C) and shaking at 1500 rpm for 20 min (Eppendorf® Thermomixer R Dry Block Heating and Cooling Shaker). Immunoblot analysis (2.2.2) was performed using antibodies against MyD88 and IRAK1 from Cell Signaling (anti-MyD88 D80F5, anti-IRAK1 D51G7) and against

tubulin from Sigma (dilutions of antibodies in appendix). ECL signal quantification was conducted on the Paqlab Fusion SL CCD system.

2.2.4 2D-PAGE of overexpressed MyD88 in I3A cells

Posttranslational modification of MyD88 was investigated by two-dimensional polyacrylamide gel electrophoresis (2D-PAGE). MyD88-deficient I3A cells were transfected with MyD88 WT and L265P encoding plasmids (pOW030 and pOW031, both with N-terminal Strep-HA protein fusion tag, see appendix) with the calcium phosphate method in 10 cm dish format and cultured for 48 h (transfection protocol see 2.3.2). Immunoprecipitated MyD88-enriched samples (protocol see 2.3.7) were resuspended in 13 µl lysis buffer (composition see appendix) and incubated while shaking at 400 rpm (Eppendorf® Thermomixer R Dry Block Heating and Cooling Shaker) at room temperature for 30 min. Afterwards 117 µl of rehydration buffer (see appendix) was added and the samples were vortexed and centrifuged at maximum speed to pellet agarose beads for 2 min. Subsequently 120 µl of the supernatant was evenly distributed on ceramic strip holders and covered with 7 cm Immobiline™ DryStrip (GE Healthcare) resulting in an immobilized non-linear gradient ranging from pH 3 to pH 10. The strips were covered with 600 µl oil (GE Healthcare Plus One Dry Strip cover fluid) and the whole ceramic holder was closed with a proper plastic lid and applied to the Ettan™ IPGphor™ system from GE Healthcare. Proteins migrated to the IPG agarose strips by incubating at 30 V overnight. Isoelectric focusing of the first dimension was performed by first maintaining 300 V for 1 h, than applying a gradient increase to 1000 V over 30 min, followed by another gradient increase to 5000 V over 1.5 h and lastly keeping voltage constant at 5000 V over 36 min. Afterwards IPG agarose strips were rinsed briefly with distilled water and prepared for the second dimension protein separation by equilibrating the strips first with 1x LDS buffer (Invitrogen) containing 1% DTT and afterwards with 1x LDS buffer supplemented with 2.5 % iodoacetamide with incubation each condition for 15 min. The IPG strips were mounted on NuPAGE® Novex® 4-12% Bis-Tris ZOOM® gels (Life Technologies) and separation by molecular size was performed in MES running buffer (Life Technologies) by applying 100 V for 5 min and then increasing to 200 V with incubation for 45 min. MyD88 protein species were analyzed by immunoblot (2.2.2) with the hemagglutinin-tag specific antibody C29F4 from Cell Signaling (Table 5.4 appendix).

2.3 Cell biology methods

2.3.1 Cell lines and cultivation

Human HEK293 cell line was obtained from Dr. Alexander Dalpke (Department of Medical Microbiology and Hygiene, University of Heidelberg, Germany). The HEK-derived cell lines I1A (IRAK1-deficient) and I3A (MyD88-deficient)[113] were a kind gift from George R. Stark (Department of Molecular Genetics, Lerner Research Institute, Cleveland, USA). All HEK-derived cells were cultured in Dulbecco's modified Eagle medium minimal (DMEM, Sigma Aldrich) supplemented with 10% heat-inactivated fetal calf serum (FCS), 1% penicillin/streptomycin and 1% glutamine (Invitrogen).

Different human-derived B cell lymphoma lines expressing either WT MyD88 (I83E95, RPMI-8226, Namalwa, OCI-LY19, BJAB and U2392) or one mutated allele of MYD88 (OCI-LY10, TMD8, HBL1 with L265P; HLY1 with S219C and SUDHL2 with S222R) or homozygously MyD88 L265P (OCI-LY3) were investigated for MyD88 and IRAK1 protein aggregation. OCI-LY19, OCI-LY3, TMD8, HBL1 and SUDHL2 DLBCL cells were kindly gifted from Dr. Manfred Kögl (Boehringer Ingelheim RCV, Vienna, Austria), HLY1 DLBCL cells from Dr. Irina Bonzheim (Pathology Department, University Hospital Tübingen), BJAB, U2392 and OCI-LY10 DLBLC cells from Dr. Stephan Hailfinger (Department of Biochemistry, University of Tübingen) and the CLL line I83E95 from Dr. Daniel Mertens (Department of Internal Medicine III, University of Ulm). B cell lymphoma cell lines were cultured in RPMI Medium 1640 (Life Technologies) supplemented with 20% heat-inactivated FCS, except lines OCI-LY19 (Minimum Essential Medium Alpha, 10% FCS, life technologies), OCI-LY10 (Iscove's Modified Dulbecco's Medium IMDM from Lonza, 20% heat-inactivated human serum from Biochrom AG) and I83E95 (IMDM supplemented with 20% FCS). All media were supplemented with 1% penicillin/streptomycin. All cell lines were cultivated at 37°C and 5% CO_2.

2.3.2 Transfection of HEK293-derived cells by the calcium phosphate precipitation method

HEK293, I3A and I1A cells were transiently transfected with the standard calcium phosphate method which was generally used for signaling and gene expression assays. Premade stocks (stored at -80°C) of 2 M $CaCl_2$ and 2x HBS (buffer composition see appendix) were applied for the transfection. Variable amounts of transfection reagents were required for respective plate formats (Table 2.3). Transfection mixtures were carefully pipetted to the wells in order not to destroy the layer of adherent cells. Transfection efficacy was controlled by fluorescence

microscopy of EGFP expressing cells and normally reached about 90% at the time of harvesting after 48 h.

Table 2.3: Calcium phosphate transfection shame for different plate formats and different experiments.

Format	24 well/pipet per well	10 cm dish
Assay	DLA, gene expression analysis by immunoblot	Co-IP, 2D-PAGE
Cells seeded per well in DMEM complete	$7.5x10^4$ in 500 µl media	$1.5x10^6$ in 10 ml media
µl of Gateway GOI expression plasmid containing GOI (100 ng/µl)	1 for immunoblot; various for DLA,	50
µl of EGFP plasmid (100 ng/µl)	1	10
µl of firefly luciferase reporter plasmids (varying concentrations, see 2.3.5)	1 for DLA; 0 for immunoblot	0
µl of Renilla luciferase expression plasmid (10 ng/µl)	1 for DLA; 0 for immunoblot	0
µl of 2 M $CaCl_2$	1.2	61
Adjust with sterile H_2O to a volume of µl	10	500
µl of 2x HBS	10	500
Total volume of transfection mixture µl	20	1000

2.3.3 Gene expression analysis of plasmid-transfected HEK cells by immunoblot

All destination vectors created with the Gateway system used in this study were analyzed for correct protein expression of respective cloned genes. HEK293 or I3A cells were plated in 24 well format and transfected with appropriate plasmids (100 ng, see list in appendix) by the calcium phosphate method (see 2.3.2). Cells were lysed 48 hours later in 60 µl RIPA lysis buffer supplemented with protease and phosphatase inhibitors (see appendix) for 15 min. Lysates were transferred to 1.5 ml tubes and spun at maximum speed to pellet cellular debris at 4 °C for 10 min. Afterwards the protein containing supernatants were transferred to new tubes and prepared for SDS-PAGE and immunoblot (see 2.2.2). Information about antibodies used to detect fusion tags of respective constructs (anti-HA, anti-Protein A, anti-Renilla, anti-MyD88 to detect untagged MyD88 constructs) are listed in the appendix.

2.3.4 siRNA-mediated knock-down of MyD88 protein in HEK293T

40 nM of Qiagen siRNA oligonucleotides (AllStars Negative Control siRNA 1027280, Hs_MYD88_10 SI02100902) were transfected (Lipofectamine® 2000, Life Technologies) in parallel with plasmids encoding for MyD88 TIR domain (amino acid sequence 155-294) WT or L265P (10, 50, or 100 ng of pOW028 or pOW029; pT-Rex-Dest30-based plasmids containing an N-terminal Strep-HA protein fusion tag) and reporters for NF-κB inducible firefly luciferase (100 ng) and constitutive Renilla luciferase (10 ng of pEX351) in 24-well format ($7.5x10^4$ HEK293T cells seeded in 500 µl of DMEM complete medium see 2.3.1). Before transfection the siRNA, plasmids and Lipofectamine were mixed in Opti-MEM® I Reduced Serum Media (Life Technologies) and incubated for 20 min. Cells were lysed 48 h after transfection (Promega passive lysis buffer) and either luciferase activity was measured by DLA (see 2.3.5) or the same lysates were analyzed by immunoblot (see 2.2.2; for detailed information about antibodies D80F5 and C29F4 from Cell Signaling Technologies against MyD88 and HA-tag please refer to appendix).

2.3.5 Dual luciferase reporter assay

Induction of signaling pathways culminating in the activation of the transcription factors NF-κB, STAT3 and Elk-1 was analyzed by the Dual-Luciferase® Reporter Assay System (Promega). Reporter plasmids contained the inducible Firefly luciferase gene whose expression is controlled by specific promotor binding consensus sequences of respective transcription factors. Transfections of cell lines HEK293T, I3A and I1A were conducted in 24 well plate format (calcium phosphate method, see 2.3.2) in triplicates with Gateway destination vectors encoding for GOIs in various concentrations and 100 ng per well of NF-κB- or 250 ng of STAT3-(pEX331) reporter or in case of Elk-reporter plasmid amounts were used according to the manual (PathDetect Elk1 *trans*-Reporting System, Agilent Technologies). In addition, cells were co-transfected with a control vector expressing constitutively Renilla luciferase (pRL-TK from Promega, see pEX351) which served as a transfection efficacy control. For STAT3 activation, cells were stimulated 24 h after transfection with IL-6 (100 ng/ml, from Biolegend) for another 24 h. Cells were harvested 48 h post transfection and lysed on ice in 60 µl Passive Lysis Buffer (Promega) and a subsequent freeze thaw cycle (incubation at -80 °C for 15 min) aided in improving disruption of the cells. Lysates were cleared from cell debris by centrifugation (2500xg, 4 °C for 10 min) and 10 µl of the supernatant was transferred to white 96 well plates (Nunc) for analysis in the Fluostar Optima device (BMG Labtech). 50 µl of each substrate (Promega kit) for respective luciferases were injected sequentially with firstly the Luciferase Assay Reagent II (LAR II) to

quantify firefly luminescence and secondly the Stop & Glo® Reagent which quenches the first reaction and simultaneously initiates the luminescence signal from the Renilla luciferase. Luminescence signals were captured individually for both luciferases every 0.5 s in a timeframe of 10 s and expressed as relative light units (RLU). Signals of Firefly reporter RLU were normalized to control reporter Renilla RLU. For detailed information about IFN-β reporter assay please refer to Avbelj, Wolz et al.[42].

2.3.6 Luminescence-based mammalian interactome mapping (LUMIER)

Protein interaction studies were done by a technique called LUMIER[114]. Gateway expression clones were generated with N- or C- terminal Renilla or Protein A tags, detailed information about plasmids transfected for LUMIER studies are listed in the appendix. Per well 10^4 HEK293T or IA3 cells were seeded in 100 µl media in 96 well format and transfected with 20 ng Protein A- and Renilla fusion plasmids each (Lipofectamine® 2000, Life Technologies). 48 h post transfection cells were lysed on ice in 10 µl per well lysis buffer (composition see appendix) for 15 min. The buffer contained additionally 10 % v/v of PBS-washed Dynabeads® M-280 Sheep Anti-Mouse IgG slurry (Life Technologies) to allow precipitation of the Protein A fusion proteins and co-precipitation of their respective Renilla-tagged interaction partners. Lysates were diluted with 100 µl PBS, 10% of the suspensions were retained to measure the raw Renilla luciferase activity in the sample (Fluostar Optima, BMG Labtech). The residual lysate suspension was washed with ice cold PBS on a magnetic plate washer (Hydro Flex plate washer from Tecan) whereby Protein A-tagged proteins and Renilla-tagged interactors were co-purified. The Renilla luciferase substrate coelenterazine (PJK GmbH) was diluted to a final concentration of 3 µM in Renilla assay buffer (recipe in appendix) and 70 µl of the substrate containing buffer was injected to each sample well and subsequent signals were measured every 0.5 s in a timeframe of 1.5 s. Each interaction analysis included control conditions, therefore the Renilla-tagged protein constructs were co-transfected with plasmids expressing only Protein A tag (plasmid pEX140). This aided in quantifying unspecific binding between Renilla-fusion proteins with the Protein A fusion tag of the respective binding partner. Bound Renilla luciferase activity was measured and an interaction signal was processed by dividing the activity of bound Renilla luciferase by the amount of raw Renilla activity for each transfection, and then subtracting the signal for the Protein A-only (no bait) control condition. In accordance to the literature[114] to rule out false positive events, an interaction was only defined as positive if activity of bound Renilla luciferase divided by raw Renilla activity was at least three fold higher than the respective Protein A-only control.

2.3.7 Protein immunoprecipitation (IP) from transfected I3A cells for consequent 2D-PAGE analysis

In order to enrich proteins for consequent 2D-PAGE analysis, imunoprecipitation (IP) assays were performed. I3A cells were transfected in 10 cm dish format (see 2.3.2) with 5 µg of Gateway expression plasmids encoding for N-terminal tagged Strep-HA MyD88 fusion protein (pOW030 for MyD88 WT, pOW031 for L265P). 48 h post transfection adherent cells were carefully washed with PBS and afterwards lysed at 4°C in 850 µl of RIPA buffer (see appendix) for 45 min. Lysates were spun (4 °C, 10000xg for 10 min) to remove cell debris and afterwards supernatants were transferred to new tubes. Protein concentrations were measured by BCA (2.2.1) and adjusted by dilution with adequate lysis buffer. 800 µl of lysate was applied for immunoprecipitations and incubated with respective antibodies at 4°C for 2 h. For IP 2.5 µg of monoclonal anti-HA antibody (Sigma-Aldrich H9658, clone HA-7) was used and subsequently 30 µl of lysis buffer-equilibrated Protein A/G coupled beads (Pierce™ Protein A/G UltraLink™ Resin) was applied for over-head mixing at 4 °C for another 2 h. The beads with immune-complexed proteins were pelleted by centrifugation (2500xg, 4 °C for 2 min) and washed three times with cold lysis buffer. Lastly proteins were further processed for 2D-PAGE (2.3.7).

2.3.8 CCK-8 viability assay of MyD88 inhibitor-treated B cell lines

For the Cell Counting Kit-8 (CCK-8) colorimetrical cell viability assay (Dojindo Molecular Technologies) cells were seeded in triplicates in 96 well format (5x 10^4 cells per condition in 100 µl of proper media, see 2.3.1). MyD88-inhibitor (Pepinh-MYD) or control peptides (Invivogen) were added to the media at indicated concentrations (30 µM, 40 µM, 50 µM and 80 µM) and cell viability was measured after 48 h. Cell suspensions were mixed with 10 µl of CCK-8 reagent and incubated for 2 h at 37°C. Absorbance was measured at 450 nm (Fluostar Optima, BMG Labtech). Viability was calculated by normalizing absorbance of inhibitor-treated cells to absorbance of control-peptide treated cells at respective concentrations.

2.4 Data analysis and statistics

Data were analyzed with Microsoft Excel 2010 and GraphPad Prism 6. For statistical analysis (done using GraphPad Prism 6) an unpaired t-test was used, if Gaussian distribution was fulfilled as assessed by the D'Agostino-Pearson, Shapiro-Wilk, and Kolmogorov-Smirnov tests. Otherwise, the Mann Whitney U t-test of unpaired samples was used to account for non-Gaussian distribution. Throughout, * indicates statistical significance at the 5% level, i.e. $p<0.05$.

3 Results

3.1 Oncogenic MyD88 mutants display increased signaling

Ngo[80] and Puente[81] et al. firstly described that oncogenic MyD88 mutations and in particular the most frequent L265P mutation, contribute to elevated NF-κB activation in different B cell Non-Hodgkin lymphomas. We re-evaluated the signaling potential of these frequent somatic lymphoma-associated MyD88 mutants in terms of NF-κB and other MyD88-dependent signaling pathways. Therefore luciferase reporter assays were conducted in the HEK293T cell line system as well as in the HEK293-derived MyD88-deficient I3A cell line or the IRAK1-deficient I1A cells[113].

3.1.1 Oncogenic MyD88 mutants hyperactivate NF-κB also when expressed as isolated TIR domains

We first overexpressed different MyD88 constructs at indicated concentrations in HEK293T to compare their activation potential for the NF-κB in luciferase reporter. Figure 3.1 A shows activation of the NF-κB transcription factor for plasmids expressing MyD88 full-length. In line with previous studies were oncogenic full-length MyD88 mutant GFP-fusion constructs were overexpressed in DLBCL lines[80] the L265P-version of the protein hyperactivated NF-κB in comparison to WT MyD88 in a concentration dependent manner.

Based on the fact that nearly all described somatic MyD88 mutations are located in the proteins' TIR domain (residues 155-294) we assumed that effects on signaling might emanate from altered conformations of this domain. However, to activate the NF-κB signaling pathway MyD88 recruits kinases of the IRAK-family through heterotypic DD interaction forming the so-called Myddosome complex[63]. In this context the TIR domain is not participating in binding DDs of IRAKs[115]. Expressing isolated MyD88 TIR domains has been suggested to block NF-κB pathway signaling[116]. Nevertheless, L265P-mutated MyD88 TIR overexpression induced constitutive NF-κB activation (Figure 3.1 B) when 100 ng of plasmid were transfected, whereas WT TIR domains revealed activation levels comparable to empty vector background control, i.e. was inactive as expected.

Higher NF-κB promotor activation for MyD88 full-length and TIR domain-only expression was also observed for other described lymphoma-associated MyD88-mutations (Figure 3.2 A, C) as it was shown by our partners from the laboratory of Roman Jerala, Ljubljana, Slovenia. MyD88 mutants located on the BB loop and

hydrophobic core of the TIR domain displayed the most elevated activation (i.e. M232T and L265P in the core, S219C on BB loop; more than a tenfold higher activation as WT). Remarkably, despite rather lower protein expression of mutants (note especially TIR L265P, lanes 4 of immonoblots) compared to WT (lanes 3), significantly higher NF-κB signaling was observed (Figure 3.2 B, D) compared to non-mutated MyD88. It was previously described by the Jerala lab[117] that similar as for the MyD88 TIR mutants shown here, fusion proteins of MyD88 WT TIR-dimers (tethered TIR domains) activate NF-κB when expressed at higher concentrations. Given the similar effect on activation proposes that TIR dimerization/oligomerization, may account for the consequent pathway induction by oncogenic mutants.

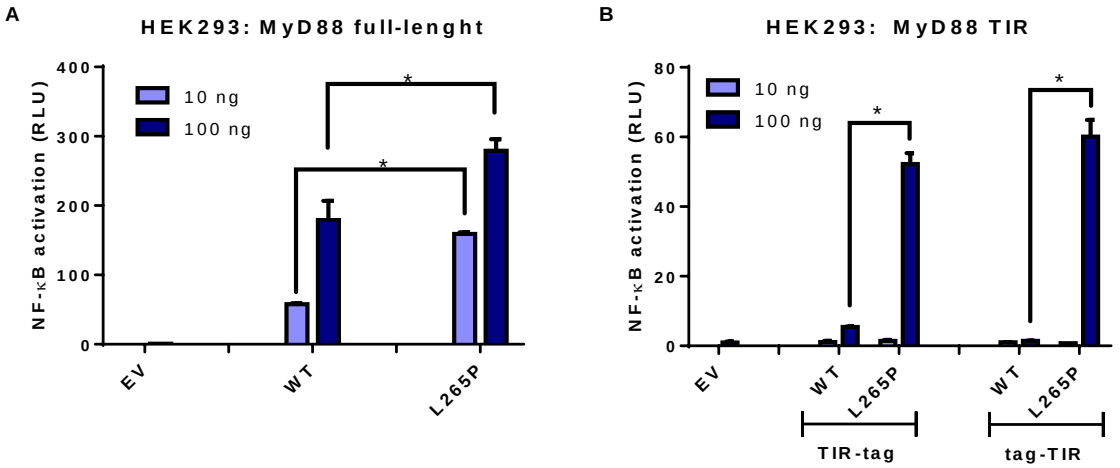

Figure 3.1: The oncogenic MyD88 mutation L265P and its isolated TIR domain hyperactivate the NF-κB transcription factor.

HEK293T cells were transfected with indicated amounts of plasmids coding for human MyD88 full-length (A) or TIR domain versions (B) containing either the WT or L265P sequence. Plasmids encoding for GFP (to monitor transfection efficiency, 100 ng), constitutive Renilla luciferase (10 ng) as well as NF-κB-inducible firefly luciferase (100 ng) were transfected in parallel. Luciferase activity was measured by Promega DLA 48 h after transfection. (A) Full-length constructs were expressed with N-terminal streptavidin-hemagglutinin (Strep-HA) fusion protein. (B) TIR-domain plasmids (MyD88 residues 155-294) were either expressed with a C-terminal (TIR-tag) or N-terminal (tag-TIR) Strep-HA fusion protein. Data represent the means + standard error of the mean (SEM) of 3 independent experiments (A) or means + standard deviation (SD) of technical triplicates from one representative out of 3 identical experiments (B). EV, empty vector. * $p < 0.05$.

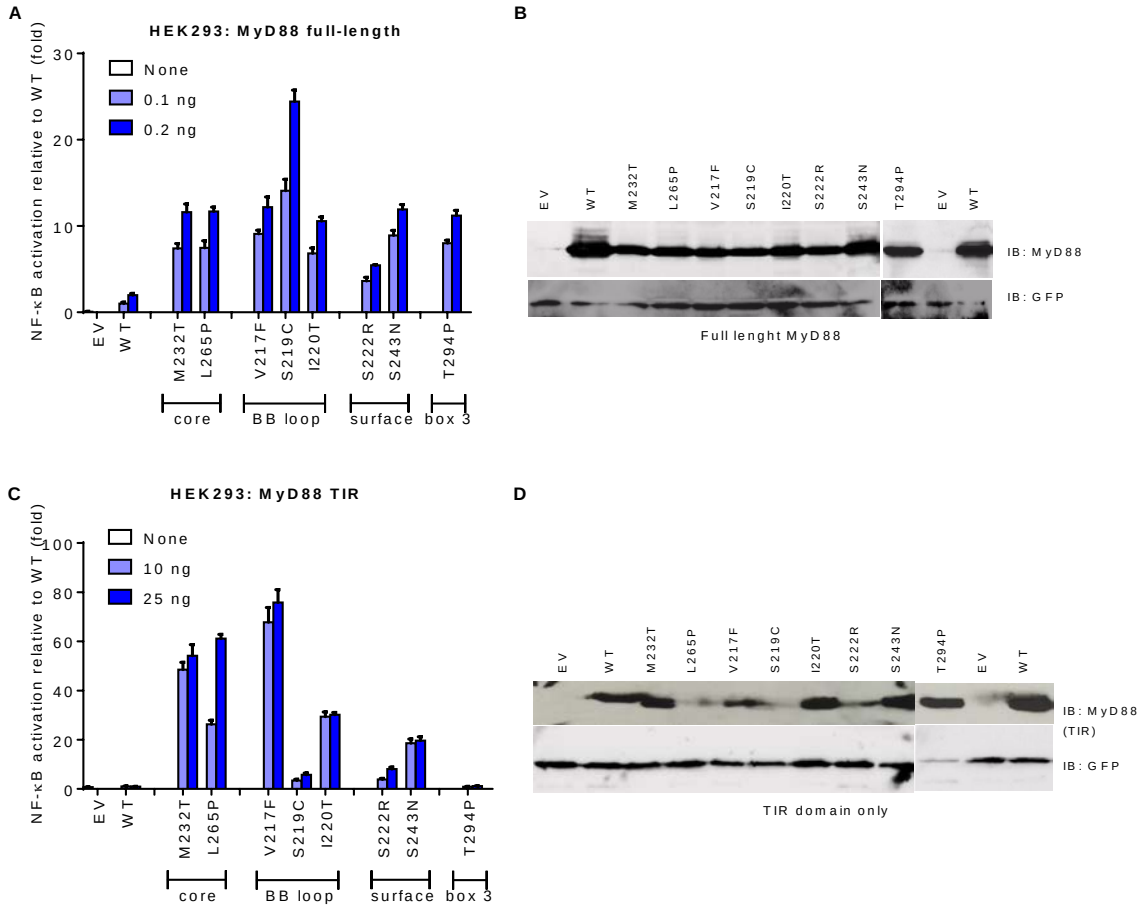

Figure 3.2: Frequent oncogenic MyD88 mutants constitutively activate the NF-κB transcription factor in both a full-length and TIR domain-only context.
Figure adapted from[42], experiments performed by Avbelj et al. (A-D) HEK293 cells were transfected with the indicated amounts of plasmids for full-length (A, B) or TIR-domain-only (C, D) constructs of MyD88 mutants, in parallel with NF-κB-inducible firefly luciferase and constitutive Renilla luciferase reporters. Cells were harvested 24 h later. Luciferase activity was measured by DLA (A, C) or separately transfected cell lysates analyzed by immunoblot. GFP served as transfection and loading control (B, D). For panels A and C data presented are means + SD of triplicate samples. Data illustrate fold change of NF-κB activity of mutant MyD88 in comparison to WT. In panels B and D the data shown are representatives of at least 3 independent experiments. EV, empty vector; IB, immunoblot.

3.1.2 The constitutive activity of oncogenic MyD88 mutants emanates from their TIR domain

For downstream signal propagation MyD88 recruits kinases of the IRAK family via heterotypic DD-interactions. The question to be answered here is how isolated TIR domains could entail constitutive signaling pathway activation when MyD88 DDs are absent and IRAKs could thus not be recruited. We speculated that overexpressed mutant MyD88 TIR domains might utilize MyD88 full-length WT which is endogenously expressed in HEK293T cells (see immunoblot Figure 3.5 B) for the previously described NF-κB induction. To prove this assumption we performed

NF-κB luciferase reporter assays in the HEK293-derived I3A cell line which is deficient for MyD88[113]. Indeed, the hyperactivation phenotype of full-length MyD88 L265P in comparison to WT was reduced (less than twofold for 1 ng of transfected plasmid) or abolished (10 ng and 100 ng transfections), see Figure 3.3 A. For L265P TIR domain-only constructs expressed in I3A (Figure 3.3 B) reporter activation was absent (1 ng and 10 ng transfection) or only less than twofold higher than empty vector control background (100 ng transfection), respectively.

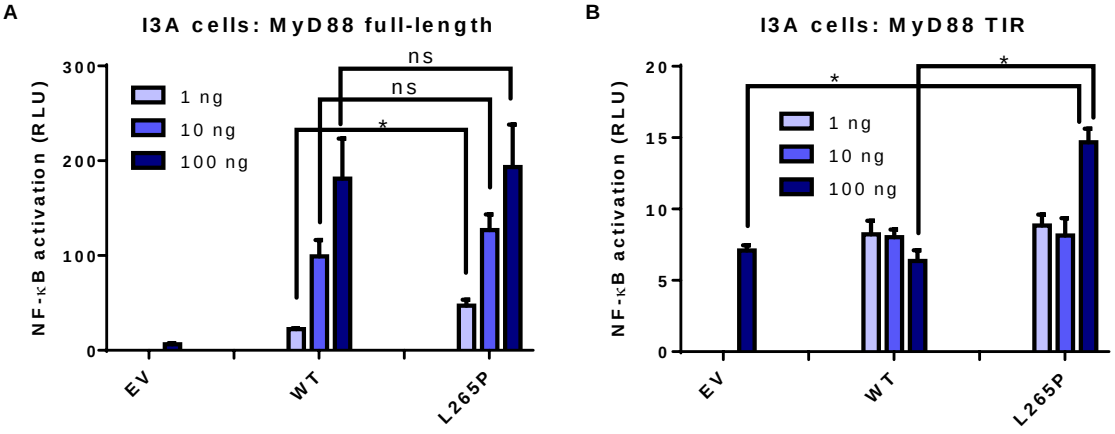

Figure 3.3: The hyperactive phenotype of the MyD88 L265P TIR construct is absent in cells lacking endogenous full-length MyD88.
HEK293-derived MyD88-deficient I3A cells were transfected with plasmids at indicated concentrations (1 ng, 10 ng and 100 ng) coding for N-terminal tagged (Strep-HA) human MyD88 full-length (A) or TIR domain versions (B) corresponding to either WT or the L265P mutation. DLAs performed as described for Figure 3.1. Mutant full-length constructs (A) or TIR domain-only constructs (B) do not show hyperactivation in comparison to WT. Data represent the means + SEM of 4 independent experiments (A) or a representative of technical triplicates from one experiment (B). EV, empty vector. * $p < 0.05$.

This finding was in good agreement with observations made by our Slovenian collaborators (compare to Figure 3.4) showing that both L265P as well as other oncogenic MyD88 mutations lose their capacity to hyperactivate NF-κB when expressed in MyD88-deficient I3A cells. For the Myd88 full-length constructs NF-κB induction was only about twofold higher for mutants and not tenfold as shown in HEK293, see Figure 3.2 A. For TIR-only expressed constructs none of them induced NF-κB (all at background level, see Figure 3.2 C). In summary our observations propose that oncogenic MyD88 TIR mutants may cooperate with endogenous WT MyD88, being expressed under natural circumstances in HEK293, for NF-κB hyperactivation.

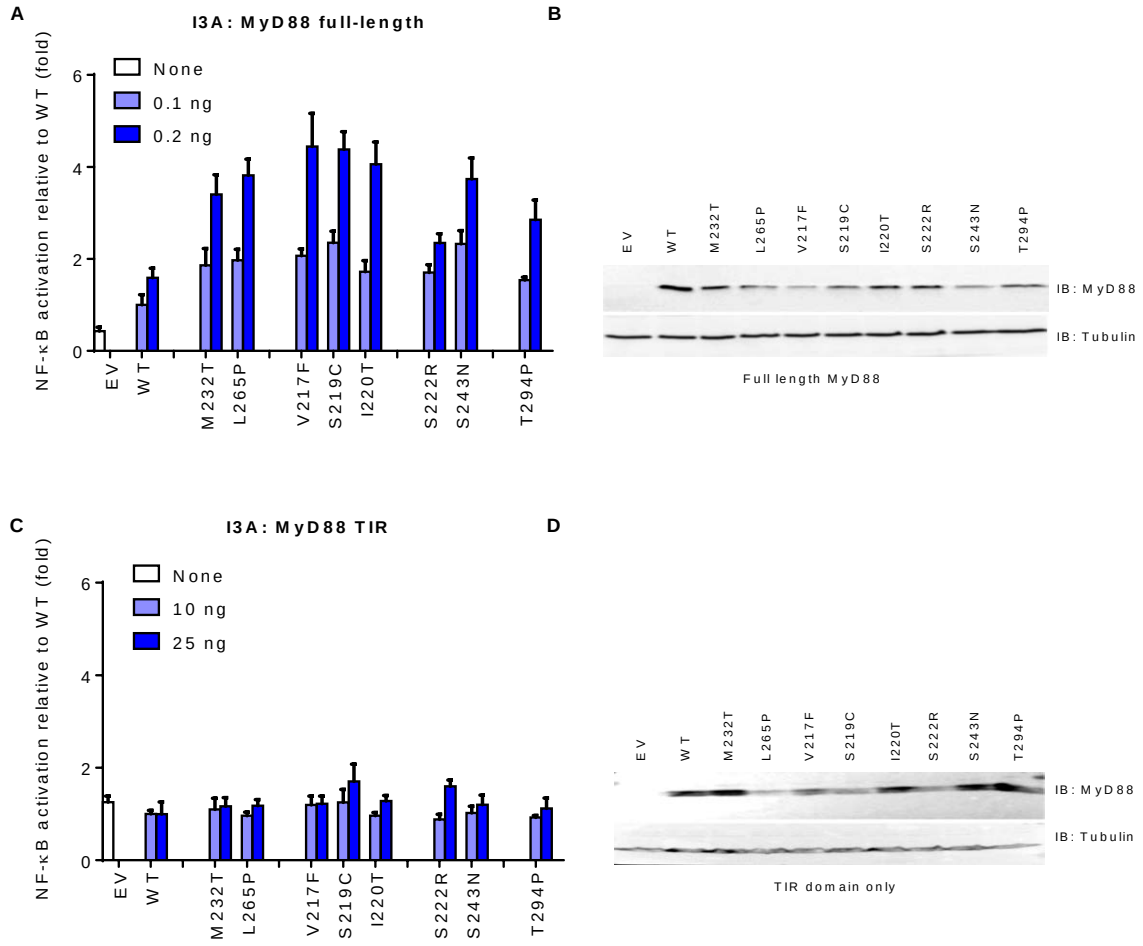

Figure 3.4: The hyperactive phenotype of various oncogenic MyD88 TIR mutants is absent in cells lacking endogenous full-length MyD88.
Figure adapted from[42], experiments performed by Avbelj et al. (A-D) MyD88-defient I3A cells were transfected with plasmids for full-length (A, B) or TIR-domain-only (C, D) constructs of MyD88 mutants, in parallel with NF-κB-inducible firefly luciferase and constitutive Renilla luciferase reporters. Cells were harvested 48 h later. Aliquots from the same lysate were used for DLA measurement (A, C) or analyzed by immunoblot. GFP served as transfection control for DLAs and for immunoblots Tubulin was used as loading control (B, D). For panels A and C, data presented are means + SD of triplicate samples, and for panels B and D, data shown are representative of at least 3 independent experiments. EV, empty vector; IB, immunoblot.

3.1.3 The constitutive activity of L265P-mutated TIR domains involves WT MyD88

Because of possible clonal influences it is difficult to compare NF-κB promotor activation between HEK293T and I3A cells side by side (see section 3.1.2). Therefore siRNA-mediated knockdown of endogenous WT MyD88 was performed in HEK293T cells in parallel with MyD88 TIR overexpression and consequent NF-κB DLA (Figure 3.5). TIR L265P mediated constitutive NF-κB activation (red bars, note hyperactivation despite much lower expression of mutant HA-MyD88 in immunoblot Figure 3.5 C) was effectively reduced by knockdown of endogenous WT MyD88 (checkered red bars; CCD immunoblot quantification Figure 3.5 C revealed protein reduction of about 40 %) suggesting that the hyperactive signaling phenotype of the L265P TIR mutant in HEK293T relies on endogenously expressed WT MyD88. Thus a reasonable conclusion is that mediated through constitutive TIR-oligomerization, oncogenic MyD88 mutants cooperate with WT MyD88 in hyperactivating NF-κB. Therefore, in an in vivo context in lymphoma cells, only one allelic copy of mutant MyD88 would be necessary and sufficient to trigger potent NF-κB activation. In fact, nearly all B cell tumor samples bare MyD88 mutations heterozygously with still one WT MyD88 allele being present ([79,80,82,118], see also section 1.4.2) which is in agreement with our findings.

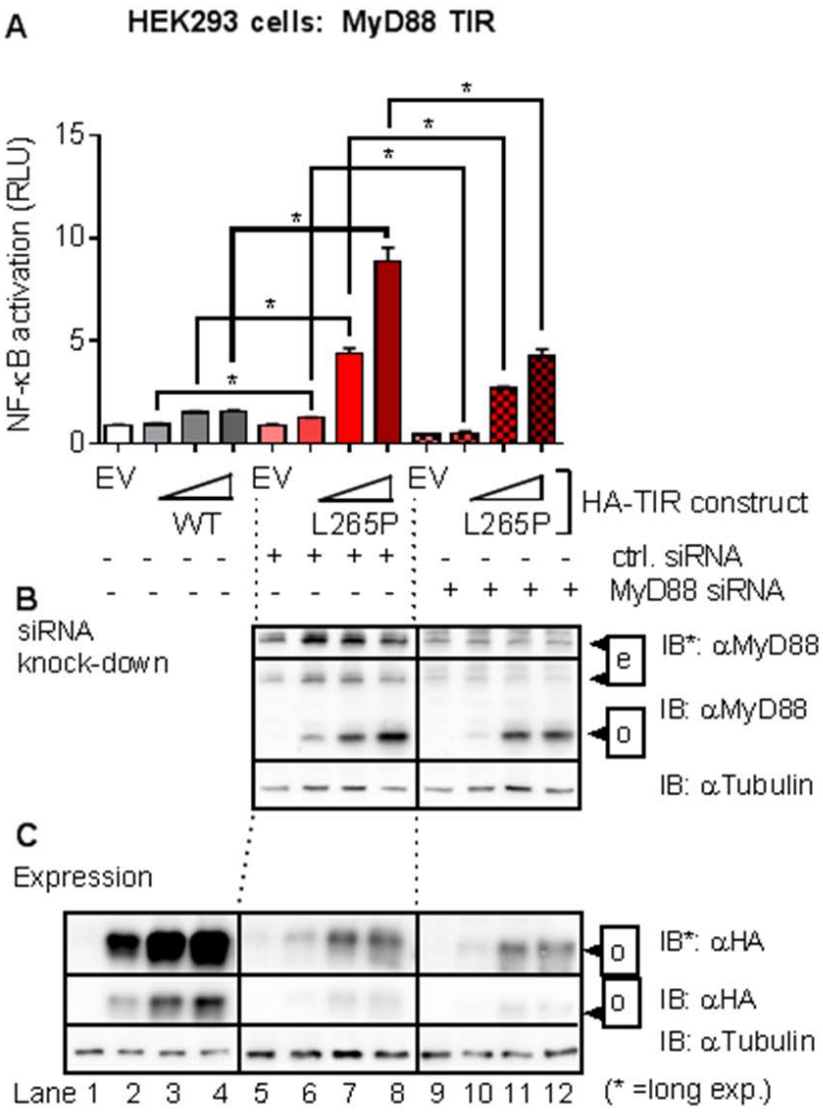

Figure 3.5: Hyperactivation of NF-κB by isolated MyD88 L265P TIR domains depends on endogenously expressed full length WT MyD88.

DLA and immunoblot analysis of HEK293T transfected with increasing amounts (0, 10, 50, or 100 ng) of plasmids for N-terminally Strep-HA-tagged MyD88 TIR domain-only constructs, in parallel with NF-κB inducible firefly luciferase, constitutive Renilla luciferase reporters and EGFP as transfection control. Where indicated, control (ctrl.) or a siRNA targeting the *MYD88* 3' UTR (i.e. only endogenous MyD88) were co-transfected. Cells were harvested 48 h later and either luciferase activity measured by DLA or the same lysates analyzed by immunoblot to verify siRNA knock-down of endogenous (e) full length MyD88 (B, one representative out of three identical experiments shown) or overexpressed (o) Strep-HA-tagged TIR domain-only constructs (C, same representative out of 3 identical experiments shown). MyD88 specific antibody (D80F5) detects both endogenous full length (e) and overexpressed Strep-HA-tagged MyD88 TIR domains (o), respectively. HA-specific antibody (C29F4) only detects overexpressed tagged TIR domains (o). Tubulin served as a loading control. (B-C) * denotes a longer exposure of the same membrane. Means + SDs are shown from triplicates from one representative experiment out of three similar experiments and differences tested using an unpaired t-test. * $p < 0.05$.

3.1.4 Constitutive NF-κB induction by oncogenic MyD88 L265P may only partially depend on IRAK1 signaling

RNA interference screening revealed that the kinases IRAK1 and IRAK4 are essential for MyD88-mutated ABC DLBCL cell survival. Based on co-immunoprecipitations MyD88 was found to be constitutively associated with IRAK1 in L265P mutated cells [80,81]. Therefore, the L265P mutant has been thought to promote cell survival by spontaneously assembling a protein complex containing IRAK1 and IRAK4, leading to IRAK4 kinase activity, IRAK1 phosphorylation and subsequent NF-κB signaling[80,81]. However mutated MyD88-mediated NF-κB hyperactivation might not exclusively depend on IRAK1 signaling. Despite IRAK1 deficiency of the HEK293-derived I1A cell line[113] the L265P mutant induced NF-κB stronger in comparison to non-mutated MyD88, at least at lower concentrations of transfected plasmids (10 ng and 50 ng, see Figure 3.6 A). Even more strikingly, L265P mutated TIR domain alone induced NF-κB in an IRAK1-deficient background (100 ng transfection, see Figure 3.6 B). Thus, IRAK1 appears redundant and might be compensated for by IRAK2 (compare to increased interaction of MyD88 L265P with IRAK2 in Figure 3.14 D).

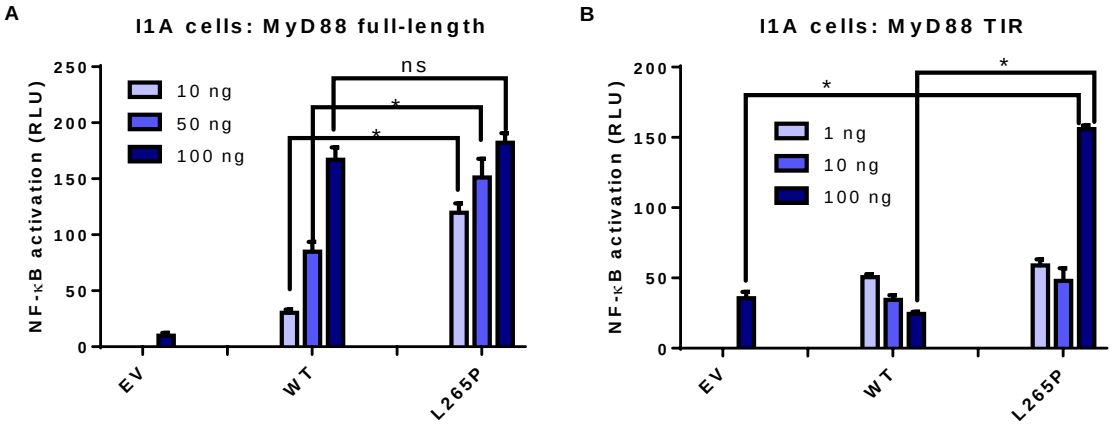

Figure 3.6: NF-κB hyperactivity by MyD88 L265P is only partially dependent on IRAK1.
HEK293-derived IRAK1-deficient I1A[113] cells were transfected with the indicated amounts of plasmids coding for human untagged MyD88 full-length (A) or N-terminal tagged (Strep-HA) TIR domain versions (B) corresponding to either WT or the oncogenic L265P mutation. DLAs performed as described for Figure 3.1. (A) Mutant full-length MyD88 conducts NF-κB hyperactivation in an IRAK1-deficient background. (B) L265P-mutated TIR-domains activate NF-κB in an IRAK1-deficient background. Data show the means + standard deviation (SD) of one representative from 3 similar experiments (A) or of technical triplicates from one experiment (B). EV: empty vector. * $p < 0.05$.

3.1.5 Oncogenic MyD88 mutations affect activation of transcription factors other than NF-κB

MyD88 plays a key role in inflammation but also in other crucial cellular processes like differentiation, proliferation and survival by regulating diverse transcriptional activators which involve diverse families of factors such as NF-κB, AP-1 and IRF (see introduction section 1.2.1). Ngo et al. found elevated amounts of the immune-modulatory cytokine IFN-β in culture supernatants of L265P-mutated DLBCL lines which were reduced by shRNA-mediated knockdown of MyD88[80]. They speculated in their report that elevated secretion of immune-modulatory cytokines such as IFN-β might positively impact tumor growth by influencing tumor-infiltrating immune cells and creating a suitable microenvironmental niche. The transcription of the type I interferon IFN-β is normally rapidly induced following infection by viruses or bacteria in an TRIF (and TLR3) or MyD88 (TLR7/8/9) dependent manner[16]. Thereby transcription factors of the IRF-family (interferon regulatory factors) control the expression of genes encoding for type I interferons such as IFN-β. Therefore we wondered if oncogenic MyD88 mutations have an effect on IRF-signaling. Of note, our partners from the group of Roman Jerala demonstrated that WT and mutant MyD88 activate IRF-dependent signaling, whereby mutated MyD88 induced a two- to threefold higher IRF-dependent IFN-β promotor activation (Figure 3.7 A).

NF-κB cooperates with MAPK pathways in the control of inflammatory responses by inducing the secretion of inflammatory cytokines. NF-κB and MAPK signaling is linked by the kinase TAK1 which simultaneously activates both pathways[16]. It was reported that heightened MyD88-L265P/IRAK/TRAF6 oligomerization activates TAK1[96]. Furthermore, Coste et al.[119] showed that MyD88 is required for MAPK activation and cell transformation in primary cancer tissues. Mechanistically, the MyD88 DD interacted with the activated key MAPK Erk, suggesting the relevance of this mechanism in human neoplasia. Among other transcription factors, Erk activates Elk-1 which is a member of the ETS oncogene family[120]. We therefore investigated the consequences of MyD88 overexpression on the canonical MAPK pathway by using an Elk-1 dependent reporter assay. We found that overexpression of MyD88 enhanced MAPK/Erk-dependent activation of Elk-1 (Figure 3.7 B) but there was no observable significant difference between WT and L265P MyD88.

DLBCL lines with oncogenic MyD88 mutations exhibited a strong JAK kinase activation of the transcription factor STAT3[80]. Moreover MyD88 was proposed to have an important role in STAT3 induction upon TLR9 stimulation and this was essential for naïve B cell differentiation to memory B cells and the secretion of Immunglobulins[121,122]. In this model MyD88 forms a trimeric complex together with the

GDP/GTP exchange factor DOCK8 and the kinase Pyk2, which mediates Src and Syk kinases to consequently induce STAT3. Indeed, by using a STAT3-dependent reporter assay (Figure 3.7 C), we observed that MyD88 overexpression activated STAT3. This was potentiated by IL-6-induced STAT3-activation but both WT and L265P displayed STAT3-induction to the same extent.

Taken together cancer-associated MyD88 mutants induced IFN-β promoter more strongly than non-mutated MyD88, but not the MAPK Elk1- or STAT3- reporters. Our obtained results by DLA in MyD88-overexpressed HEK293 cells allow only to draw limited conclusions and we can only speculate about the relevance in cancer. Therefore further studies in primary B lymphomas i.e. by ChIP-based methods or by expression analysis of transcription factor target genes should be conducted to verify aforementioned assumptions. Nevertheless our observations indicate that oncogenic MyD88 mutations could principally affect diverse downstream signaling pathways interfering with cell differentiation and survival.

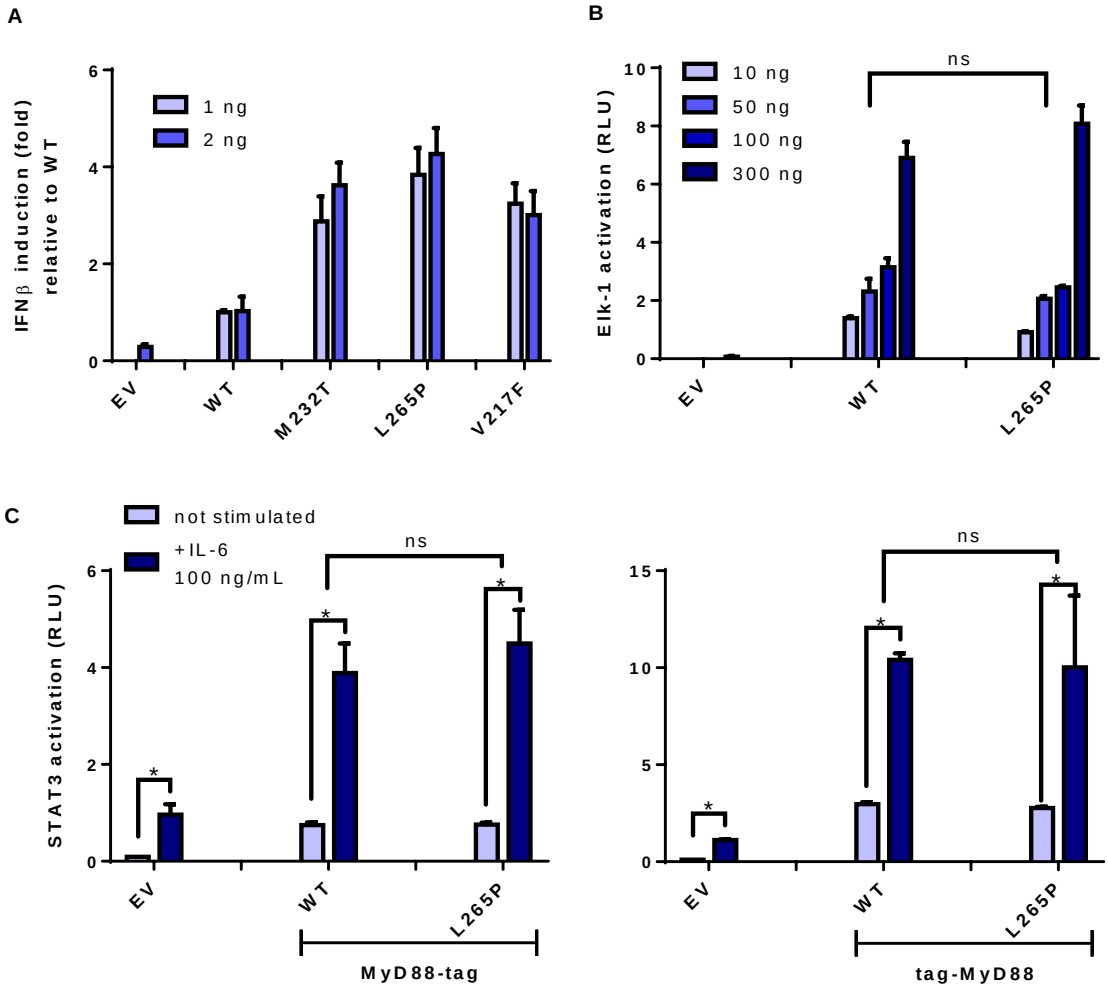

Figure 3.7: MyD88 L265P mediated induction of transcription factors other than NF-κB.
(A) WT and mutant MyD88 activate IRF-dependent signaling. Adapted from[42], experiments performed by Avbelj et al.: HEK293 cells were transfected with plasmids for WT or oncogenic MyD88 mutants together with IFN-β promotor-regulated firefly luciferase reporter, and constitutive Renilla reporter plasmids. 24 h after transfection cells were lysed and luciferase activity was measured. Data showed as mean + SD of triplicate samples and is representative of at least three independent experiments. (B) MyD88 L265P does not hyperactivate an Elk-1 transcription factor-dependent luciferase reporter. HEK293 cells were transfected with plasmids coding for MyD88 (N-terminal Strep-HA fusion protein) corresponding to either WT or L265P mutation. Plasmids from Agilent Technologies' "PathDetect Elk1 *trans*-Reporting System" were transfected in parallel. Luciferase activity was measured by Promega DLA 48 h after transfection. Data represent means + SD of technical triplicates from one experiment. Shown is one representative out of two independent repetitions. (C) MyD88 L265P does not hyperactivate a STAT3-dependent luciferase reporter. HEK293 cells were transfected with plasmids coding for MyD88 C- (MyD88-tag) or N-terminal (tag-MyD88) Strep-HA fusion protein corresponding to either WT or L265P mutation. Firefly luciferase reporter under control of STAT3 promotor together with constitutive Renilla reporter plasmids were transfected in parallel. 24 h after transfection cells were stimulated for another 24 h with IL-6 or left untreated. Luciferase activity was measured by Promega DLA 48 h after transfection. Data represent means + SD of technical triplicates from one experiment. Shown is one representative out of two independent repetitions. EV, empty vector. * $p < 0.05$.

3.2 The constitutive activity of oncogenic MyD88 mutants depends on TIR oligomerization

3.2.1 L265P-mutated TIR domains mediate a strong augmented MyD88 oligomerization

Expressing mutated MyD88 TIR constructs hyperactivated NF-κB in HEK293T cells (see section 3.1.1) but not in MyD88-deficient I3A (see 3.1.2). This suggested that mutated TIR domains employed full-length WT MyD88 by homotypic TIR interactions to form a scaffold for additional recruitment of IRAKs to initiate Myddosome signaling complex formation. To confirm this hypothesis at the level of protein interactions we used a technique called LUMIER (luminescence-based mammalian interactome mapping[114]), to quantify protein binding. In brief, protein interaction is measured by co-expressing two putative interacting candidates as Protein A- (bait) or Renilla luciferase- (prey) fusion proteins and subsequently determining the level of specific binding of the Renilla-fused partner upon Protein A purification.

For MyD88 full-length (Figure 3.8 A) and TIR (Figure 3.8 B) constructs, dimerization was increased for both heteromeric WT-L265P (or conversely L265P-WT) and the homomeric L265P-L265P combinations, compared to the WT-WT condition. Homomeric L265P-L265P interactions of TIRs were significantly weaker than heteromeric WT-L265P, but still more prominent than WT-WT. Interactions of full length versions in MyD88-deficient I3A cells showed comparable levels of binding (Figure 3.8 C). On the other hand TIR-TIR interactions were nearly tenfold lower in I3A compared to HEK293T cells (see binding values of Figure 3.8 D and A). Also in I3A, association between the homomeric L265P-L265P was on the same level as for the heteromeric WT-L265P combination. Furthermore interactions between MyD88 full-length and TIR domains were determined in HEK293T (Figure 3.8 E) and I3A (Figure 3.8 F). Augmented binding was measured for all combinations of L265P with other constructs in both cell lines and again this was slightly reduced for the homomeric L265P-L265P interaction in comparison to heteromeric WT-L265P. Taken together, our results suggest that strong L265P-mediated TIR interactions in HEK293T cells are promoted by endogenous WT MyD88, in line with our findings on NF-κB activation. This support the idea that L265P TIRs utilize endogenous WT MyD88 in HEK293T to activate NF-κB and thus the mutated TIR domain is responsible for hyperactivity.

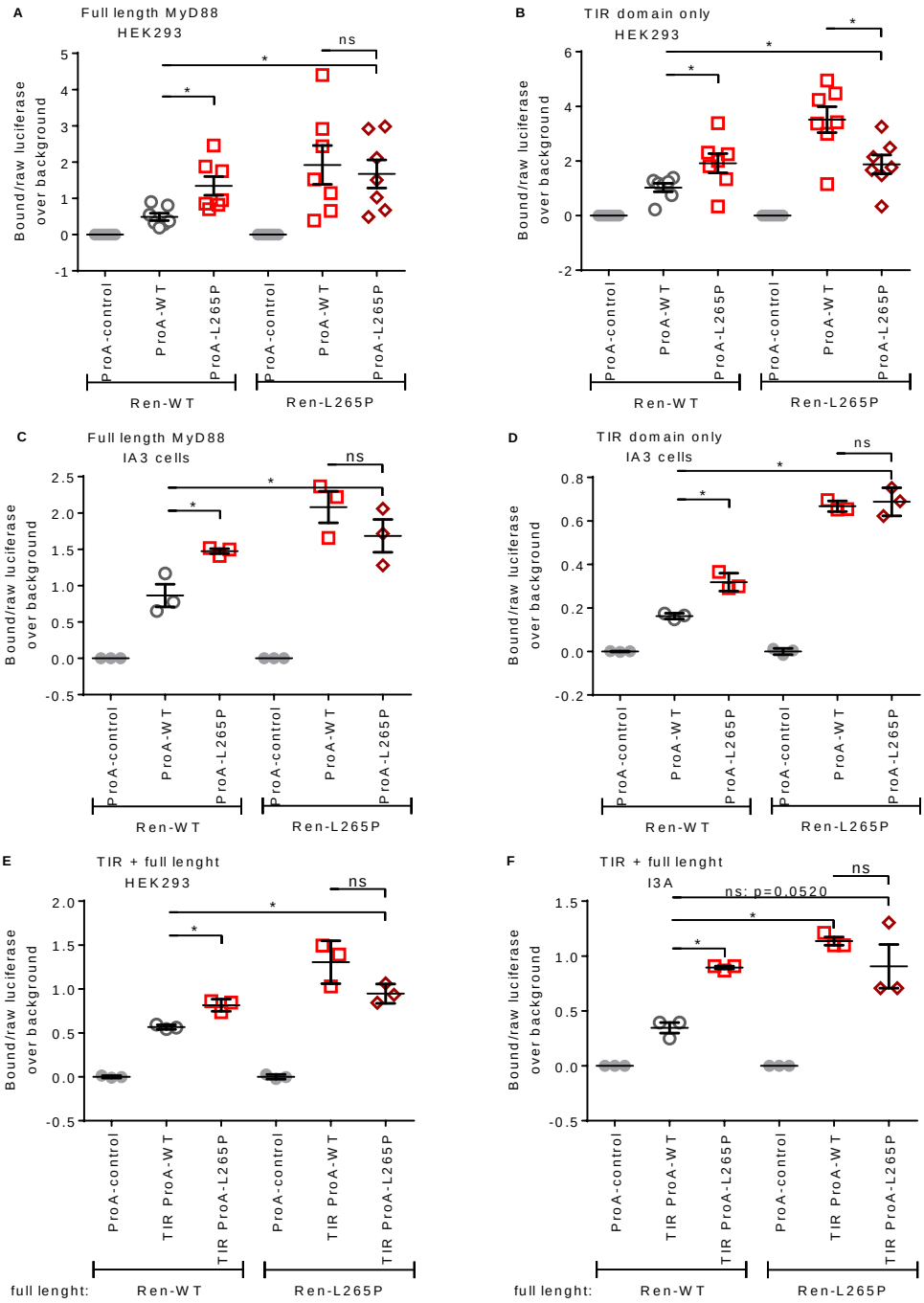

Figure 3.8: Augmented MyD88-dimerization is mediated by L265P-mutated TIR domains. LUMIER luciferase analysis from HEK293T (A, B, E) or MyD88-deficent I3A (C, D, F) cells transfected with Protein A-tagged (ProA) and Renilla luciferase-tagged (Ren) WT or L265P mutant full-length (A, C, E-F) or TIR-domain-only (MyD88 residues 155-294; B, D, E-F) MyD88 constructs (all with N-terminal protein fusion tags). 48 h post transfection, cells were lysed and raw luciferase measured in 10% of the sample. The remainder was used for Protein A purification with immunoglobulin G-coupled magnetic beads and subsequent measurement of bound luciferase. Data represent ratios of bound versus raw luciferase for each transfection upon subtraction of background (Protein A-only control bait) combined from at least three identical experiments (A-C and F, shown are means +/- SEM) or exemplary technical triplicates from two independent experiments (D, E; Means +/- SDs). Differences were tested using Mann-Whitney U (A, B) or unpaired t test (C-F). * $p < 0.05$.

3.2.2 The L265P TIR-mediated MyD88 dimerization could be blocked by decoy peptides

Loiarro et al.[123] described that MyD88 TIR BB-loop mimicking peptides effectively inhibited MyD88 homodimerization in vitro. A cell permeable analog of these TIR mimicking peptides is linked to antennapedia-derived residues to introduce the inhibitor in cells in vivo. To see if those peptide inhibitors were capable to efficiently block the augmented dimerization between WT and L265P-mutated TIRs, we conducted LUMIER assays in MyD88-deficient I3A cells as described for Figure 3.8 D. Additionally, cells were treated by addition of a MyD88-peptide inhibitor (Pepinh-MYD from Invivogen) or respective control peptides to the culture supernatant at indicated concentrations, 6 h prior harvesting (Figure 3.9). Indeed, incubation of cells with inhibitor significantly lowered the heteromeric TIR WT-L265P binding at a concentration of 80 µM for about 25% in comparison to the control treatment. Therefore, the MyD88 peptide inhibitor is not only capable to block dimerization of WT MyD88 as described by Loiarro et al., but also to block elevated interactions between WT and mutant MyD88 TIR domains.

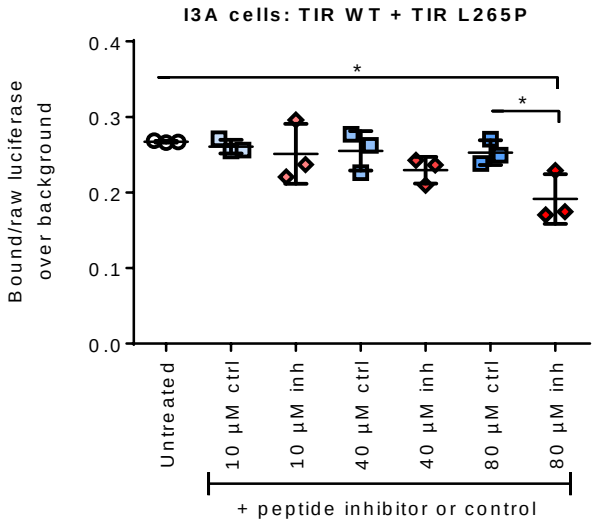

Figure 3.9: A TIR blocking peptide prevents L265P-mediated MyD88 TIR oligomerization.
LUMIER experiments were conducted in MyD88-deficent I3A cells as described for Figure 3.8 D (with transfection of N-terminally tagged Pro A-TIR WT and Renilla-TIR L265P plasmid constructs) except that a control peptide (ctrl, blue) or MyD88 blocking peptide[123] (inh, red) was added at indicated concentrations (10, 40 and 80 µM) 6 h prior to cell lysis. Data represent ratios of bound vs. raw luciferase upon subtraction of background (Protein A-only control bait). Means +/- SDs are shown and differences tested by unpaired t test. One representative out of 5 experiments with similar results is shown. * $p < 0.05$.

3.2.3 L265P-mediated MyD88 dimerization is initiated by TIR-TIR contacts without DDs being involved

Since L265P-mutated TIR domains augment MyD88 dimerization we wondered if such complexes might have a higher tendency to incorporate DDs. Indeed, there was interaction observed between MyD88 full-length and DDs (Figure 3.10 A, B). Interestingly in HEK293T binding between MyD88 L265P and DD was significantly elevated compared to the WT. Since the L265P mutation is located in the TIR domain which is not directly participating in DD binding (Figure 3.10 C, D and[115]) this observation might be explained by an elevated integration of DDs in a preexisting L265P-mediated protein complex. In line with this, neither WT nor L265P mutated TIR-domains interacted directly with isolated MyD88 DD-domains (Figure 3.10 C, D; note low binding values for both HEK293T and I3A) which excludes the involvement of DDs as oligomerization inducers and further corroborates the crucial role of MyD88 TIR-oligomerization in Myddosome signal complex formation.

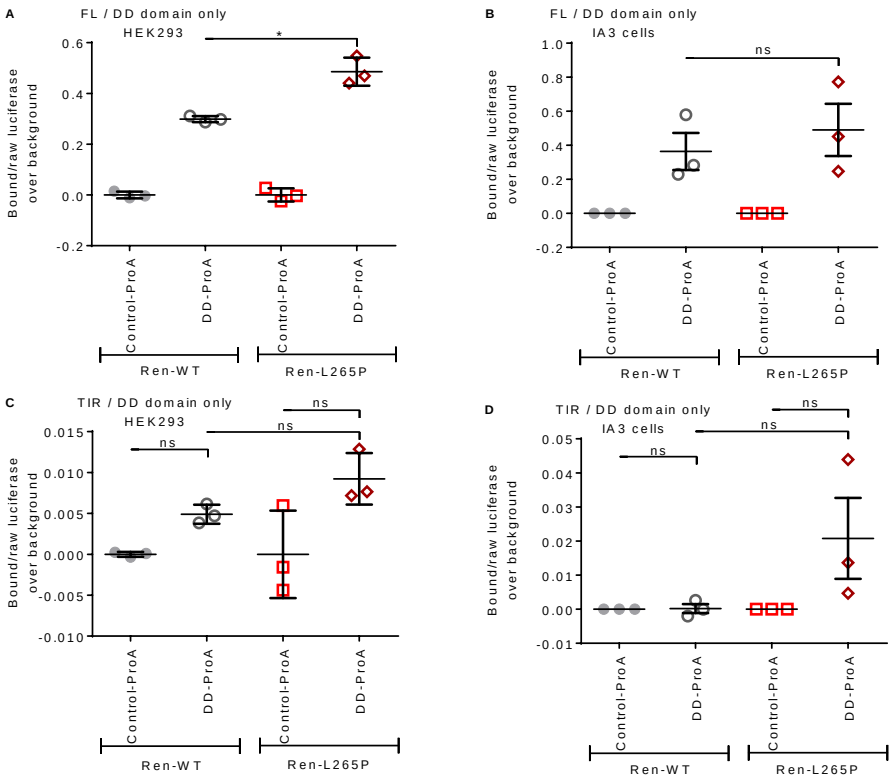

Figure 3.10: MyD88 L265P dimerizes via TIR-TIR and not TIR-DD contacts.
LUMIER luciferase analysis from HEK293T (A, C) or MyD88-deficent I3A (B, D) cells transfected with MyD88 Protein A-tagged (ProA) death domain only (DD) and Renilla luciferase-tagged (Ren) WT or L265P mutant full length (FL; A-B) or TIR domain only (residues 155-294, C-D) MyD88 constructs. 48 h post transfection, cells were lysed and LUMIER measurement conducted as described in Figure 3.8. Data represent triplicates from one experiment (A, C; means +/- SDs) or combined from three identical experiments (B, D; means +/- SEMs). Statistical differences were tested by using unpaired t test. * $p < 0.05$.

3.3 Oncogenic MyD88 mutations cause excessive oligomerization and molecular aggregation

The L265P mutation caused a strong binding between MyD88 TIR domains (section 3.2.1). To visualize the extend of MyD88 oligomerization in situ, MyD88 TIRs fused to the fluorescent protein mCitrine were analyzed by our partners (Jerala et al., Figure 3.11 A, B) in HEK293. Whereas mCitrine-TIR WT revealed a diffuse pattern of staining (yellow pseudocolor), lymphoma-associated TIR mutants (in particular L265P), clustered in the cytoplasm (Figure 3.11 A), an observation also described for tethered WT MyD88 TIR domains[117]. However, TIR mutant protein aggregates (Figure 3.11 B) revealed a similar NF-κB hyperactivation phenotype as their non-tagged equivalents (compare to Figure 3.2 C). Mutant MyD88 TIRs co-localized with WT full-length MyD88 (not shown, see our publication[42]) which supports the assumption that mutated TIR domains aggregate and can further recruit WT full-length MyD88 via its TIR domain. To further test if aggregation of mutant TIR domains creates a scaffold for nucleating Myddosome assembly, colocalization with downstream binding proteins of MyD88 was investigated by confocal microscopy. Therefore, plasmids coding for ECFP-MyD88 WT or L265P together with IRAK1-EGFP or IRAK4-EGFP were expressed in HEK293 cells (Figure 3.11 C, D). IRAK1 or IRAK4 transfected alone resulted in a diffuse staining pattern (magenta pseudocolor), but expressed together with MyD88 (cyan pseudocolor), a fraction of both IRAK1 and IRAK4 co-localized with MyD88 (indicated by white arrows). Levels of colocalization with IRAKs were not distinguishable between MyD88 WT and the L265P mutant. Nevertheless our observations indicate spontaneous mutant MyD88 TIR-mediated assembly of Myddosomes what is in agreement with previous findings where MyD88 L265P binds strongly to IRAK1 (compare to Figure 3.14 C) and utilizes IRAK4 for constitutive signal transduction[80,81,97].

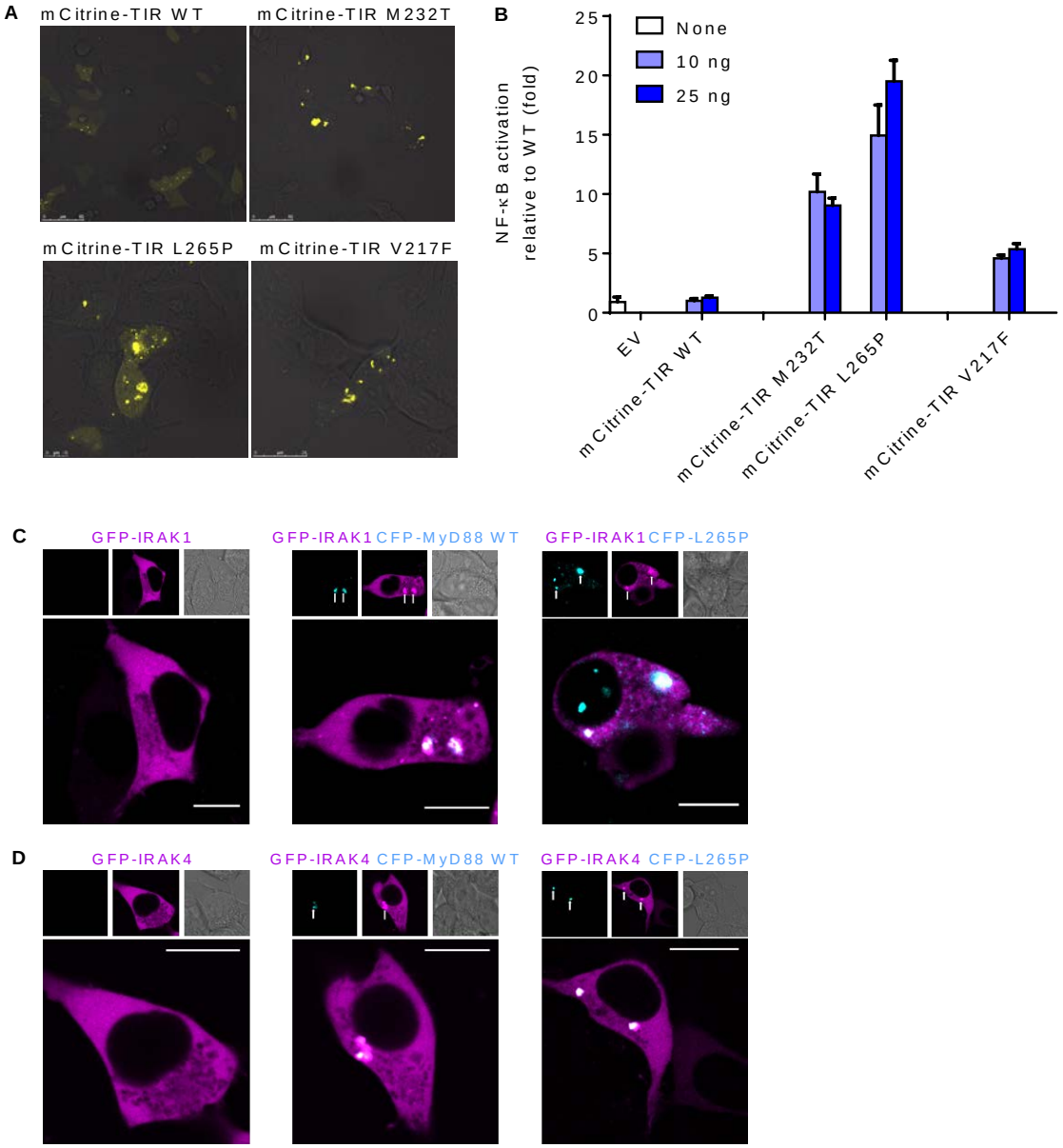

Figure 3.11: Oncogenic MyD88 mutants aggregate and colocalize with IRAK1 and IRAK4. Experiments performed by Avbelj et al., figure adapted from[42]: (A, B) HEK293 cells were transfected with plasmids coding for mutant or WT MyD88 mCitrine-TIR alone (A, yellow pseudocolor) or (B) together with NF-κB inducible firefly luciferase and constitutive Renilla luciferase reporter plasmids for DLA analysis. After 48 h cells were (A) visualized by confocal microscopy at x1000 magnification or (B) lysed and luciferase activity measured by DLA. (A) Shown are representative images of at least three independent experiments. (B) Data show mean + SD of triplicate samples and are representatives of at least three independent experiments. (C, D) IRAK1 and IRAK4 colocalize with MyD88 WT and L256P mutant: MyD88 deficient I3A cells were transfected with plasmids expressing (C-tagged EGFP) IRAK1 (C) or IRAK4 (D) without (left panels) or in combination with (N-tagged CFP) MyD88 WT (center panels) or MyD88 L265P (right panels). Cyan=CFP (extinction 405 nm / emission 460-480 nm); magenta=EGFP (extinction 514 nm / emission 525-600 nm); white = colocalization of IRAK1 or IRAK4 with MyD88 WT or L265P. White arrows indicate the position of MyD88 aggregates. Shown are representative cells from one experiment of two identical repetitions.

Next it was examined if MyD88 mutant aggregation also occurs in B cell lymphoma-derived cell lines where MyD88 is expressed at natural levels. Therefore lysates from B cell lines of different tumor entities with MyD88 mutations (n = 6) or WT (n = 6) were fractionated by centrifugation, and lysates as well as pelleted high molecular weight fractions analyzed by immunoblot. Relative MyD88 levels were quantified by charge-coupled device (CCD) image acquisition and plotted as the tubulin-normalized ratios of lysate (WCL) vs. pelleted insoluble MyD88. In Figure 3.12 A there is a significantly reduced lysate to pellet ratio for L265P mutated cells (dark red), compared with MyD88 WT lines (grey). MyD88 mutated cell lines including L265P, S219C and S222R mutations exhibited a tendency (not significant with p = 0,051) towards a lower lysate to pellet ratio proposing higher amounts of insoluble MyD88-containing aggregates. As an example (see Figure 3.12 B and C) the GCB DLBCL OCI-LY19 cell line, which expresses WT MyD88, is compared to the homozygously L265P-mutated ABC DLBCL line OCI-LY3. Despite higher *MYD88* mRNA expression (Figure 3.12 B) in mutated OCI-LY3 cells, there is less MyD88-protein found in the whole cell lysate (WCL, Figure 3.12 C immunoblot below), whereas more mutant MyD88 is found aggregated in the pelleted fraction (quantification upper part of Figure 3.12 C, immunoblot lower part). MyD88 L265P containing protein aggregates found in OCI-LY3 cells correspondingly included higher amounts of IRAK1 compared to OCI-LY19 MyD88 WT cells (Figure 3.12 D). Because MyD88 L265P was described to constitutively interact with IRAK1[80,81,97] in a Myddosome context (see also Figure 3.11 C and Figure 3.14 C), the MyD88 clusters observed by microscopy (Figure 3.11 A) as well as the aggregates verified by centrifugation and immunoblot experiments, probably resemble signaling-active Myddosomes. Thus, oncogenic MyD88 mutations have an intrinsic propensity to form TIR-mediated homo-oligomers which serves as a platform for recruiting downstream IRAKs via a death domain scaffold and therefore initiating downstream signaling in both the HEK293 cell model system and B cell lymphoma lines.

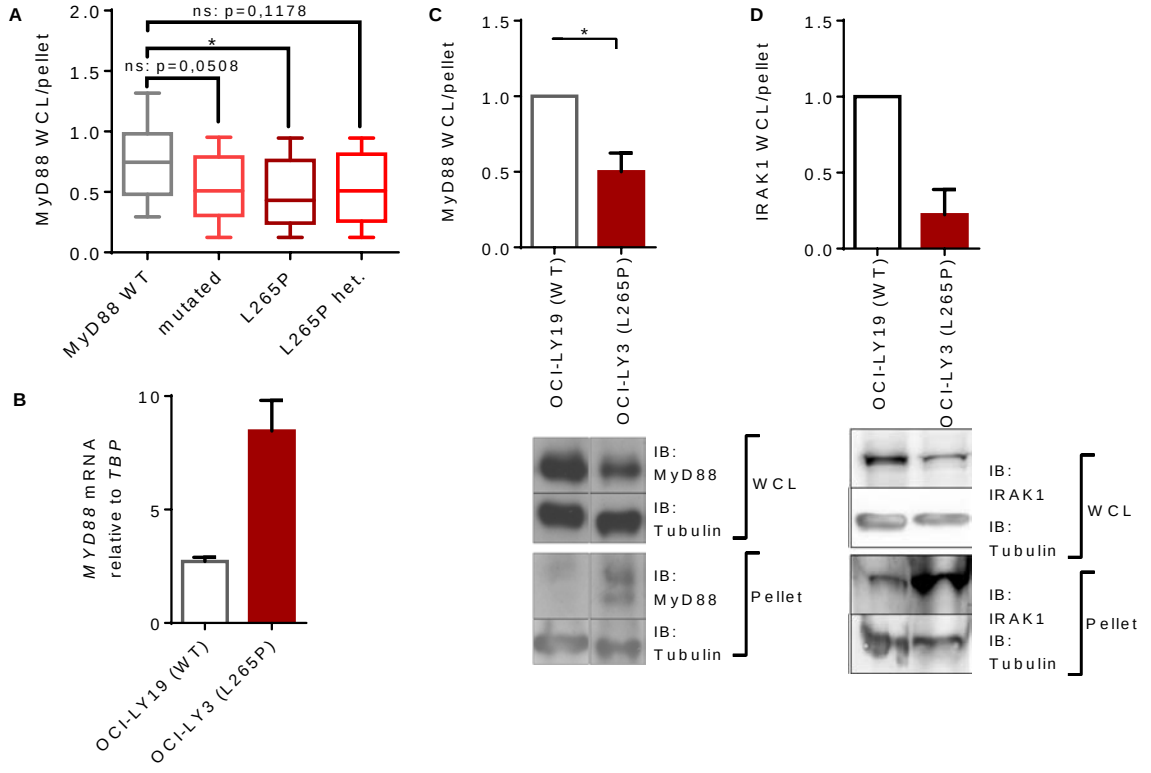

Figure 3.12: Aggregation of the MyD88 L265P mutant in lymphoma cell lines.
(A, C) Augmented amounts of mutant MyD88 in aggregates in different B cell lymphoma lines. Cell lysates were fractionated by centrifugation. Lysate and pellet fractions were analyzed by SDS-PAGE followed by anti-MyD88 (A, C) or IRAK1 (D) and anti-tubulin immunoblot (see blots in panels C, D). MyD88, IRAK1 and tubulin levels were quantified by charge-coupled device (CCD) detection and plotted as the tubulin-normalized ratios of lysate (WCL) vs. pelleted MyD88 (A, C) or IRAK1 (D). (A) Data were combined from 4 experiments and are illustrated as min-to-max box-and whisker plots with differences tested using Mann-Whitney U test. WT MyD88 B cell lymphoma lines (I83E95, RPMI-8226, Namalwa, OCI-LY19, BJAB, U2392) were compared with MyD88-mutated cell lines (OCI-LY10, TMD8 and HBL1 with heterozygous L265P (het.); OCI-LY3 with homozygous (hom.) L265P; HLY1 with heterozygous S219C, SUDHL2 with heterozygous S222R). (B) Differences in MyD88 lysate expression in L265P-mutated OCI-LY3 cells are not due to lower mRNA expression in comparison to OCI-LY19, as assessed by quantitative PCR. One representative shown of 3 independent experiments done in triplicates. (C) Comparison of MyD88 WT OCI-LY19 vs. L265P homozygous OCI-LY3; lysate vs. pellet ratio from 9 combined experiments and showing a representative immunoblot. (D) MyD88 L265P aggregates also contain higher amounts of IRAK1. Comparison of WT OCI-LY19 vs. L265P homozygous OCI-LY3 lysate vs. pellet ratio from 3 combined experiments and showing a representative immunoblot. IB, immunoblot; * $p < 0.05$.

3.4 Aggregation of the MyD88 L265P mutant is basal to tumor cell persistence

It was already discussed that oncogenic MyD88 mutants tend to oligomerize due to a TIR-intrinsic mechanism and thereby initiate downstream signaling. The question arises if L265P-mediated nucleation of signaling platforms by augmented TIR oligomerization is a prerequisite for tumor cell survival. Therefore we treated tumor cell lines with cell-permeable TIR BB-loop mimicking peptides (Loiarro et al.[123]), which were capable to lower heteromeric TIR WT-L265P binding, as demonstrated before by LUMIER protein interaction assay (Figure 3.9). Indeed, in a colorimetrical CCK8 viability assay (Figure 3.13), L265P-mutated DLBCL lines were more sensitive to exposure to the inhibitory peptides in a concentration specific manner, compared to cells expressing non-mutated MyD88 (significant between 30-50 µM, see Figure 3.13 A and B). Thus, aggregation of L265P-mutated MyD88 is mechanistically a process basal to oncogenic B cell persistence and blocking hyperactive signaling at the level of MyD88 oligomerization might be therapeutically an option to pursue (see discussion).

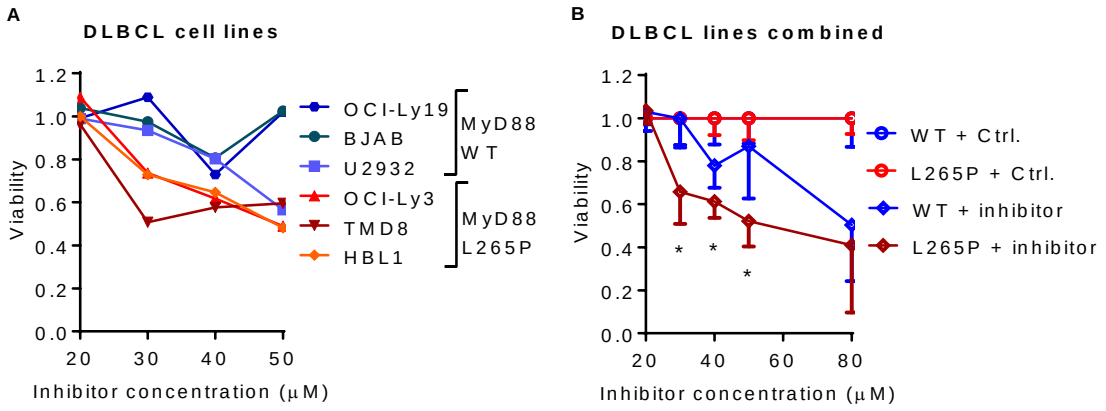

Figure 3.13: A MyD88 TIR blocking peptide sensitizes viability of L265P-mutated DLBCL cell lines.

DLBCL cell lines were grown in the presence of control (Ctrl.) or MyD88 blocking peptide (inhibitor) at indicated concentration (30, 40, 50 and 80 µM). Cell viability was determined by using the Cell Counting Kit-8 (CCK8) method after 48 h. Data were generated from 3 MyD88 WT and 3 L265P-mutated DLBCL cell lines, combined from 3 identical experiments and shown either for each individual cell line (A, error bars omitted for clarity) or combined (B, means - SDs shown). Where indicated, differences were tested using an unpaired t-test. * $p<0.05$.

3.5 The L265P mutation strongly impacts binding to known interactor proteins of the Myddosome

We stated that oncogenic MyD88-mutations found in B-NHLs have an intrinsic propensity to oligomerize and nucleate aggregates likely corresponding to Myddosomes. To prove our assumptions further in the Myddosome setting we analyzed protein interactions of WT and L265P mutated MyD88 with previously reported partner proteins by LUMIER[114].

3.5.1 The L265P mutation modulates binding of MyD88 to other TIR domain-containing proteins

From the previously displayed results it is obvious that the L265P mutation increases homo-oligomerization of MyD88 TIR domains. Therefore it was assessed if mutated MyD88 shapes the interaction to other TIR-domain comprising proteins upstream in the Myddosome signaling complex.

3.5.1.1 Unexpectedly the L265P-mutation does not affect TLR9 TIR interaction

CpG-rich DNA-sensing TLR9 is the most abundant TLR expressed in B cells, including also transformed B cells in Burkitt- and follicular lymphoma and multiple myeloma[25]. The receptor plays a crucial role in lymphomagenesis as it was described that CpG ODN stimulated NF-κB activation in a B cell lymphoma cell line[124]. Wang et al.[101,125] recently expressed mutated MyD88 versions corresponding to oncogenic human orthologues in a murine model. *MYD88*-mutated B cells were proliferating even in the absence of B cell mitogens (i.e. CpG DNA) but using cells from *tr9*$^{-/-}$ mice prevented proliferation indicating that malignant cells may, at least in part, depend on an intact TLR9 signaling apparatus. From our previous data from MyD88 TIR-oligomerization (Figure 3.8) we hypothesized that L265P mutation might increase protein interaction between MyD88 and the cytoplasmic TLR9 TIR domain. In such case it is conceivable that mutant MyD88 shapes the receptor's affinity to ligands by influencing leucine rich repeats (LRRs) conformation (see discussion). However interaction between MyD88 and ectopically expressed TLR9 TIR was rather low in general without any obvious differences between MyD88 WT or L265P mutation (Figure 3.14 A). The question if MyD88 mutations directly influence TLR-stimuli as a trigger for Myddosome formation still remains elusive.

3.5.1.2 The L265P mutation abolishes interaction with the adaptor protein Mal

TLR4 and TLR2 recruit MyD88 to their cytoplasmic domains via the TIR-domain-containing bridging adaptor Mal (also termed as TIRAP, reviewed in[14,15]). With its phosphoinositide-binding domain Mal gets directed to membranes of different cell compartments[35,38,126]. There it also acts as a sorting adaptor for TLR9 between the plasma and endosomal membranes, where it triggers from both locations the assembly of Myddosomes in response to TLR stimuli. Mal is tyrosine-phosphorylated at its TIR domain by the Bruton's tyrosine kinase (BTK)[49] and moreover BTK was recognized to be fundamental for TLR9 signaling in human plasmacytoid dendritic cells (pDCs)[127]. Interfering in so many pathways we analyzed if Mal also plays a role for Myddosomes nucleated by mutated MyD88 and if L265P-mediated effects might be a consequence of altered MyD88-Mal heterodimer formation. In Figure 3.14 B it is displayed that MyD88 WT binds Mal but surprisingly this high interaction is (in opposite to MyD88-dimerization see Figure 3.8) completely suppressed by the L265P mutation (see also supplemental Figure 5.1 in appendix). We failed to validate this findings in tumor cells due to the lack of specific antibodies against Mal, but the results based on LUMIER propose that effects mediated by oncogenic MyD88 mutations on i.e. TLR and BTK signaling might be rather more direct and not include the TIR-containing co-adaptor Mal.

3.5.2 The L265P mutation increases binding of MyD88 to DD-containing proteins downstream of the Myddosome

Next it was explored how lymphoma-associated mutations influence the interaction of MyD88 with proteins downstream in the Myddosome complex. Through its amino-terminal DD, MyD88 interacts with DDs of all known IRAK family members, whereby the MyD88 TIR domain is not participating in DD binding DDs of IRAKs[115] (compare also to Figure 3.10 C-D). In the DD-stack crystal structure from Lin et al.[63] Myddosome formation follows a hierarchical assembly, in which MyD88 recruits IRAK4 thereby recruiting IRAK2 or the related IRAK1. In line with other reports[80,81,97] and our own observations by microscopy (see Figure 3.11 C) we found MyD88 L265P strongly associated with IRAK1 in LUMIER protein-interaction assays (Figure 3.14 C) and both WT and mutant variant interacting with IRAK4 (Figure 3.14 E) to the same extend. Interestingly the L265P mutant tended to interact significantly stronger with IRAK2 than WT MyD88 which was never reported before (Figure 3.14 D). This observation is a plausible explanation for the constitutive induction of NF-κB by the MyD88 L265P mutant in IRAK1-deficient I1A cells (see Figure 3.6) and indicates that IRAK2 might be alternatively employed to form Myddosome signaling complexes also in tumor cells. Formation of Myddosome complexes brings the kinase domains of IRAKs into proximity for phosphorylation

and activation of the E3 ubiquitin ligase TRAF6[14,15,21,128]. MyD88 L265P was stronger associated with TRAF6 than the non-mutated form (Figure 3.14 F, not significant with p = 0,056), as it was also published in the meantime by another group[96]. Since TRAF6 lacks DDs, we assume that augmented co-precipitation with MyD88 L265P is not due to direct interaction, but rather happens in a complex with other proteins, likely Myddosomes. Taken together the MyD88 TIR homo-dimerization of oncogenic MyD88 mutants is probably the first step in oncogenic signaling complex formation. A crucial preformed platform of DDs stemming from mutant MyD88 would further nucleate the hierarchical assembly of the Myddo-some by recruiting IRAKs via their DDs and consequently incorporating TRAF6 in the complex.

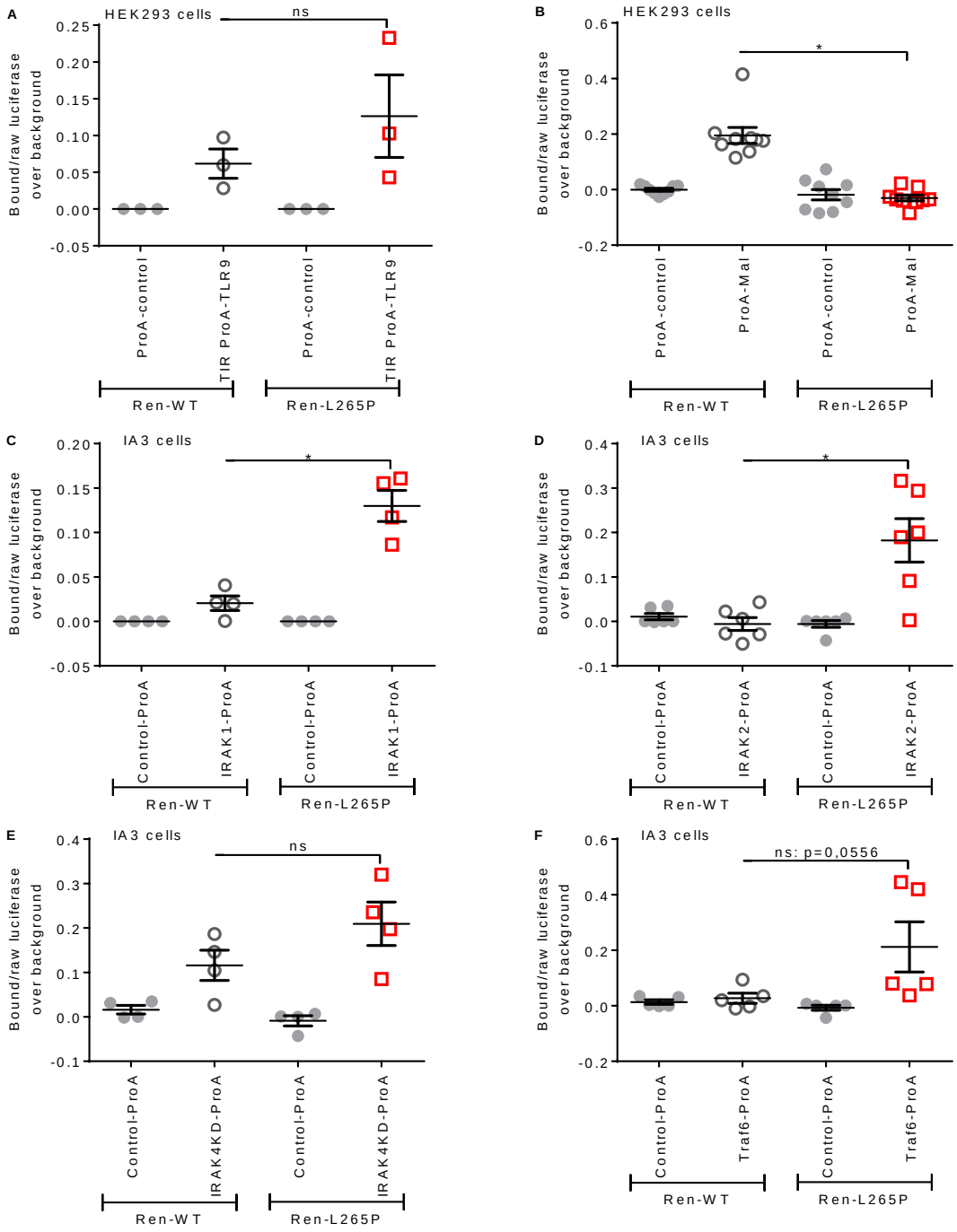

Figure 3.14: MyD88 L265P modulates binding to partner proteins of the Myddosome.
LUMIER luciferase analysis from HEK293T (A-B) and MyD88-deficent I3A (C-F) cells transfected with Protein A-tagged (ProA) MyD88 binding partners and N-terminally Renilla luciferase-tagged (Ren) WT or L265P mutant MyD88 constructs. 48 h post transfection, cells were lysed and LUMIER measurement conducted as described in Figure 3.8. Data were combined from at least 3 identical experiments and show means +/- SEMs. Statistical differences were tested by using Mann-Whitney U test. * $p < 0.05$.

3.5.3 The MyD88 L265P mutation may effect binding to SH2-domain containing tyrosine kinases

Recent evidence highlighted MyD88 to be involved in additional non-canonical intracellular pathways besides signaling via the Myddosome. During generation of memory B cells the SH2 (Src homology 2) domain-containing tyrosine kinases Src and Syk (spleen tyrosine kinase) appear to directly link mitogen BCR with TLR9 stimuli which together synergize in persistent cellular survival and immunoglobulin production by activating STAT3[121,122]. Further interaction studies were conducted to dissect if MyD88 L265P exerts its hyperactive phenotype by utilizing Src and Syk tyrosine kinases which are highly expressed in different B cell tumor cells (see appendix supplemental Figure 5.2). In comparison to WT, mutated MyD88 revealed a slightly increased interaction with both Src (not significant) and Syk (significant, but interaction less than threefold higher as negative control), see Figure 3.15. Our data remain to be verified with Co-IPs from endogenously expressed proteins in DLBCL lines. As Src was demonstrated to be pivotal in Waldenström's macroglobulinemia[129] and Syk pathway inhibitors show promise in lymphoma therapy[95,130,131], we plan to validate this link in patient cells and a murine model.

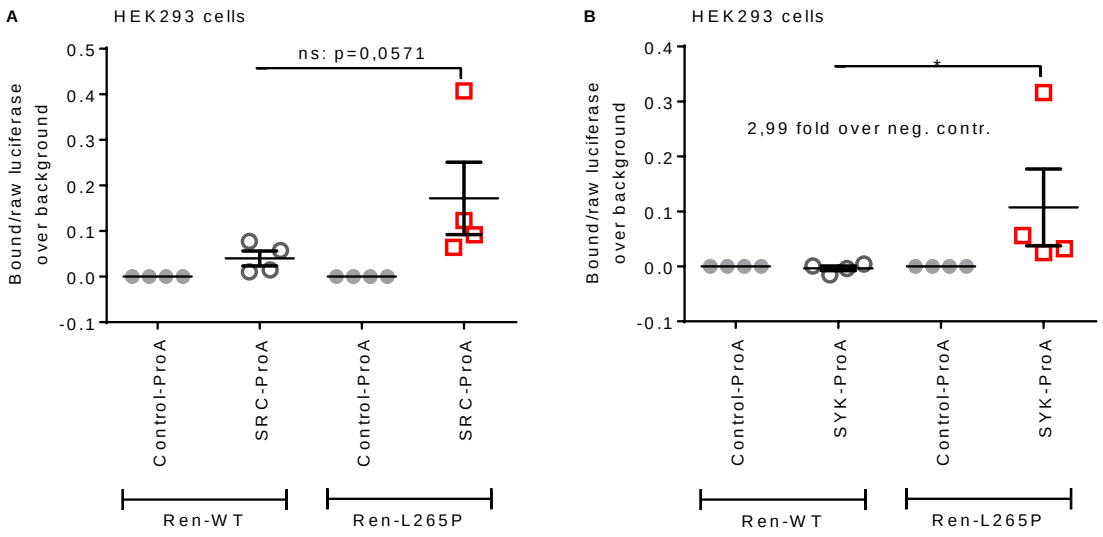

Figure 3.15: MyD88 L265P modulates binding to SH2-domain containing tyrosine kinases. LUMIER luciferase analysis from HEK293T cells transfected with C-terminal Protein A-tagged (ProA) tyrosine kinases Src (A) or Syk (B) together with N-terminal Renilla-tagged (Ren) WT or L265P MyD88 plasmids. Assay performed as described for Figure 3.8. (B) Interaction L265P-Syk did not excess the defined false positive rate of threefold excess over the negative control, see Material and Methods for detailed explanation. Means from 4 independent experiments are shown +/- SEM and differences tested using Mann-Whitney U test. * $p < 0.05$.

3.6 WT and L265P-mutated MyD88 may differ in post-translational modifications

It is of interest whether described oncogenic properties of the L265P mutation may rely on altered post-translational modification (PTM) of mutant protein, such as phosphorylation. In order to address this 2D-PAGE analysis was performed from HA-precipitated MyD88 which was overexpressed in I3A cells. Both WT and L265P-mutated MyD88 revealed to be post-translationally modified, showing multiple protein species of similar molecular size of approximately 35 kDa (Figure 3.16). There are observable differences in number and abundance of protein species differing in isoelectric characteristics, indicative of phosphorylation (Figure 3.16 upper and middle panel). Simultaneous expression of both WT and L265P-mutated MyD88 constructs (Figure 3.16 lower panel) aided to simulate heterozygousity of the mutant allele found in most tumors (see section 1.4.2). The combination of WT and L265P shows a modification pattern similar to L265P, suggestive of a possible *trans* effect which is executed by the oncogenic mutant. To confirm this very preliminary analysis it should be considered to enrich MyD88 from primary B cell lysates by IP and by using whole proteome approaches to investigate modification changes (not only phosphorylation but also ubiquitination and acetylation) of L265P vs. WT MyD88 cells. It remains elusive to determine the interactors mediating specific MyD88 phosphorylation and if this observation is of functional relevance in B cell lymphoma. Principally this could be addressed by RNAi knockdown of putative MyD88 L265P interactor candidates followed by mass spectrometric analysis of protein modifications and investigation of cell viability.

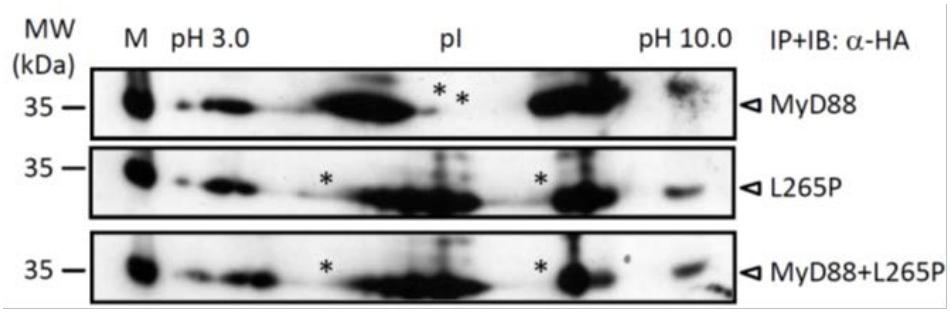

Figure 3.16: The L265P mutation affects post-translational modifications of MyD88.
2D-PAGE analysis of MyD88 WT (upper), L265P (middle) or WT+L265P mixed in a 1:1 ratio (lower) N-terminal Strep-HA-tagged constructs expressed and HA-precipitated from MyD88-deficient I3A cell lysates. * WT species not found in L265P and vice versa. Preliminary data from one experiment. pI = isoelectric point; MW = molecular weight; M = 35 kDa band of molecular size marker; IP = immunoprecipitation; IB = immunoblot.

4 Discussion

MyD88 is the central signaling adaptor protein of TLR and IL-1R receptors. Features and mechanisms of this protein were mainly investigated in innate immune cells, i.e. macrophages, but components of the TLR pathway are also highly expressed in a variety of other cell types like B cells, where their precise function still remains elusive. For example, recent studies reported that in B cell lymphomas *MYD88* is frequently mutated, which maintains malignant cell-survival by constitutive NF-κB activation. However, how MyD88 contributes to oncogenesis is not fully understood. The aim of this study was to advance knowledge in this area and in the following it is debated how oncogenic MyD88 mutations directly contribute to Myddosome formation and signal hyperactivation. A malfunctioning molecular mechanism will be discussed which delivers a plausible explanation why one copy of mutated *MYD88* in patients might be sufficient for disease progression. I speculate about altered regulation of MyD88 mutants modulating the TLR sensitivity and mediating interaction with SH2-domain tyrosine kinases. Furthermore, general concepts for developing mutation-specific therapies to target MyD88-mediated oncogenic signaling will be argued.

4.1 Aggregation of oncogenic MyD88 mutants is a prerequisite of B cell tumorigenesis

Patients with rare germline *MYD88* loss-of-function mutations have been described to suffer from severe susceptibility to pyogenic bacterial infection during childhood and they survive into adulthood only on a strict therapy of antibiotics[132]. Conversely, somatic *MYD88* gain-of-function mutations were recently discovered with high frequency in diverse B cell NHLs[80,81]. These somatic mutations are restricted to highly conserved TIR residues whereby only very particular substitutions are likely providing an advantage in clonal selection. In our publication[42] we describe that i.e. the L265P mutant is strongly hyperactive, but their designed counterpart I266P affecting the neighboring residue lost this ability, although it would expectedly render similar chemical properties. Therefore, the oncogenic substitutions are presumably to have emerged as a result of the selection in B cells, which is in line with a study showing that MyD88 L265P is an early driver for CLL tumorigenesis and is found in nearly all subclones[87].

NF-κB hyperactivation has been described as a key feature in MyD88-mutated B cell lymphomas, nevertheless the underlying molecular mechanism how one amino acid alteration exerts the described phenotypes has to be resolved in more de-

tail. In line with studies in DLBCL lines[80] and primary CLL cells[81], we confirmed the hyperactivation potential of such oncogenic MyD88 mutants. Isolated MyD88 TIR domains block signal transduction, but fused TIR-TIR tandem constructs initiate signaling what proposes that TIR dimerization nucleates Myddosomes[117]. If this observation is related to relevant physiological conditions has never been described. Here it was hypothesized that in HEK293 cells, TIR mutants employ endogenously expressed MyD88 WT for consequent signaling. Indeed, there was no NF-κB activation resulting from mutant TIR overexpression in MyD88-deficient I3A cells and siRNA-knockdown of endogenous MyD88 in HEK293T reduced the L265P-TIR mediated NF-κB induction (see Figure 3.3, Figure 3.4 and Figure 3.5). These observations suggest that mutated TIR domains form a scaffold together with endogenous WT MyD88 which in turn recruits IRAKs and initiates Myddosome complex formation. LUMIER experiments revealed that protein binding between molecules of MyD88 full-length, TIRs, or TIR with full-length was considerably higher for all L265P-combinations in comparison to WT-WT interactions, confirming the key role of TIR domains in oligomerization of mutant MyD88 (Figure 3.8). Therefore, even if artificially expressed TIRs in HEK293T cells do not reflect the natural conditions in tumors, these findings imply that in vivo, oncogenic MyD88 mutants intrinsically possess a higher ability to aggregate. In line with this, microscopy of HEK293 cells expressing MyD88 mCitrine-TIR, revealed a diffuse staining pattern for WT, whereas mutant TIR constructs were strongly aggregated, but still capable to hyperactive NF-κB (Figure 3.11). MyD88 L265P colocalized with IRAK1 and IRAK4 (Figure 3.11), suggesting that mutant TIR aggregates trigger Myddosome nucleation. To prove if spontaneous oligomerization/aggregation is a natural incident in cancer, MyD88 protein levels were compared in lymphoma cell lines between lysates and pelleted HMW fractions after centrifugation by immunoblot. In L265P-mutated cells there was significantly more MyD88 pelleted in comparison to WT lines, indicative for a potent mutant-mediated MyD88 oligomerization (Figure 3.12). Protein aggregates of homozygously L265P-mutated OCI-LY3 cells also contained elevated amounts of IRAK1 which is in agreement with the observation that IRAK1 is the essential kinase mediating constitutive signaling of MyD88 L265P Myddosomes[80]. We failed to monitor MyD88 aggregates and colocalization with IRAKs indicative for Myddosomes by microscopy/ImageStream since lacking fluorescently labeled antibodies specific for the proteins. Therefore we proved indirectly if this aggregation phenotype is of relevance for Myddosome formation by blocking TIR-dimerization with decoy peptides[123] and therefore preventing MyD88 aggregation. In fact, DLBCL cell lines were specifically killed by the inhibitory peptides in a L265P mutation-dependent manner (Figure 3.13). This is in line with two studies showing that MyD88 inhibition caused cell death by diminishing phosphorylation of IRAK1 and phospho-p65 nuclear translocation in L265P

mutated WM cells[79,97]. Taken together, MyD88-L265P has a TIR-intrinsic tendency to oligomerize/aggregate to Myddosome-like complexes and therefore hyperactivating signaling, which is a prerequisite of tumor cells to persist.

4.1.1 Aggregation of oncogenic MyD88 mutants happens in an ordered manner suggesting allosteric oligomerization

Oncogenic MyD88 mutant 'aggregation' may be an improper term since this implies misfolded proteins forming cellular inclusion bodies i.e. as reported for the so-called Lewy bodies in Parkinson's disease. But circular dichroism spectroscopy revealed a preserved global secondary structure of mutant TIR domains (personal communication with Roman Jerala). Furthermore computational molecular dynamics simulation, based on a NMR structure of the MyD88 TIR domain (Protein Data Bank accession 2JS7, described in our publication[42]), indicated that oncogenic mutants are as stable as the WT-structures and are therefore unlikely to act via a gross disturbance of the TIR fold as a whole. Highly stable positions within the domain were noted, corresponding to frequently mutated residues in lymphoma, i.e. at positions 177, 204, 232 and 265. In the globular folding of the domain those residues are all buried and located on adjacent β strands along the proposed MyD88 TIR dimerization interface[133], suggesting that oncogenic mutations might modulate force transduction during oligomerization. Thus, lymphoma-associated mutations may facilitate MyD88 oligomerization by affecting residues involved in TIR dimer formation, possibly by an allosteric effect.

Under normal circumstances Myddosome formation is a highly regulated hierarchical process in order to protect the organism from overreaction of the immune system. For instance, TLR4 needs the co-receptor MD-2 to get activated by LPS (endotoxin) and recruitment of MyD88 to activated receptors is additionally controlled by the co-adaptor Mal. If this strict hierarchy is intermitted, i.e. by L265P-mutated MyD88 oligomerization, one would assume a bidirectional complex nucleation towards crosslinking upstream TLR TIRs and downstream IRAK recruitment. Healthy Myddosome signaling is thought to be a transient process with variable stoichiometry of proteins involved. For instance IRAK1 is crucial in early phase of cytokine production in mouse BMDMs and pDCs, but prolonged TLR stimulation causes rapid turnover, whereby IRAK2 is incorporated into Myddosomes for a sustained activation of signaling networks[134]. Taken in advance that oncogenic mutant-mediated nucleation happens spontaneously without being triggered/controlled by receptor-stimulation, one would expect stable signaling complexes of high molecular weight, what we referred to as MyD88 L265P 'aggregates'. Such mutation-mediated protein aggregation leading to over-activation of distinct signaling pathways is a pathological phenomenon also reported else-

where[135,136]. Germline encoded gain-of-function mutations in CARD11 (caspase recruitment domain 11), a scaffolding protein required for antigen receptor-induced NF-κB activation, are associated with lymphoproliferative disorders. In particular CARD11 C49Y and E134G were reported in DLBCL[137,138] and transfection in B cells resulted in spontaneous protein aggregation, colocalization with the signalosome components MALT1 (mucosa associated lymphoid tissue lymphoma translocation gene 1), and phosphorylation of IKK which constitutively induced NF-κB[135,136].

4.2 Oncogenic MyD88 mutations affect activation of transcription factors other than NF-κB

We analyzed by luciferase reporter assays if other signaling pathways emanating from MyD88 were influenced by lymphoma-associated MyD88 mutations.

Our partners from the Jerala lab found increased IRF-dependent IFN-β promotor activation for different overexpressed oncogenic MyD88 mutations (Figure 3.7) in HEK293 cells. Our results are in line with a report where *MYD88* knockdown in L265P-mutated DLBCL cells changed expression of several genes that are induced by type I interferons. Furthermore knockdown in the homozygously L265P-mutated OCI-LY3 ABC DLBCL line decreased the type I interferon IFN-β cytokine secretion[80], but to our knowledge, this is the only report describing IRF-signaling in the background of oncogenic MyD88 mutations so far. In general, IRFs orchestrate B lymphocyte differentiation at several maturation stages[139-142]. This is also important in lymphomagenesis, as IRF4 regulates expression of BCL-6, a key factor necessary for formation of germinal centers, but which is implicated in pathogenesis of DLBCL[143]. IFN-β transcription is normally rapidly induced following infections in a TLR7/8/9 and MyD88-dependent way[16]. The role of IFN-β regarding to B cells and lymphoma is controversial. On the one hand, mouse bone marrow B cells treated with IFN-β showed resistance to Fas-mediated apoptosis and increased survival. IFN-β also enhanced responses to BCR ligation such as calcium fluxes, IgM internalization, induction of activation markers and proliferation[144]. On the other hand, IFN-β treatment revealed a broad spectrum of antitumor activities including anti-proliferative and pro-apoptotic effects, and are potentially useful for the therapy of B cell cancers[145-149]. I.e. treatment with IFN-β fused to anti-CD20 antibody (to increase stability of the cytokine and target B cells), efficiently inhibited B cell lymphoma growth in a murine model and prolonged survival of the animals[145]. Future work should address whether the extensive secretion of immunemodulatory cytokines such as IFN-β, but also IL-6 and IL-10 by MyD88 L265P mutated tumors[80,81] favorably influences tumor- and/or immune cells in the microenvi-

ronment, such as T helper cells which could potentially provide survival signals for malignant B cells.

During work on this thesis, it was published that the kinase TAK1 is hyper-phosphorylated in L265P-mutated lymphoma lines[96]. Since TAK1 simultaneously activates both NF-κB and MAPK pathways[21] we decided to investigate consequences of MyD88 overexpression on the MAPK pathway. An important MAPK, ERK, was shown to get activated by TAK1 via both MAPKs MEK-1 and -2[150] and in turn ERK controls Elk-1 transcription factor activation, an oncogene regulating cellular growth and proliferation[119]. But MyD88 L265P overexpression in HEK293T cells showed no differences in Elk-1 activation compared to WT (Figure 3.7). Nevertheless, to our knowledge MAPK pathways have never been investigated in the background of oncogenic *MYD88* mutations so far. Future studies should address whether MAPK-signaling is elevated in primary B cell lymphomas and focus on more abundant MAPKs in B lymphocytes such as p38 or the C-Jun N-terminal kinase (JNK) which are both critical proliferation regulators[151,152]. Schmid et al. recently published that aberrant promotor methylation in both GCB and ABC DLBCL results in a loss of expression of the dual-specificity phosphatase (DUSP) 4. This prevents JNK dephosphorylation leading to its constitutive activation and inhibition of apoptosis, indicating that DLBCL cells depend on JNK signaling for survival[152]. With this regard pharmacological targeting of MAPK pathways in B cell lymphoma should be reconsidered as a variability of small molecule inhibitors of MAPKs are actually tested in different clinical trials in autoimmune and inflammatory diseases (reviewed in[153]).

It was previously reported that the transcription factor STAT3 synergizes with NF-κB in promoting cellular survival in the subset of ABC DLBCL[154]. *MYD88* RNA interference revealed an elevated gene expression signature for JAK/STAT3 pathways in L265P-mutated cell lines[80] and furthermore primary L265P-mutated CLLs gained high levels of STAT3-phosphorylation[81]. Interestingly mice deficient for IRAK1, a crucial component of oncogenic MyD88-mediated hypersignaling, failed to activate STAT3 and to produce IL-10 upon stimulation with LPS[10,155]. This led us to the assumption that MyD88 L265P might directly interfere with JAK/STAT signaling in malignant cells. Using a reporter assay we observed that overexpression of MyD88 L265P in HEK293T was not hyperactivating STAT3 in comparison to the WT, but additional stimulation of cells with recombinant IL-6 potentiated STAT3 activity (Figure 3.7). This is in agreement with the idea that induction of JAK/STAT pathways in MyD88-mutated tumors are a consequence of augmented autocrine secretion of the NF-κB targets IL-10 and IL-6, which consequently leads to auto-stimulation of JAK/STAT-associated IL-10 and IL-6 receptors[80,156-158]. On the other hand, Jabara et al.[121,122] showed that for the generation of memory B

cells, TLR9 stimulation recruits a complex of DOCK8-MyD88-Pyk2 which directly links signaling via Src/Syk to activation of STAT3, independently of an interleukin autocrine secretion/auto-stimulation loop. Given the role of STATs as critical factors in B cells and lymphomagenesis[159], prospective work should address if oncogenic mutants would influence this direct link between MyD88 and STAT3 and therefore potentiate signaling. This scenario would imply to consider Syk-inhibition (see also section 4.3.3), which was already discussed for lymphoma treatment[95,130,131], as an optional therapy in patients with L265P-mutated tumors.

4.3 The MyD88 L265P mutation alters partner protein interaction

4.3.1 MyD88 L265P strongly binds IRAK2 and NF-κB hyperactivation may only partially depend on IRAK1

MyD88 mutated tumor cells were reported to depend on the action of IRAK1; MyD88 L265P strongly associated with IRAK1 and cells were sensitive to *IRAK1* RNA interference[80]. Unexpectedly, we observed in luciferase reporter assays in the IRAK1-deficient I1A line that in comparison to WT MyD88, the L265P mutant significantly stronger activated NF-κB (Figure 3.6). In the Myddosome complex MyD88 first interacts with IRAK4 which further promotes recruitment of IRAK1 or IRAK2[63]. Knock-out studies in mice have revealed a principle redundancy between IRAK1 and IRAK2[68,69] with only partial deficiencies in TLR signal transduction. In line with this LUMIER interaction studies displayed that MyD88 L265P not exclusively employs IRAK1 but also had an increased binding affinity to IRAK2 (Figure 3.14). So far the role of IRAK2 in MyD88 L265P Myddosomes in lymphoma cells still remains to be investigated. IRAK2 will be implemented in further experiments as possible candidate to co-precipitate with mutated MyD88 in tumor cells and its expression should be targeted by RNAi screening[80] to verify its potential role in transmitting L265P-mediated effects. Those observations would strengthen the need for small molecule inhibitors specifically targeting IRAKs in clinical settings to treat patients from the broad range of various B cell lymphomas with MyD88 mutations. During our work on this present study Yang et al. proved that in Waldenström's macroglobulinemia MyD88 L265P drives constitutive NF-κB signaling also by activating an alternative pathway independently from IRAKs. MyD88 L265P supports malignant cell viability by constitutively associating with phosphorylated Bruton's tyrosine kinase (BTK)[97]. As a logical consequence, pharmacological inhibition of both BTK with the irreversible inhibitor ibrutinib specifically killed mutated WM cells. These findings demonstrate that tumor cell survival through constitutive NF-κB pathway activation may not exclusively rely on IRAK1, which implies to

combine inhibition of different driver pathways to potentiate malignant cell eradication.

4.3.2 The L265P mutation modulates protein binding of MyD88 to other TIR domain-containing proteins

From our results we concluded that the MyD88 L265P mutation increases association with other MyD88 TIR domains. Consequently it was examined by LUMIER assays if binding to other TIR domain-containing proteins which are part of the Myddosome is affected.

The cytoplasmic TLR9 TIR domain interacted only moderately with MyD88 in LUMIER studies (Figure 3.14), independently if expressed as WT or L265P. However, TLR9-deficient mouse B cells ectopically expressing MyD88 L265P lost their ability to proliferate even in the absence of mitotic TLR9 stimuli[101], which indicates that the situation in primary cells is more complex as represented by our experiments. It is generally accepted that TLR9 receptors rest in the endosomal membrane as preformed homodimers in the steady state. Merely after ligand engagement the cytoplasmic pre-dimerized TIR domains undergo conformational changes which is required for the recruitment of adaptor proteins like MyD88[32]. A conceivable explanation for the partial TLR9-dependency of oncogenic MyD88 would be that the L265P mutation influences the receptors specificity by mediating the reverse reaction: hypothetically spoken, MyD88 L265P would engage TLR9 TIR-homodimers by augmented TIR-TIR hetero-oligomerization and therefore forcing the LRR ectodomains to bind improper ligands. Hence, positive allostery of receptors (TLR9) may be influenced by preformed intracellular signaling scaffolds like Myddosomes, which could potentially increase the affinity of receptors to their ligands. Or formulated in another way, reduce the receptors threshold that it binds also ligands not fitting that well to the corresponding LRRs, i.e. in case of TLR9 potentially self DNA from necrotic cells with comparatively high CpG contend. To verify those suppositions, co-IP and co-localization studies for MyD88 and TLR9 are planned in CpG-stimulated primary CLLs. Given that intact TLR9 signaling is critical for B cells with oncogenic MyD88 mutations[101] targeting this pathways would be an attractive option for lymphoma therapy. In this sense the clinical use of chloroquine, an agent which blocks endosomal acidification leading to inadequate folding of TLRs 7, 8, 9, is discussed[106] or inhibitory oligonucleotides capable of suppressing nucleotide-sensing TLR responses[160].

Surprisingly, although Mal was reported to be crucial for robust TLR9 responses[35], mRNA expression and protein levels of Mal in CLL cells were severely lowered compared with that of healthy B lymphocytes[161]. We found Mal to be dissociated from MyD88 L265P in contrast to WT in LUMIER assays (Figure 3.14). If this is of

any biological relevance in oncogenic MyD88-mutated malignancies has never been investigated so far and explanations remain hypothetical. Mal locates through its promiscuous phosphoinositide-binding domain at both plasma and endosomal membranes from where it acts as a bridging adaptor to recruit MyD88 to activated receptors, whereby Mal is an integral part of Myddosomes[35,162]. In this sense the TIR-domain of Mal controls an ordered Myddosome assembly by supporting cooperativity of heteromeric TIR oligomerization of receptors and adaptor proteins. One could speculate that in case of L265P-mutated MyD88, where a strong binding affinity to MyD88 TIRs was observed, the absence of Mal leads to an unordered and spontaneous MyD88 aggregation nucleating Myddosome signaling complexes. We are planning to verify the absent binding between these two TLR adaptors in lymphoma cells and are interested if binding is partially compensated for heterozygous mutations where one WT allelic copy of MyD88 is present. It is difficult to experimentally address if gain-of-function mutations in MyD88 simultaneously cause loss-of-function for Mal-controlled cooperativity in signaling complex assembly. One possibility would be to knockdown (i.e. with shRNAs) Mal or to (over-)express Mal WT or mutants described to disrupt MyD88 interaction[133] in lymphoma cells with subsequent investigation of Myddosome signaling and cellular survival outcome. That functionally loss of Mal not necessarily abrogates TLR signaling was showed by Horng et al.[163]: Mal-deficient mice displayed defects in NF-κB/MAPK activation and cytokine production after stimulation with LPS, but they retained intact responses to TLR7 and TLR9 ligands.

4.3.3 MyD88 L265P might alter signaling via SH2-domain containing tyrosine kinases

Yang et al. identified in co-IP studies that phosphorylated BTK complexed with MyD88 in L265P-expressing WM cells, which was vital for a robust NF-κB activation by synergizing with signaling via the MyD88-IRAK-axis[97]. Interestingly, treatment with a MyD88 peptide inhibitor (Loiarro et al.[123]), but not with a compound targeting IRAK4 and 1, effectively reduced the phosphorylation level of BTK, indicating that activation of the BTK axis (and not solely activation of the IRAK-axis) depends on MyD88 L265P-mediated oligomerization. Nevertheless the molecular basis for the interaction between MyD88 L265P and BTK remains unclear.

TLR4-mediated signaling leads to rapid activation of PI3K, a kinase family involved in regulation of cell growth, apoptosis, and motility. For instance, in LPS-treated mouse macrophages the p85 subunit of PI3K has been reported to co-precipitate with MyD88[164]. It is thought that the regulatory p85 subunit binds via its SH2 domain to phosphorylated tyrosine residues within a YXXM motif (SH2-binding motif) of distinct partner proteins. This in turn causes phosphorylation of the pre-

associated p110 kinase subunit leading to full activation of the PI3K complex[165]. Gelman et al.[166] showed that proliferation of mouse CD4+ T cell is influenced by TLR9-MyD88 responses mediating PI3K activation. Moreover PI3K activation was dependent on a single tyrosine residue (Y257 in mouse, corresponds to human Y270) located in a putative SH2 YKAM binding motif in the MyD88 TIR domain. Site-directed mutagenesis to Y257F (phenylalanine is similar to tyrosine in size but never phosphorylated) effectively prevented CpG-mediated PI3K-depedent phosphorylation of AKT and proliferation of cells. Laird et al.[165] confirmed this by comparing MyD88 mutation variants within the putative YKAM SH2-binding motif and measured their capacities to bind PI3K p85 by co-immunoprecipitation analysis. The MyD88 Y257A mutation (alanine not phosphorylated) showed slightly reduced interaction with p85. Intriguingly Y257A also revealed attenuated dimerization with WT MyD88. These observations may suggest a reciprocal activation and positive feedback loop between MyD88 (tyrosine phosphorylated at putative YKAM SH2 binding motif causes higher dimerization) and p85/p110 (recruited to MyD88 YKAM via its SH2 domain when Y270 is phosphorylated). The aforementioned study by Yang et al. supports our proposal of mutual feedback between MyD88 and SH2-domain tyrosine kinases in L265P-mutated WM cells. On the one hand inhibition of MyD88-dimerization reduced phosphorylation of the SH2-domain protein BTK and conversely, BTK inhibition with ibrutinib lowered interaction between both proteins[97]. The direct vicinity of oncogenic MyD88 L265P mutation might influence presumed Y270 phosphorylation and therefore create a beneficial binding interface for SH2-domain tyrosine kinases being involved in BCR signaling, such as BTK or PI3Ks. Indeed 2D-PAGE analysis of transfected MyD88 L265P precipitated from I3A cells (Figure 3.16) revealed a different pattern of posttranslational modifications between the mutant and WT, suggesting an altered phosphorylation for mutant MyD88. We investigated interactions between MyD88 and various SH2-domain tyrosine kinases known to intervene in B cell lymphoma growth, apoptosis and motility[95,129,167], by LUMIER. MyD88 L265P revealed a moderate affinity to both Src and Syk (Figure 3.15) but protein interactions were too low for explicit statements. For confirmation we will repeat LUMIER and test TIR interactions with SH2-domains of Src/Syk/BTK where we expect strong binding for the L265P which in turn is expectedly attenuated when Y270F is mutated in parallel. We also want to further investigate in DLBCL lines or primary CLL potential L265P-mediated MyD88 phosphorylation and interaction with SH2 domain-containing proteins. Therefore we consider performing IPs which will be subjected to 2D-PAGE or mass spectrometry. New potential candidates will be validated for their role as drivers in lymphomagenesis with shRNA-mediated knockdown or pharmacological inhibition. Consequently we hope to deliver a rationality why inhibition of SH2 domain-containing tyrosine kinases such as BTK, Syk and PI3K which already show

promise in lymphoma therapy[97,130,131,168], might be an option for the treatment of MyD88-mutated cases.

4.4 Potential treatment options of MyD88 L265P-mediated pathologies

MyD88 appears to act as a master regulator of intracellular signaling particularly in B cells. In case of oncogenic mutations recent evidence has highlighted the involvement of MyD88 in NF-κB, but additional also in non-canonical intracellular signaling pathways. Increasing publications suggest a variety of different treatment options (reviewed in[125]) in L265P-mutated lymphomas, including pharmaceutical kinase-inhibition (i.e. IRAKs, BTK, TAK1), or blocking TLR responses (inhibitory oligonucleotides and chloroquine). But inhibitors and their advancements are still tested in clinical settings in different phase trials. To our knowledge, only BTK inhibitor ibrutinib has already been tested successfully against L265P-mutated WM[168] and was also approved by the US Food and Drug Administration for the treatment of mantle cell lymphoma in 2013. Nevertheless, in CLL bypass mutations in *BTK* were reported leading to ibrutinib resistance[169-171], which corroborates the investigation of new inhibition strategies.

Given the unfavorable prognosis for many B cell cancers harboring MyD88 mutations, targeting its oligomerization would expand the portfolio of recently suggested inhibition strategies. But for clinical usage previously discussed MyD88 inhibitory peptides are rather inappropriate. Specific killing of L265P-mutated cells was effective only at high micromolar concentrations (Figure 3.13) and peptides might have only a restricted cell permeability and short half-life in vivo. I propose that a pharmacological blockade of TIR dimer formation by a small molecule would be a promising option. B-NHLs with MyD88 mutations are exclusively malignancies of the elderly. Therefore, for a good specific inhibitor interrupting MyD88 signaling, one would expect only moderate side effects, since patients with functional MyD88-deficiencies suffer from severe infections in childhood but remain healthy after reaching adulthood[132]. But, TIR homo- or heterotypic interactions are not well understood and some predictions are contradictory[39,40,133,172], and on a structural level dimers have never been crystalized, which hampers the design of small molecule inhibitors targeting MyD88.

Additionally, we suggest to evaluate oncogenic MyD88 mutations for individualized peptide-based T cell immunotherapy[173]. Since aforementioned lymphomas are cancerous neoplasms of the elderly and therefore gained after T cell selection in the thymus, HLA (human leukocyte antigen)-presented somatic mutations (in par-

ticular L265P) on cancer cells could potentially be recognized by CTLs as foreign epitopes and tumors eliminated.

But best therapeutic outcomes will probably not be achieved by using single but rather to combine various treatments. That such combinations could be beneficial was indicated by Yang et al.[97] where they report a synergistic effect of two small molecule inhibitors targeting BTK (with ibrutinib) and IRAKs (IRAK1 and 4) caused apoptosis selectively in MyD88 L265P-mutated primary WM cells, but not in WT B cells.

4.5 Conclusions and future plans

Genomic sequencing of B cell lymphoma samples revealed that several mutations of the MyD88 TIR domain, with L265P being the most frequent, acquired constitutive activation of signaling. Although others described that oncogenic MyD88 mutations hyperactivate NF-κB by effecting different kinases such as IRAKs[80,81], BTK[97] and TAK1[96] the fundamental molecular basis of these surveillances has remained elusive. Observations described in this report now deliver a rational molecular elucidation of this phenomenon. For instance, we could show that oncogenic MyD88 mutations display enlarged TIR domain oligomerization resulting in cytosolic aggregates, possibly signaling-active Myddosomes. Showing that mutated MyD88 employs WT for NF-κB activation might explain why one mutant allele is sufficient for tumorigenesis as suggested by heterozygosity of MyD88 L265P in the majority of B cell lymphomas. In this regard a single mutated allele would be necessary and sufficient to drive clonal expansion by providing a selective advantage. Taken together, our data suggest mutant MyD88 TIR dimer formation is a crucial key event for subsequent oncogenesis. In fact, we demonstrated sensitiveness of MyD88 L265P-mutated DLBCL lines towards decoy peptides blocking the TIR dimerization interface.

Cancer is the second most malignancy connected with morbidity in Germany and the United States (source: World Health Organization). Among all tumors, B cell Non-Hodgkin-Lymphomas with somatic MyD88 mutations are a considerable group associated with unfavorable outcome, i.e. in case of the frequent aggressive ABC subtype of DLBCL with MyD88 mutation rates higher than 30%. Standard treatments like surgical resection of tumors and chemotherapy often cause severe cytotoxic side effects and are frequently not an option because of progressed age of patients, i.e. the median of patients diagnosed with CLL is 72 years[174-176]. Thus, there is a crucial need for new forms of therapies being more selective against only cancer cells to avoid severe side effects.

However, for further improvement and clinical investigation there is an urgent need for good animal models. Since the MyD88 TIR is highly conserved among species and MyD88 mutations were shown to be early events and driver-mutations in lymphomagenesis, one would expect that mice with B cells expressing MyD88 L265P develop human-like diseases. Such a murine model would be entirely novel and ideal to verify observed changes in MyD88 interactions, post-translational modification, as well as effects on cellular growth and other B cell intrinsic signaling pathways. Although in vitro data from human cells are very insightful, L265P-mediated changes and evaluation of treatment options need to be addressed in vivo and therefore we propose to generate a murine model.

5 Appendix

5.1 Supplemental data

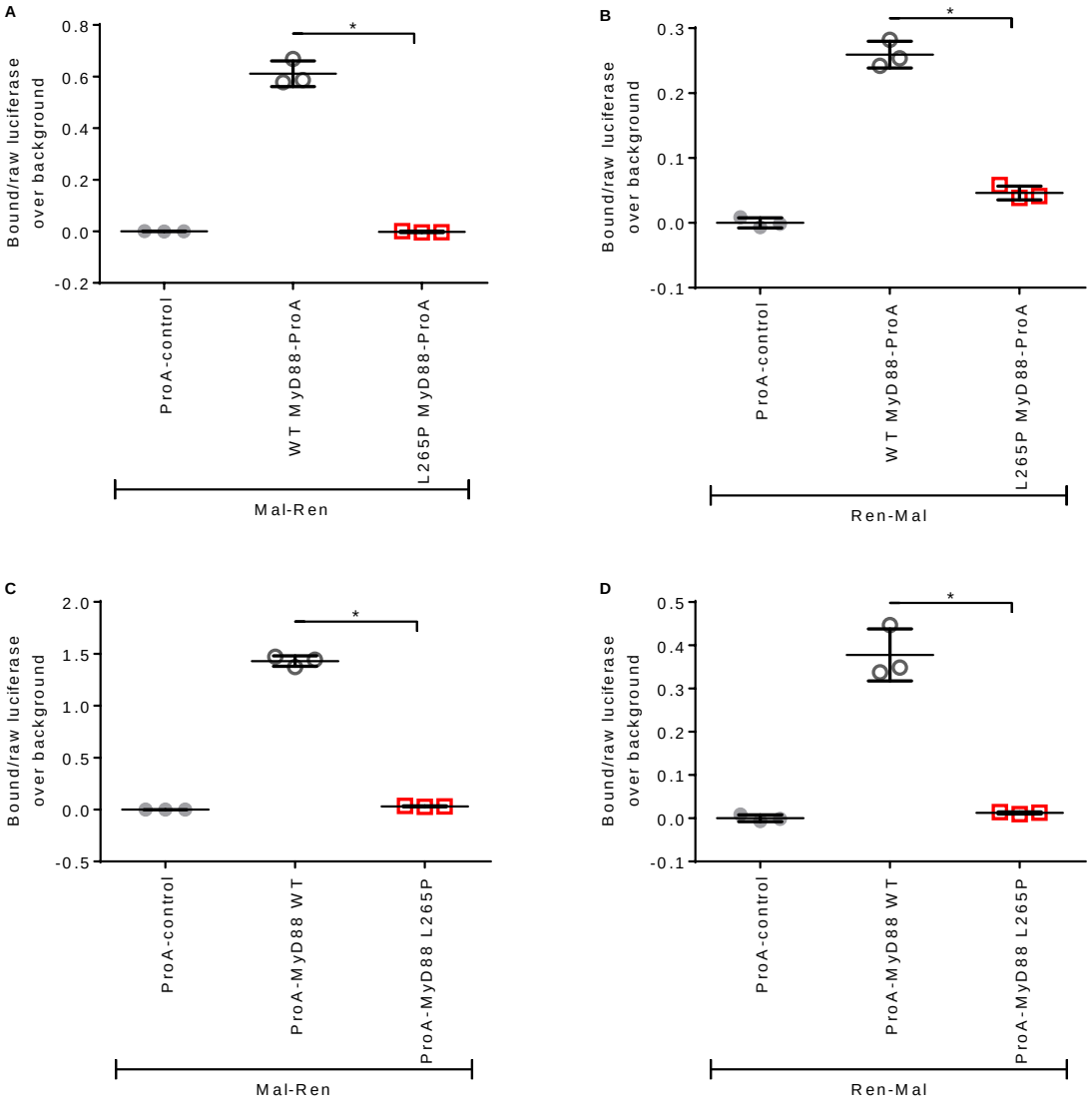

Figure 5.1: MyD88 L265P has a reduced binding affinity to Mal compared to MyD88 WT. LUMIER luciferase analysis from MyD88-deficient I3A cells transfected with C- (A, B) or N-terminal (C, D) Protein A-tagged (ProA) MyD88 WT or L265P together with C- (A, C) or N-terminal (B, D) Renilla-tagged (Ren) Mal. Assay performed as described for Figure 3.8. (A-D) Data represent triplicates from one experiment showing means +/- SDs. Statistical differences were tested by using unpaired t test. * $p < 0.05$.

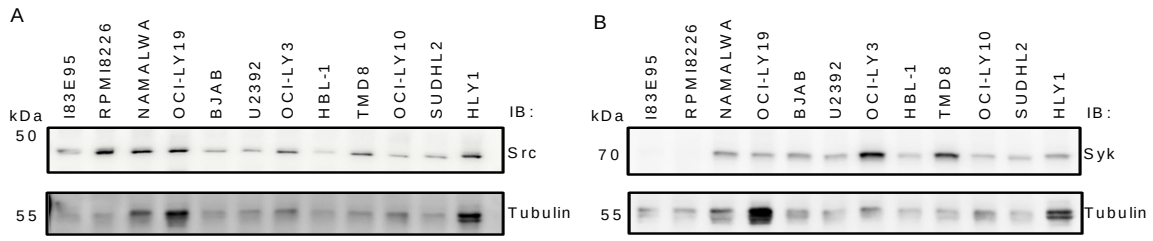

Figure 5.2: The SH2 domain-containing proteins Src and Syk are expressed in various B cell lymphoma lines.
Lysates (Promega passive lysis buffer) from different B cell Non-Hodgkin lymphoma lines were applied for SDS-PAGE and consequent immunoblot by probing with antibodies from Thermo Scientific specific for Src (clone 1F11) and Syk (clone 12E3). Nitrocellulose membranes were stripped (Restore™ Western Blot Stripping Buffer, Thermo Scientific) and re-probed for Tubulin which serves as a loading control.

5.2 Recipes of buffers and media

Table 5.1: Media and buffer solutions.
For media and buffers not listed in the table but used in this study please refer to[42].

Buffer/media	Recipe
2D-PAGE lysis buffer	7 M urea, 2 M thiourea, 4% CHAPS, 2% IPG buffer 3-10, supplemented with Complete Mini EDTA-free Protease Inhibitor Cocktail tablets from Roche
2D-PAGE rehydration buffer	7 M urea, 2 M thiourea, 4% CHAPS, 0.5% IPG buffer 3-10, 40 mM DTT
Blocking buffer immunoblot	TBS, 0.05% Tween® 20, 5% w/v BSA Fraction V from Biomol GmbH
HBS for calcium phosphate transfection	For 2x HBS stock mix 50 mM HEPES pH 7.05, 10 mM KCl, 12 mM dextrose, 280 mM NaCl, 1.5 mM Na_2HPO_4, aliquot and store at -80° C
LUMIER lysis buffer	20 mM Tris pH 7.5, 250 mM NaCl, 1% Triton-X100, 10 mM EDTA, 10 mM DTT, protease and phosphatase inhibitors from Roche, 0.0125 U/µl Benzonase from Sigma-Aldrich. Additionally buffer was supplemented with 10 % v/v of PBS-washed Dynabeads® M-280 Sheep Anti-Mouse IgG (Life Technologies).
LUMIER Renilla assay buffer	220 mM potassium phosphate buffer (1 M K2HPO4, 1 M KH2PO4, pH 5.1), 1.1 M NaCl, 2.2 mM EDTA, 0.44 mg/ml BSA
PBS (phosphate buffered saline)	8 g NaCl, 0.2 g KCl, 1.44 g Na_2HPO_4, fill with distilled water to a final volume of 1 l, adjust to pH 7.4
SDS running buffer	Tris 25 mM, glycine 250 mM, SDS 0.1%
Sodium borate buffer	5 mM di-sodium borate

Buffer/media	Recipe
RIPA lysis buffer	50 mM HEPES, 150 mM NaCl, 1% NP-40, 20 mM ß-glycerophosphate, 2 mM DTT, adjust to pH 6.9, freshly supplemented with Roche inhibitor tablets Complete Mini Protease Inhibitor and Phosstop Phosphatase inhibitor
TBS (Tris buffered saline)	50 mM Tris HCl pH 7.4, 150 mM NaCl
TE buffer	10 mM Tris pH 7.5, 0.5 M EDTA
Washing buffer immunoblot	TBS, 0.05% Tween® 20
LB media	1% w/v bacto tryptone, 0.5 % w/v yeast extract, 0.5% w/v NaCl, pH 7.5
S.O.C. media	2% w/v bacto tryptone, 0.5 % w/v yeast extract, 10 mM NaCl, 2.5 mM KCl, 20 mM glucose

5.3 Oligonucleotides

Table 5.2: Oligonucleotides used in this study to clone diverse Gateway entry clones.
All primers were purchased from biomers.net GmbH.

Name of primer	DNA sequence 5'-3'
AWx273_ F MYD88 5' attB1 KOZAK ATG	GGGGACAAGTTTGTACAAAAAAGCAGGCTACCATGG-CAGAGCTGGCGGGCATCACC
AWx274_ R MyD88 3' attB2 delStop ct	GGGGACCACTTTGTACAAGAAAGCTGGGTCGGG-CAGGGACAAGGCCTTGGCAAGGCG
AWx275_ F MyD88 FL attB1 nt	GGGGACAAGTTTGTACAAAAAAGCAGGCTTCATGGCTG-CAGGAGGTCCCGGCGC
AWx276_ F MyD88 TIR attB1 nt	GGGGACAAGTTTGTACAAAAAAGCAGGCTTCATGG-CAGAGCTGGCGGGCATCACC
AWx277_ R MyD88 Stop attB2 nt	GGGGACCACTTTGTACAAGAAAGCTGGGTCTCAGGG-CAGGGACAAGGCCTTGGC
AWx340_ F MYD88 FL attB1 KOZAK ATG	GGGGACAAGTTTGTACAAAAAAGCAGGCTACCATGGCTG-CAGGAGGTCCCGGCGC

5.4 Plasmid constructs used in this study

Table 5.3: Plasmids used in this study.
For plasmids not listed in the table but described in this study please refer to[42]

Plasmid	Description	Bacterial resistance	Reference
NF-κB reporter	Firefly luciferase reporter gene the under control of NF-κB p65 consensus promotor sequence	Ampicillin	Purchased from Stratagene
pEX008	pC1-EGFP plasmid constitutively encoding for enhanced green fluorescent protein (EGFP)	Ampicillin	From Clontech Laboratories
pEX118	pcDNA3-derived Gateway destination vector for expressing proteins with N-terminal Renilla fusion tag	Ampicillin	Gift from Manfred Kögl, DKFZ
pEX127	pDONR223 Gateway donor vector (entry clone) with human full length MyD88 WT aa 13-296 open construct without stop codon	Spectinomycin	DKFZ core facility clone number 100847135
pEX140	pT-Rex-derived Gateway destination vector expressing Protein A fused to N-terminal Protein A tag (control for LUMIER, see 2.3.6)	Ampicillin	Gift from Manfred Kögl, DKFZ
pEX141	pENTR221 Gateway donor vector (entry clone) with human IRAK1 open construct (no stop-codon) inserted	kanamycin	Purchased from imaGenes GmbH
pEX144	pTO-N-SH Gateway destination vector for expressing proteins with N-terminal Strep-hemagglutinin fusion tag	Ampicillin	Gift from Andreas Pichlmair
pEX145	pTO-C-SH Gateway destination vector for expressing proteins with C-terminal Strep-hemagglutinin fusion tag	Ampicillin	Gift from Andreas Pichlmair
pEX146	pT-Rex-DEST30-derived Gateway destination vector for expressing proteins with C-terminal Protein A fusion tag	Ampicillin	Gift from Manfred Kögl, DKFZ
pEX147	pT-Rex-DEST30-derived Gateway destination vector for expressing proteins with N-terminal Protein A fusion tag	Ampicillin	Gift from Manfred Kögl, DKFZ
pEX167	pdECFP-C1 Gateway compatible destination vector for expressing proteins with C-terminal CFP fusion tag	Ampicillin	Gift from Stefan Wiemann

Plasmid	Description	Bacterial resistance	Reference
pEX193	Gateway compatible destination vector for expressing proteins with C-terminal EGFP fusion tag	Ampicillin	Stefan Pusch
pEX194	Gateway compatible destination vector for expressing proteins with N-terminal EGFP fusion tag	Ampicillin	Stefan Pusch
pEX234	pDONR207 Gateway donor vector (entry clone) with ccdB lethal gene flanked by attP recombination sites	Gentamycin	Life Technologies
pEX331	pLG4.47(luc2P/SIE/Hygro) firefly reporter gene under the control of a STAT3 promotor consensus sequence	Ampicillin	Purchased from Promega
pEX332	pDONR223 Gateway donor vector (entry clone) with human Syk (CV025937) construct without stop codon	Spectinomycin	human ORFome Version 1.1, send by Jelena Knezevic
pEX351	pRL-TK Renilla luciferase control reporter vector	Ampicillin	Purchased from Promega
pEX467	pUC57 human TLR9 (Q9NR96) cytoplasmic domain aa 840-1032 closed (with stop-codon) flanked by *attL* sites (Gateway entry clone-like)	Kanamycin	Purchased from GENEWIZ
pEX506	pENTR221 Gateway donor vector (entry clone) with human SRC (EU831519) open (no stop-codon) inserted	Kanamycin	Gift from Christopher Oakes, DKFZ
pHW011	pT-Rex-DEST30-derived Gateway destination vector (pEX117) expressing human Mal Iso A with C-terminal Renilla tag	Ampicillin	Hui Wang
pHW012	pcDNA3-derived Gateway destination vector (pEX118) expressing human Mal Iso A with N-terminal Renilla tag	Ampicillin	Hui Wang
pHW014	pT-Rex-DEST30-derived Gateway destination vector (pEX147) expressing human TRAF6 with C-terminal Protein A tag	Ampicillin	Hui Wang
pHW041	pT-Rex-DEST30-derived Gateway destination vector (pEX147) expressing human IRAK2 with C-terminal Protein A tag	Ampicillin	Hui Wang

Plasmid	Description	Bacterial resistance	Reference
pHW143	pDONR223 Gateway donor vector (entry clone) with human full length MyD88 L265P aa 13-296 open construct without stop codon (site directed mutagenesis of pEX127)	Spectinomycin	Hui Wang
pHW161	pT-Rex-DEST30-derived Gateway destination vector (pEX147) expressing human IRAK1 with C-terminal Protein A tag	Ampicillin	Hui Wang
pJG072	pT-Rex-DEST30-derived Gateway destination vector (pEX147) expressing human MyD88 death domain fused to Myc with N-terminal Protein A tag	Ampicillin	Julie George, described[64]
pJG117	pT-Rex-DEST30-derived Gateway destination vector (pEX146) expressing human IRAK4 dead kinase mutation with C-terminal Protein A tag	Ampicillin	Julie George
pOW005	pDONR207 Gateway donor vector (entry clone) with inserted human MyD88 WT TIR aa 155-296 open construct without stop codon	Gentamycin	This study
pOW006	pDONR207 Gateway donor vector (entry clone) with inserted human MyD88 L265P TIR aa 155-296 open construct without stop codon	Gentamycin	This study
pOW011	pDONR207 Gateway donor vector (entry clone) with human full length MyD88 WT aa 13-296 closed construct with stop codon	Gentamycin	This study
pOW012	pDONR207 Gateway donor vector (entry clone) with human full length MyD88 L265P aa 13-296 closed construct with stop codon	Gentamycin	This study
pOW013	pDONR207 Gateway donor vector (entry clone) with human MyD88 WT TIR aa 155-296 closed construct with stop codon	Gentamycin	This study
pOW014	pDONR207 Gateway donor vector (entry clone) with human MyD88 L265P TIR aa 155-296 closed construct with stop codon	Gentamycin	This study
pOW016	pT-Rex-DEST30-derived Gateway destination vector (pEX147) expressing human full length MyD88 WT aa 13-296 with N-terminal Protein A tag	Ampicillin	This study

Plasmid	Description	Bacterial resistance	Reference
pOW017	pT-Rex-DEST30-derived Gateway destination vector (pEX147) expressing human full length MyD88 L265P aa 13-296 with N-terminal Protein A tag	Ampicillin	This study
pOW018	pcDNA3-derived Gateway destination vector (pEX118) expressing human full length MyD88 WT aa 13-296 with N-terminal Renilla tag	Ampicillin	This study
pOW019	pcDNA3-derived Gateway destination vector (pEX118) expressing human full length MyD88 L265P aa 13-296 with N-terminal Renilla tag	Ampicillin	This study
pOW020	pT-Rex-DEST30-derived Gateway destination vector (pEX147) expressing human MyD88 WT TIR aa 155-296 with N-terminal Protein A tag	Ampicillin	This study
pOW021	pT-Rex-DEST30-derived Gateway destination vector (pEX147) expressing human MyD88 L265P TIR aa 155-296 with N-terminal Protein A tag	Ampicillin	This study
pOW022	pcDNA3-derived Gateway destination vector (pEX118) expressing human MyD88 WT TIR aa 155-296 with N-terminal Renilla tag	Ampicillin	This study
pOW023	pcDNA3-derived Gateway destination vector (pEX118) expressing human MyD88 L265P TIR aa 155-296 with N-terminal Renilla tag	Ampicillin	This study
pOW024	pTO-C-SH Gateway destination vector (pEX145) expressing human full length MyD88 WT aa 13-296 with C-terminal StrepHA tag	Ampicillin	This study
pOW025	pTO-C-SH Gateway destination vector (pEX145) expressing human full length MyD88 L265P aa 13-296 with C-terminal StrepHA tag	Ampicillin	This study
pOW026	pTO-C-SH Gateway destination vector (pEX145) expressing human MyD88 WT TIR aa 155-296 with C-terminal StrepHA tag	Ampicillin	This study
pOW027	pTO-C-SH Gateway destination vector (pEX145) expressing human MyD88 L265P TIR aa 155-296 with C-terminal StrepHA tag	Ampicillin	This study

Plasmid	Description	Bacterial resistance	Reference
pOW030	pTO-N-SH Gateway destination vector (pEX144) expressing human full length MyD88 WT aa 13-296 with N-terminal StrepHA tag	Ampicillin	This study
pOW031	pTO-N-SH Gateway destination vector (pEX144) expressing human full length MyD88 L265P aa 13-296 with N-terminal StrepHA tag	Ampicillin	This study
pOW028	pTO-N-SH Gateway destination vector (pEX144) expressing human MyD88 WT TIR aa 155-296 with N-terminal StrepHA tag	Ampicillin	This study
pOW029	pTO-N-SH Gateway destination vector (pEX144) expressing human MyD88 L265P TIR aa 155-296 with N-terminal StrepHA tag	Ampicillin	This study
pOW035	pDONR207 Gateway donor vector (entry clone) with human full length MyD88 WT aa 13-296 (contains KOZAK and ATG start codon, closed construct with stop codon) inserted	Gentamycin	This study
pOW035	pDONR207 Gateway donor vector (entry clone) with human full length MyD88 L265P aa 13-296 (contains KOZAK and ATG start codon, closed construct with stop codon) inserted	Gentamycin	This study
pOW060	pTO-C-SH Gateway destination vector (pEX145) expressing human full length MyD88 WT aa 13-296 without fusion tag	Ampicillin	This study
pOW061	pTO-C-SH Gateway destination vector (pEX145) expressing human full length MyD88 L265P aa 13-296 without fusion tag	Ampicillin	This study
pOW101	pT-Rex-DEST30-derived Gateway destination vector (pEX146) expressing human Syk (entry pEX332) with C-terminal Protein A tag	Ampicillin	This study
pOW114	pT-Rex-DEST30-derived Gateway destination vector (pEX147) expressing human Mal isoform A (entry clone pEX126) with N-terminal Protein A tag	Ampicillin	This study

Plasmid	Description	Bacterial resistance	Reference
pOW140	pT-Rex-DEST30-derived Gateway destination vector (pEX146) expressing human SRC (entry pEX506) with C-terminal Protein A tag	Ampicillin	This study
pOW143	pT-Rex-DEST30-derived Gateway destination vector (pEX147) expressing human TLR9 cytoplasmic domain aa 840-1032 (entry clone pEX467) with N-terminal Protein A tag	Ampicillin	This study
pOW146	pdECFP-C1 Gateway destination vector (pEX167) expressing human full length MyD88 WT aa 13-296 with N-terminal CFP fusion tag	Ampicillin	This study
pOW147	pdECFP-C1 Gateway destination vector (pEX167) expressing human full length MyD88 L265P aa 13-296 with N-terminal CFP fusion tag	Ampicillin	This study
pOW148	Gateway destination vector (pEX193) expressing IRAK1 with C-terminal EGFP fusion tag	Ampicillin	This study

5.5 List of used antibodies in immunoblot analysis

Table 5.4: Antibodies used in this study.
For antibodies not listed in the table but described in this study please refer to[42]. All antibodies were dilute in TBS-based blocking buffer (Table 5.1).

Antibody	Raised in species	Working dilution	Manufacturer (catalogue number)
Anti-mouse HRP conjugated		1:5000	Promega (W4028)
Anti-rabbit HRP conjugated	Goat	1:5000	Vector Laboratories (PI-1000)
Anti-rabbit conformation specific HRP conjugated	Mouse	1:2000	Cell Signaling (L27A9)
Anti-rat HRP conjugated	Goat	1:2000	Cell Signaling (7077)
Anti-HA (hemagglutinin) C29F4 monoclonal	Rabbit	1:1000	Cell Signaling (3724)
Anti-IRAK1 D51G7 monoclonal	Rabbit	1:1000	Cell Signaling (4504)
Anti-TIRAP (Mal) Sebi-1 clone	Rat	1:500	Abnova (MAB3447)
Anti-MyD88 D80F5 monoclonal	Rabbit	1:1000	Cell Signaling (4283)
Anti-Protein A	Rabbit	1:625000	Sigma Aldrich (P3775)
Anti-Renilla Luciferase clone 1D5.2	Mouse	1:2500	Merck Millipore (MAB4410)
Anti-Tubulin clone TUB 2.1	Mouse	1:5000	Sigma Aldrich (T5201)
Anti-Src clone 1F11	Mouse	1:1000	Thermo Scientific (MA5-15924)
Anti-Syk clone 12E3	Mouse	1:1000	Thermo Scientific (MA5-17207)

References

1. Chaplin DD. Overview of the immune response. *J Allergy Clin Immunol*. 2010;125(2 Suppl 2):S3-23.

2. Janeway CA, Jr. Approaching the asymptote? Evolution and revolution in immunology. *Cold Spring Harb Symp Quant Biol*. 1989;54 Pt 1:1-13.

3. Lemaitre B, Nicolas E, Michaut L, Reichhart JM, Hoffmann JA. The dorsoventral regulatory gene cassette spatzle/Toll/cactus controls the potent antifungal response in Drosophila adults. *Cell*. 1996;86(6):973-983.

4. Medzhitov R, Preston-Hurlburt P, Janeway CA, Jr. A human homologue of the Drosophila Toll protein signals activation of adaptive immunity. *Nature*. 1997;388(6640):394-397.

5. Poltorak A, He X, Smirnova I, et al. Defective LPS signaling in C3H/HeJ and C57BL/10ScCr mice: mutations in Tlr4 gene. *Science*. 1998;282(5396):2085-2088.

6. Ausubel FM. Are innate immune signaling pathways in plants and animals conserved? *Nat Immunol*. 2005;6(10):973-979.

7. Didierlaurent A, Simonet M, Sirard JC. Innate and acquired plasticity of the intestinal immune system. *Cell Mol Life Sci*. 2005;62(12):1285-1287.

8. Takeuchi O, Akira S. Pattern recognition receptors and inflammation. *Cell*. 2010;140(6):805-820.

9. O'Neill LA, Golenbock D, Bowie AG. The history of Toll-like receptors - redefining innate immunity. *Nat Rev Immunol*. 2013;13(6):453-460.

10. Flannery S, Bowie AG. The interleukin-1 receptor-associated kinases: critical regulators of innate immune signalling. *Biochem Pharmacol*. 2010;80(12):1981-1991.

11. Parkin J, Cohen B. An overview of the immune system. *Lancet*. 2001;357(9270):1777-1789.

12. Bekeredjian-Ding I, Jego G. Toll-like receptors--sentries in the B-cell response. *Immunology*. 2009;128(3):311-323.

13. Gay NJ, Gangloff M, O'Neill LA. What the Myddosome structure tells us about the initiation of innate immunity. *Trends Immunol*. 2011;32(3):104-109.

14. O'Neill LA. The interleukin-1 receptor/Toll-like receptor superfamily: 10 years of progress. *Immunol Rev*. 2008;226:10-18.

15. Watters TM, Kenny EF, O'Neill LA. Structure, function and regulation of the Toll/IL-1 receptor adaptor proteins. *Immunol Cell Biol*. 2007;85(6):411-419.

16. Kawai T, Akira S. Toll-like receptor and RIG-I-like receptor signaling. *Ann N Y Acad Sci*. 2008;1143:1-20.

17. Gay NJ, Gangloff M, Weber AN. Toll-like receptors as molecular switches. *Nat Rev Immunol*. 2006;6(9):693-698.

18. Gay NJ, Symmons MF, Gangloff M, Bryant CE. Assembly and localization of Toll-like receptor signalling complexes. *Nat Rev Immunol*. 2014;14(8):546-558.

19. Deng L, Wang C, Spencer E, et al. Activation of the IkappaB kinase complex by TRAF6 requires a dimeric ubiquitin-conjugating enzyme complex and a unique polyubiquitin chain. *Cell*. 2000;103(2):351-361.

20. Ninomiya-Tsuji J, Kishimoto K, Hiyama A, Inoue J, Cao Z, Matsumoto K. The kinase TAK1 can activate the NIK-I kappaB as well as the MAP kinase cascade in the IL-1 signalling pathway. *Nature*. 1999;398(6724):252-256.

21. Kawai T, Akira S. Toll-like receptor and RIG-I-like receptor signaling. *Annals of the New York Academy of Sciences*. 2008;1143:1-20.

22. De Nardo D. Toll-like receptors: Activation, signalling and transcriptional modulation. *Cytokine*. 2015.

23. Kagan JC, Su T, Horng T, Chow A, Akira S, Medzhitov R. TRAM couples endocytosis of Toll-like receptor 4 to the induction of interferon-beta. *Nat Immunol*. 2008;9(4):361-368.

24. West AP, Koblansky AA, Ghosh S. Recognition and signaling by toll-like receptors. *Annu Rev Cell Dev Biol*. 2006;22:409-437.

25. Bourke E, Bosisio D, Golay J, Polentarutti N, Mantovani A. The toll-like receptor repertoire of human B lymphocytes: inducible and selective expression of TLR9 and TLR10 in normal and transformed cells. *Blood*. 2003;102(3):956-963.

26. Abreu MT. Toll-like receptor signalling in the intestinal epithelium: how bacterial recognition shapes intestinal function. *Nat Rev Immunol*. 2010;10(2):131-144.

27. Panter G, Jerala R. The ectodomain of the Toll-like receptor 4 prevents constitutive receptor activation. *J Biol Chem*. 2011;286(26):23334-23344.

28. Yoon SI, Kurnasov O, Natarajan V, et al. Structural basis of TLR5-flagellin recognition and signaling. *Science*. 2012;335(6070):859-864.

29. Kang JY, Nan X, Jin MS, et al. Recognition of lipopeptide patterns by Toll-like receptor 2-Toll-like receptor 6 heterodimer. *Immunity*. 2009;31(6):873-884.

30. Jin MS, Kim SE, Heo JY, et al. Crystal structure of the TLR1-TLR2 heterodimer induced by binding of a tri-acylated lipopeptide. *Cell*. 2007;130(6):1071-1082.

31. Liu L, Botos I, Wang Y, et al. Structural basis of toll-like receptor 3 signaling with double-stranded RNA. *Science*. 2008;320(5874):379-381.

32. Latz E, Verma A, Visintin A, et al. Ligand-induced conformational changes allosterically activate Toll-like receptor 9. *Nat Immunol*. 2007;8(7):772-779.

33. Tanji H, Ohto U, Shibata T, Miyake K, Shimizu T. Structural reorganization of the Toll-like receptor 8 dimer induced by agonistic ligands. *Science*. 2013;339(6126):1426-1429.

34. Casrouge A, Zhang SY, Eidenschenk C, et al. Herpes simplex virus encephalitis in human UNC-93B deficiency. *Science*. 2006;314(5797):308-312.

35. Bonham KS, Orzalli MH, Hayashi K, et al. A promiscuous lipid-binding protein diversifies the subcellular sites of toll-like receptor signal transduction. *Cell*. 2014;156(4):705-716.

36. Lingwood D, Kaiser HJ, Levental I, Simons K. Lipid rafts as functional heterogeneity in cell membranes. *Biochem Soc Trans*. 2009;37(Pt 5):955-960.

37. Motshwene PG, Moncrieffe MC, Grossmann JG, et al. An oligomeric signaling platform formed by the Toll-like receptor signal transducers MyD88 and IRAK-4. *J Biol Chem*. 2009;284(37):25404-25411.

38. Kagan JC, Medzhitov R. Phosphoinositide-mediated adaptor recruitment controls Toll-like receptor signaling. *Cell*. 2006;125(5):943-955.

39. Ohnishi H, Tochio H, Kato Z, et al. Structural basis for the multiple interactions of the MyD88 TIR domain in TLR4 signaling. *Proceedings of the National Academy of Sciences of the United States of America*. 2009;106(25):10260-10265.

40. Snyder GA, Cirl C, Jiang J, et al. Molecular mechanisms for the subversion of MyD88 signaling by TcpC from virulent uropathogenic Escherichia coli. *Proc Natl Acad Sci U S A*. 2013;110(17):6985-6990.

41. Bartfai T, Behrens MM, Gaidarova S, Pemberton J, Shivanyuk A, Rebek J, Jr. A low molecular weight mimic of the Toll/IL-1 receptor/resistance domain inhibits IL-1 receptor-mediated responses. *Proc Natl Acad Sci U S A*. 2003;100(13):7971-7976.

42. Avbelj M, Wolz OO, Fekonja O, et al. Activation of lymphoma-associated MyD88 mutations via allostery-induced TIR-domain oligomerization. *Blood*. 2014;124(26):3896-3904.

43. Funami K, Sasai M, Ohba Y, Oshiumi H, Seya T, Matsumoto M. Spatiotemporal mobilization of Toll/IL-1 receptor domain-containing adaptor molecule-1 in response to dsRNA. *J Immunol*. 2007;179(10):6867-6872.

44. Burns K, Janssens S, Brissoni B, Olivos N, Beyaert R, Tschopp J. Inhibition of interleukin 1 receptor/Toll-like receptor signaling through the alternatively spliced, short form of MyD88 is due to its failure to recruit IRAK-4. *J Exp Med*. 2003;197(2):263-268.

45. Avbelj M, Horvat S, Jerala R. The role of intermediary domain of MyD88 in cell activation and therapeutic inhibition of TLRs. *J Immunol*. 2011;187(5):2394-2404.

46. He B, Santamaria R, Xu W, et al. The transmembrane activator TACI triggers immunoglobulin class switching by activating B cells through the adaptor MyD88. *Nat Immunol*. 2010;11(9):836-845.

47. Fitzgerald KA, Palsson-McDermott EM, Bowie AG, et al. Mal (MyD88-adapter-like) is required for Toll-like receptor-4 signal transduction. *Nature*. 2001;413(6851):78-83.

48. Dunne A, Carpenter S, Brikos C, et al. IRAK1 and IRAK4 promote phosphorylation, ubiquitination, and degradation of MyD88 adaptor-like (Mal). *J Biol Chem*. 2010;285(24):18276-18282.

49. Gray P, Dunne A, Brikos C, Jefferies CA, Doyle SL, O'Neill LA. MyD88 adapter-like (Mal) is phosphorylated by Bruton's tyrosine kinase during TLR2 and TLR4 signal transduction. *J Biol Chem*. 2006;281(15):10489-10495.

50. Mansell A, Smith R, Doyle SL, et al. Suppressor of cytokine signaling 1 negatively regulates Toll-like receptor signaling by mediating Mal degradation. *Nat Immunol*. 2006;7(2):148-155.

51. Miggin SM, Palsson-McDermott E, Dunne A, et al. NF-kappaB activation by the Toll-IL-1 receptor domain protein MyD88 adapter-like is regulated by caspase-1. *Proc Natl Acad Sci U S A*. 2007;104(9):3372-3377.

52. Khor CC, Chapman SJ, Vannberg FO, et al. A Mal functional variant is associated with protection against invasive pneumococcal disease, bacteremia, malaria and tuberculosis. *Nat Genet*. 2007;39(4):523-528.

53. Zhang YX, Xue Y, Liu JY, et al. Association of TIRAP (MAL) gene polymorhisms with susceptibility to tuberculosis in a Chinese population. *Genet Mol Res*. 2011;10(1):7-15.

54. von Bernuth H, Picard C, Jin Z, et al. Pyogenic bacterial infections in humans with MyD88 deficiency. *Science*. 2008;321(5889):691-696.

55. George J, Kubarenko AV, Rautanen A, et al. MyD88 adaptor-like D96N is a naturally occurring loss-of-function variant of TIRAP. *J Immunol*. 2010;184(6):3025-3032.

56. Tatematsu M, Ishii A, Oshiumi H, et al. A molecular mechanism for Toll-IL-1 receptor domain-containing adaptor molecule-1-mediated IRF-3 activation. *J Biol Chem*. 2010;285(26):20128-20136.

57. Sancho-Shimizu V, Perez de Diego R, Lorenzo L, et al. Herpes simplex encephalitis in children with autosomal recessive and dominant TRIF deficiency. *J Clin Invest*. 2011;121(12):4889-4902.

58. Gangloff M. Different dimerisation mode for TLR4 upon endosomal acidification? *Trends Biochem Sci*. 2012;37(3):92-98.

59. Rowe DC, McGettrick AF, Latz E, et al. The myristoylation of TRIF-related adaptor molecule is essential for Toll-like receptor 4 signal transduction. *Proc Natl Acad Sci U S A*. 2006;103(16):6299-6304.

60. McGettrick AF, Brint EK, Palsson-McDermott EM, et al. Trif-related adapter molecule is phosphorylated by PKC{epsilon} during Toll-like receptor 4 signaling. *Proc Natl Acad Sci U S A*. 2006;103(24):9196-9201.

61. Carty M, Goodbody R, Schroder M, Stack J, Moynagh PN, Bowie AG. The human adaptor SARM negatively regulates adaptor protein TRIF-dependent Toll-like receptor signaling. *Nat Immunol*. 2006;7(10):1074-1081.

62. Ferrao R, Wu H. Helical assembly in the death domain (DD) superfamily. *Curr Opin Struct Biol*. 2012;22(2):241-247.

63. Lin SC, Lo YC, Wu H. Helical assembly in the MyD88-IRAK4-IRAK2 complex in TLR/IL-1R signalling. *Nature*. 2010;465(7300):885-890.

64. George J, Motshwene PG, Wang H, et al. Two human MYD88 variants, S34Y and R98C, interfere with MyD88-IRAK4-Myddosome assembly. *The Journal of biological chemistry*. 2011;286(2):1341-1353.

65. Li S, Strelow A, Fontana EJ, Wesche H. IRAK-4: a novel member of the IRAK family with the properties of an IRAK-kinase. *Proc Natl Acad Sci U S A*. 2002;99(8):5567-5572.

66. Picard C, Puel A, Bonnet M, et al. Pyogenic bacterial infections in humans with IRAK-4 deficiency. *Science*. 2003;299(5615):2076-2079.

67. von Bernuth H, Picard C, Puel A, Casanova JL. Experimental and natural infections in MyD88- and IRAK-4-deficient mice and humans. *Eur J Immunol*. 2012;42(12):3126-3135.

68. Kawagoe T, Sato S, Matsushita K, et al. Sequential control of Toll-like receptor-dependent responses by IRAK1 and IRAK2. *Nat Immunol*. 2008;9(6):684-691.

69. Thomas JA, Allen JL, Tsen M, et al. Impaired cytokine signaling in mice lacking the IL-1 receptor-associated kinase. *J Immunol*. 1999;163(2):978-984.

70. Keating SE, Maloney GM, Moran EM, Bowie AG. IRAK-2 participates in multiple toll-like receptor signaling pathways to NFkappaB via activation of TRAF6 ubiquitination. *J Biol Chem*. 2007;282(46):33435-33443.

71. Wang Z, Liu J, Sudom A, et al. Crystal structures of IRAK-4 kinase in complex with inhibitors: a serine/threonine kinase with tyrosine as a gatekeeper. *Structure*. 2006;14(12):1835-1844.

72. Kuglstatter A, Villasenor AG, Shaw D, et al. Cutting Edge: IL-1 receptor-associated kinase 4 structures reveal novel features and multiple conformations. *J Immunol*. 2007;178(5):2641-2645.

73. Powers JP, Li S, Jaen JC, et al. Discovery and initial SAR of inhibitors of interleukin-1 receptor-associated kinase-4. *Bioorg Med Chem Lett*. 2006;16(11):2842-2845.

74. Wang Z, Wesche H, Stevens T, Walker N, Yeh WC. IRAK-4 inhibitors for inflammation. *Curr Top Med Chem*. 2009;9(8):724-737.

75. Hou J, Wang P, Lin L, et al. MicroRNA-146a feedback inhibits RIG-I-dependent Type I IFN production in macrophages by targeting TRAF6, IRAK1, and IRAK2. *J Immunol*. 2009;183(3):2150-2158.

76. Netea MG, Wijmenga C, O'Neill LA. Genetic variation in Toll-like receptors and disease susceptibility. *Nat Immunol*. 2012;13(6):535-542.

77. Hoarau C, Gerard B, Lescanne E, et al. TLR9 activation induces normal neutrophil responses in a child with IRAK-4 deficiency: involvement of the direct PI3K pathway. *J Immunol*. 2007;179(7):4754-4765.

78. Yamamoto T, Tsutsumi N, Tochio H, et al. Functional assessment of the mutational effects of human IRAK4 and MyD88 genes. *Mol Immunol*. 2014;58(1):66-76.

79. Treon SP, Xu L, Yang G, et al. MYD88 L265P somatic mutation in Waldenstrom's macroglobulinemia. *N Engl J Med*. 2012;367(9):826-833.

80. Ngo VN, Young RM, Schmitz R, et al. Oncogenically active MYD88 mutations in human lymphoma. *Nature*. 2011;470(7332):115-119.

81. Puente XS, Pinyol M, Quesada V, et al. Whole-genome sequencing identifies recurrent mutations in chronic lymphocytic leukaemia. *Nature*. 2011;475(7354):101-105.

82. Poulain S, Roumier C, Decambron A, et al. MYD88 L265P mutation in Waldenstrom macroglobulinemia. *Blood*. 2013;121(22):4504-4511.

83. Choi JW, Kim Y, Lee JH, Kim YS. MYD88 expression and L265P mutation in diffuse large B-cell lymphoma. *Human pathology*. 2013;44(7):1375-1381.

84. Pasqualucci L, Trifonov V, Fabbri G, et al. Analysis of the coding genome of diffuse large B-cell lymphoma. *Nature genetics*. 2011;43(9):830-837.

85. Traverse-Glehen A, Bachy E, Baseggio L, et al. Immunoarchitectural patterns in splenic marginal zone lymphoma: correlations with chromosomal aberrations, IGHV mutations, and survival. A study of 76 cases. *Histopathology*. 2013;62(6):876-893.

86. Puente XS, Pinyol M, Quesada V, et al. Whole-genome sequencing identifies recurrent mutations in chronic lymphocytic leukaemia. *Nature*. 2011;475(7354):101-105.

87. Landau DA, Carter SL, Stojanov P, et al. Evolution and impact of subclonal mutations in chronic lymphocytic leukemia. *Cell*. 2013;152(4):714-726.

88. Varettoni M, Arcaini L, Zibellini S, et al. Prevalence and clinical significance of the MYD88 (L265P) somatic mutation in Waldenstrom's macroglobulinemia and related lymphoid neoplasms. *Blood*. 2013;121(13):2522-2528.

89. Treon SP, Xu L, Yang G, et al. MYD88 L265P somatic mutation in Waldenstrom's macroglobulinemia. *The New England journal of medicine*. 2012;367(9):826-833.

90. Xu L, Hunter ZR, Yang G, et al. MYD88 L265P in Waldenstrom macroglobulinemia, immunoglobulin M monoclonal gammopathy, and other B-cell lymphoproliferative disorders using conventional and quantitative allele-specific polymerase chain reaction. *Blood*. 2013;121(11):2051-2058.

91. Pham-Ledard A, Prochazkova-Carlotti M, Andrique L, et al. Multiple genetic alterations in primary cutaneous large B-cell lymphoma, leg type support a common lymphomagenesis with activated B-cell-like diffuse large B-cell lymphoma. *Modern pathology : an official journal of the United States and Canadian Academy of Pathology, Inc*. 2013.

92. Montesinos-Rongen M, Godlewska E, Brunn A, Wiestler OD, Siebert R, Deckert M. Activating L265P mutations of the MYD88 gene are common in primary central nervous system lymphoma. *Acta neuropathologica*. 2011;122(6):791-792.

93. Zhu D, Ikpatt OF, Dubovy SR, et al. Molecular and genomic aberrations in Chlamydophila psittaci negative ocular adnexal marginal zone lymphomas. *American journal of hematology*. 2013;88(9):730-735.

94. Gachard N, Parrens M, Soubeyran I, et al. IGHV gene features and MYD88 L265P mutation separate the three marginal zone lymphoma entities and Waldenstrom macroglobulinemia/lymphoplasmacytic lymphomas. *Leukemia*. 2013;27(1):183-189.

95. Chen L, Monti S, Juszczynski P, et al. SYK inhibition modulates distinct PI3K/AKT- dependent survival pathways and cholesterol biosynthesis in diffuse large B cell lymphomas. *Cancer Cell*. 2013;23(6):826-838.

96. Ansell SM, Hodge LS, Secreto FJ, et al. Activation of TAK1 by MYD88 L265P drives malignant B-cell Growth in non-Hodgkin lymphoma. *Blood Cancer J*. 2014;4:e183.

97. Yang G, Zhou Y, Liu X, et al. A mutation in MYD88 (L265P) supports the survival of lymphoplasmacytic cells by activation of Bruton tyrosine kinase in Waldenstrom macroglobulinemia. *Blood*. 2013;122(7):1222-1232.

98. Shapiro-Shelef M, Lin KI, McHeyzer-Williams LJ, Liao J, McHeyzer-Williams MG, Calame K. Blimp-1 is required for the formation of immunoglobulin secreting plasma cells and pre-plasma memory B cells. *Immunity*. 2003;19(4):607-620.

99. Lin FR, Huang SY, Hung KH, et al. ASK1 promotes apoptosis of normal and malignant plasma cells. *Blood*. 2012;120(5):1039-1047.

100. Catz SD, Johnson JL. Transcriptional regulation of bcl-2 by nuclear factor kappa B and its significance in prostate cancer. *Oncogene*. 2001;20(50):7342-7351.

101. Wang JQ, Jeelall YS, Beutler B, Horikawa K, Goodnow CC. Consequences of the recurrent MYD88(L265P) somatic mutation for B cell tolerance. *J Exp Med*. 2014;211(3):413-426.

102. Ding BB, Yu JJ, Yu RY, et al. Constitutively activated STAT3 promotes cell proliferation and survival in the activated B-cell subtype of diffuse large B-cell lymphomas. *Blood*. 2008;111(3):1515-1523.

103. Xu L, Hunter ZR, Yang G, et al. MYD88 L265P in Waldenstrom's Macroglobulinemia, IgM Monoclonal Gammopathy, and other B-cell Lymphoproliferative Disorders using Conventional and Quantitative Allele-Specific PCR. *Blood*. 2013.

104. Varettoni M, Zibellini S, Arcaini L, et al. MYD88 (L265P) mutation is an independent risk factor for progression in patients with IgM monoclonal gammopathy of undetermined significance. *Blood*. 2013;122(13):2284-2285.

105. Landau DA, Carter SL, Getz G, Wu CJ. Clonal evolution in hematological malignancies and therapeutic implications. *Leukemia*. 2014;28(1):34-43.

106. Martinez-Trillos A, Pinyol M, Navarro A, et al. Mutations in TLR/MYD88 pathway identify a subset of young chronic lymphocytic leukemia patients with favorable outcome. *Blood*. 2014;123(24):3790-3796.

107. Chiorazzi N, Rai KR, Ferrarini M. Chronic lymphocytic leukemia. *N Engl J Med*. 2005;352(8):804-815.

108. Choi JW, Kim Y, Lee JH, Kim YS. MYD88 expression and L265P mutation in diffuse large B-cell lymphoma. *Hum Pathol*. 2013;44(7):1375-1381.

109. Fernandez-Rodriguez C, Bellosillo B, Garcia-Garcia M, et al. MYD88 (L265P) mutation is an independent prognostic factor for outcome in patients with diffuse large B-cell lymphoma. *Leukemia*. 2014;28(10):2104-2106.

110. Birnboim HC, Doly J. A rapid alkaline extraction procedure for screening recombinant plasmid DNA. *Nucleic acids research*. 1979;7(6):1513-1523.

111. Brody JR, Kern SE. History and principles of conductive media for standard DNA electrophoresis. *Anal Biochem*. 2004;333(1):1-13.

112. Bertani G. Studies on lysogenesis. I. The mode of phage liberation by lysogenic Escherichia coli. *Journal of bacteriology*. 1951;62(3):293-300.

113. Li X, Commane M, Burns C, Vithalani K, Cao Z, Stark GR. Mutant cells that do not respond to interleukin-1 (IL-1) reveal a novel role for IL-1 receptor-associated kinase. *Mol Cell Biol*. 1999;19(7):4643-4652.

114. Barrios-Rodiles M, Brown KR, Ozdamar B, et al. High-throughput mapping of a dynamic signaling network in mammalian cells. *Science*. 2005;307(5715):1621-1625.

115. Nishiya T, Kajita E, Horinouchi T, Nishimoto A, Miwa S. Distinct roles of TIR and non-TIR regions in the subcellular localization and signaling properties of MyD88. *FEBS Lett*. 2007;581(17):3223-3229.

116. Medzhitov R, Preston-Hurlburt P, Kopp E, et al. MyD88 is an adaptor protein in the hToll/IL-1 receptor family signaling pathways. *Mol Cell*. 1998;2(2):253-258.

117. Fekonja O, Bencina M, Jerala R. Toll/interleukin-1 receptor domain dimers as the platform for activation and enhanced inhibition of Toll-like receptor signaling. *J Biol Chem*. 2012;287(37):30993-31002.

118. Hunter ZR, Xu L, Yang G, et al. The genomic landscape of Waldenstrom macroglobulinemia is characterized by highly recurring MYD88 and WHIM-like CXCR4 mutations, and small somatic deletions associated with B-cell lymphomagenesis. *Blood*. 2014;123(11):1637-1646.

119. Coste I, Le Corf K, Kfoury A, et al. Dual function of MyD88 in RAS signaling and inflammation, leading to mouse and human cell transformation. *J Clin Invest*. 2010;120(10):3663-3667.

120. Besnard A, Galan-Rodriguez B, Vanhoutte P, Caboche J. Elk-1 a transcription factor with multiple facets in the brain. *Front Neurosci*. 2011;5:35.

121. Jabara HH, McDonald DR, Janssen E, et al. DOCK8 functions as an adaptor that links TLR-MyD88 signaling to B cell activation. *Nat Immunol*. 2012;13(6):612-620.

122. Werner M, Jumaa H. DOCKing innate to adaptive signaling for persistent antibody production. *Nat Immunol*. 2012;13(6):525-526.

123. Loiarro M, Sette C, Gallo G, et al. Peptide-mediated interference of TIR domain dimerization in MyD88 inhibits interleukin-1-dependent activation of NF-{kappa}B. *J Biol Chem*. 2005;280(16):15809-15814.

124. Arunkumar N, Liu C, Hang H, Song W. Toll-like receptor agonists induce apoptosis in mouse B-cell lymphoma cells by altering NF-kappaB activation. *Cell Mol Immunol*. 2013;10(4):360-372.

125. Wang JQ, Jeelall YS, Ferguson LL, Horikawa K. Toll-Like Receptors and Cancer: MYD88 Mutation and Inflammation. *Front Immunol*. 2014;5:367.

126. Fitzgerald KA, Chen ZJ. Sorting out Toll signals. *Cell*. 2006;125(5):834-836.

127. Wang J, Lau KY, Jung J, Ravindran P, Barrat FJ. Bruton's tyrosine kinase regulates TLR9 but not TLR7 signaling in human plasmacytoid dendritic cells. *Eur J Immunol*. 2014;44(4):1130-1136.

128. Qian Y, Commane M, Ninomiya-Tsuji J, Matsumoto K, Li X. IRAK-mediated translocation of TRAF6 and TAB2 in the interleukin-1-induced activation of NFkappa B. *J Biol Chem*. 2001;276(45):41661-41667.

129. Ngo HT, Azab AK, Farag M, et al. Src tyrosine kinase regulates adhesion and chemotaxis in Waldenstrom macroglobulinemia. *Clin Cancer Res*. 2009;15(19):6035-6041.

130. Woyach JA, Johnson AJ, Byrd JC. The B-cell receptor signaling pathway as a therapeutic target in CLL. *Blood*. 2012;120(6):1175-1184.

131. Cheng S, Coffey G, Zhang XH, et al. SYK inhibition and response prediction in diffuse large B-cell lymphoma. *Blood*. 2011;118(24):6342-6352.

132. Picard C, von Bernuth H, Ghandil P, et al. Clinical features and outcome of patients with IRAK-4 and MyD88 deficiency. *Medicine (Baltimore)*. 2010;89(6):403-425.

133. Bovijn C, Desmet AS, Uyttendaele I, Van Acker T, Tavernier J, Peelman F. Identification of binding sites for myeloid differentiation primary response gene 88 (MyD88) and Toll-like receptor 4 in MyD88 adapter-like (Mal). *J Biol Chem*. 2013;288(17):12054-12066.

134. Pauls E, Nanda SK, Smith H, Toth R, Arthur JS, Cohen P. Two phases of inflammatory mediator production defined by the study of IRAK2 and IRAK1 knock-in mice. *J Immunol*. 2013;191(5):2717-2730.

135. Shinohara H, Behar M, Inoue K, et al. Positive feedback within a kinase signaling complex functions as a switch mechanism for NF-kappaB activation. *Science*. 2014;344(6185):760-764.

136. Buchbinder D, Stinson JR, Nugent DJ, et al. Mild B-cell lymphocytosis in patients with a CARD11 C49Y mutation. *J Allergy Clin Immunol*. 2015.

137. Chan W, Schaffer TB, Pomerantz JL. A quantitative signaling screen identifies CARD11 mutations in the CARD and LATCH domains that induce Bcl10 ubiquitination and human lymphoma cell survival. *Mol Cell Biol*. 2013;33(2):429-443.

138. Compagno M, Lim WK, Grunn A, et al. Mutations of multiple genes cause deregulation of NF-kappaB in diffuse large B-cell lymphoma. *Nature*. 2009;459(7247):717-721.

139. Lien C, Fang CM, Huso D, Livak F, Lu R, Pitha PM. Critical role of IRF-5 in regulation of B-cell differentiation. *Proc Natl Acad Sci U S A*. 2010;107(10):4664-4668.

140. Cattoretti G, Shaknovich R, Smith PM, Jack HM, Murty VV, Alobeid B. Stages of germinal center transit are defined by B cell transcription factor coexpression and relative abundance. *J Immunol*. 2006;177(10):6930-6939.

141. Jo SH, Schatz JH, Acquaviva J, Singh H, Ren R. Cooperation between deficiencies of IRF-4 and IRF-8 promotes both myeloid and lymphoid tumorigenesis. *Blood*. 2010;116(15):2759-2767.

142. Minamino K, Takahara K, Adachi T, et al. IRF-2 regulates B-cell proliferation and antibody production through distinct mechanisms. *Int Immunol*. 2012;24(9):573-581.

143. Lossos IS. The endless complexity of lymphocyte differentiation and lymphomagenesis: IRF-4 downregulates BCL6 expression. *Cancer Cell*. 2007;12(3):189-191.

144. Braun D, Caramalho I, Demengeot J. IFN-alpha/beta enhances BCR-dependent B cell responses. *Int Immunol*. 2002;14(4):411-419.

145. Trinh KR, Vasuthasawat A, Steward KK, Yamada RE, Timmerman JM, Morrison SL. Anti-CD20-interferon-beta fusion protein therapy of murine B-cell lymphomas. *J Immunother*. 2013;36(5):305-318.

146. Huang TH, Chintalacharuvu KR, Morrison SL. Targeting IFN-alpha to B cell lymphoma by a tumor-specific antibody elicits potent antitumor activities. *J Immunol*. 2007;179(10):6881-6888.

147. Armitage AE, Armitage JD, Armitage JO. Alpha-interferon for relapsed non-Hodgkin's lymphoma. *Bone Marrow Transplant*. 2006;38(10):701-702.

148. Armitage JO, Coiffier B. Activity of interferon-alpha in relapsed patients with diffuse large B-cell and peripheral T-cell non-Hodgkin's lymphoma. *Ann Oncol*. 2000;11(3):359-361.

149. Brown SL, Miller RA, Horning SJ, et al. Treatment of B-cell lymphomas with anti-idiotype antibodies alone and in combination with alpha interferon. *Blood*. 1989;73(3):651-661.

150. Sato S, Sanjo H, Takeda K, et al. Essential function for the kinase TAK1 in innate and adaptive immune responses. *Nat Immunol*. 2005;6(11):1087-1095.

151. Khiem D, Cyster JG, Schwarz JJ, Black BL. A p38 MAPK-MEF2C pathway regulates B-cell proliferation. *Proc Natl Acad Sci U S A*. 2008;105(44):17067-17072.

152. Schmid CA, Robinson MD, Scheifinger NA, et al. DUSP4 deficiency caused by promoter hypermethylation drives JNK signaling and tumor cell survival in diffuse large B cell lymphoma. *J Exp Med*. 2015;212(5):775-792.

153. Arthur JS, Ley SC. Mitogen-activated protein kinases in innate immunity. *Nat Rev Immunol*. 2013;13(9):679-692.

154. Lam LT, Wright G, Davis RE, et al. Cooperative signaling through the signal transducer and activator of transcription 3 and nuclear factor-{kappa}B pathways in subtypes of diffuse large B-cell lymphoma. *Blood*. 2008;111(7):3701-3713.

155. Huang Y, Li T, Sane DC, Li L. IRAK1 serves as a novel regulator essential for lipopolysaccharide-induced interleukin-10 gene expression. *J Biol Chem*. 2004;279(49):51697-51703.

156. Roschewski M, Staudt LM, Wilson WH. Diffuse large B-cell lymphoma-treatment approaches in the molecular era. *Nat Rev Clin Oncol*. 2014;11(1):12-23.

157. Boi M, Gaudio E, Bonetti P, et al. The BET Bromodomain inhibitor OTX015 affects pathogenetic pathways in pre-clinical B-cell tumor models and synergizes with targeted drugs. *Clin Cancer Res*. 2015.

158. Ceribelli M, Kelly PN, Shaffer AL, et al. Blockade of oncogenic IkappaB kinase activity in diffuse large B-cell lymphoma by bromodomain and extraterminal domain protein inhibitors. *Proc Natl Acad Sci U S A*. 2014;111(31):11365-11370.

159. O'Shea JJ, Holland SM, Staudt LM. JAKs and STATs in immunity, immunodeficiency, and cancer. *N Engl J Med*. 2013;368(2):161-170.

160. Kandimalla ER, Bhagat L, Wang D, et al. Design, synthesis and biological evaluation of novel antagonist compounds of Toll-like receptors 7, 8 and 9. *Nucleic Acids Res*. 2013;41(6):3947-3961.

161. Antosz H, Sajewicz J, Marzec-Kotarska B, Dmoszynska A, Baszak J, Jargiello-Baszak M. Aberrant TIRAP and MyD88 expression in B-cell chronic lymphocytic leukemia. *Blood Cells Mol Dis*. 2013;51(1):48-55.

162. Bernard NJ, O'Neill LA. Mal, more than a bridge to MyD88. *IUBMB Life*. 2013;65(9):777-786.

163. Horng T, Barton GM, Flavell RA, Medzhitov R. The adaptor molecule TIRAP provides signalling specificity for Toll-like receptors. *Nature*. 2002;420(6913):329-333.

164. Ojaniemi M, Glumoff V, Harju K, Liljeroos M, Vuori K, Hallman M. Phosphatidylinositol 3-kinase is involved in Toll-like receptor 4-mediated cytokine expression in mouse macrophages. *Eur J Immunol*. 2003;33(3):597-605.

165. Laird MH, Rhee SH, Perkins DJ, et al. TLR4/MyD88/PI3K interactions regulate TLR4 signaling. *J Leukoc Biol*. 2009;85(6):966-977.

166. Gelman AE, LaRosa DF, Zhang J, et al. The adaptor molecule MyD88 activates PI-3 kinase signaling in CD4+ T cells and enables CpG oligodeoxynucleotide-mediated costimulation. *Immunity*. 2006;25(5):783-793.

167. Jabara HH, McDonald DR, Janssen E, et al. DOCK8 functions as an adaptor that links TLR-MyD88 signaling to B cell activation. *Nature immunology*. 2012;13(6):612-620.

168. Treon SP, Tripsas CK, Meid K, et al. Ibrutinib in previously treated Waldenstrom's macroglobulinemia. *N Engl J Med*. 2015;372(15):1430-1440.

169. Young RM, Staudt LM. Ibrutinib treatment of CLL: the cancer fights back. *Cancer Cell*. 2014;26(1):11-13.

170. Woyach JA, Furman RR, Liu TM, et al. Resistance mechanisms for the Bruton's tyrosine kinase inhibitor ibrutinib. *N Engl J Med*. 2014;370(24):2286-2294.

171. Furman RR, Cheng S, Lu P, et al. Ibrutinib resistance in chronic lymphocytic leukemia. *N Engl J Med*. 2014;370(24):2352-2354.

172. Loiarro M, Volpe E, Ruggiero V, et al. Mutational analysis identifies residues crucial for homodimerization of myeloid differentiation factor 88 (MyD88) and for its function in immune cells. *J Biol Chem*. 2013;288(42):30210-30222.

173. Singh-Jasuja H, Emmerich NP, Rammensee HG. The Tubingen approach: identification, selection, and validation of tumor-associated HLA peptides for cancer therapy. *Cancer Immunol Immunother*. 2004;53(3):187-195.

174. Hallek M. State-of-the-art treatment of chronic lymphocytic leukemia. *Hematology Am Soc Hematol Educ Program*. 2009:440-449.

175. Hallek M. Therapy of chronic lymphocytic leukaemia. *Best Pract Res Clin Haematol*. 2010;23(1):85-96.

176. Hallek M. Chronic lymphocytic leukemia: 2013 update on diagnosis, risk stratification and treatment. *Am J Hematol*. 2013;88(9):803-816.